AN INVESTIGATION OF THE EFFECT OF IMPROVED PHYSICAL PROPERTY DATA ON HEAT TRANSFER COEFFICIENT PREDICTION

By

MITRI S. NAJJAR

Bachelor of Science
American University of Beirut
Beirut, Lebanon
1973

Master of Science
Oklahoma State University
Stillwater, Oklahoma
1977

Submitted to the Faculty of the Graduate College
of the Oklahoma State University
in partial fulfillment of the requirements
for the Degree of
DOCTOR OF PHILOSOPHY
May, 1980

AN INVESTIGATION OF THE EFFECT OF IMPROVED PHYSICAL PROPERTY DATA ON HEAT TRANSFER COEFFICIENT PREDICTION

Thesis Approved:

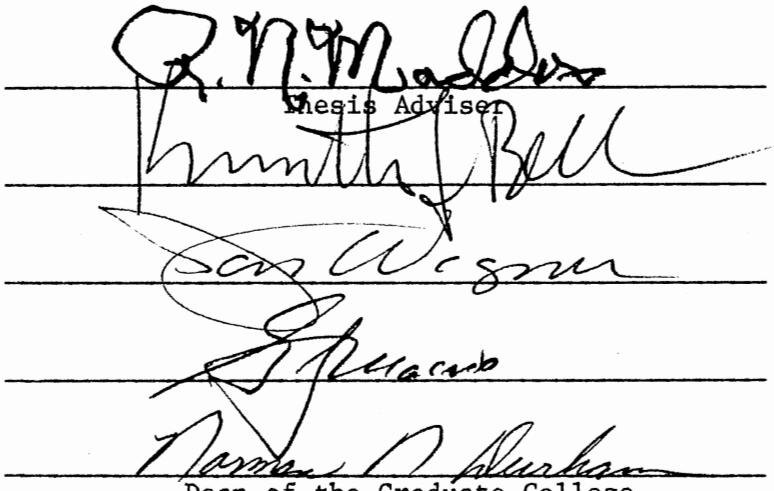

Thesis Adviser

Dean of the Graduate College

PREFACE

This dissertation is concerned with the effects well defined physical properties for pure components and/or mixtures have on estimates of the heat transfer coefficient. Experimental measurements of the heat transfer coefficient for laminar and turbulent flow inside a straight horizontal tube were made. The test fluids were distilled water, methanol, toluene, 85 wt % ethylene glycol-water mixture, 50 wt % ethylene glycol-water mixture, heavy premium coker, 30 wt % diethanolamine-water mixture, and n-octane.

I am gratefully indebted to my adviser, Dr. R. N. Maddox, for his counsel, encouragement, and patience throughout my graduate program. I am also grateful to my Advisory Committee, Dr. K. J. Bell, Dr. J. Wagner, and Dr. G. J. Mains, for their suggestions and help. I would like to thank Drs. M. Moshfeghian and C. B. Panchal for providing me the computer program and their assistance. I am grateful to Mr. E. E. McCroskey, Storeroom Manager, for his assistance in the construction of the experimental apparatus. I appreciate the financial assistance provided by the School of Chemical Engineering and the Chemistry Department during the course of my study. Also, I owe a great deal to my uncle, Dr. E. I. Shaheen, for helping me get started on my graduate work.

Finally, I would like to thank my parents, especially my mother, for their love and encouragement and sacrifices throughout my education.

My sister, Maryana, and brother-in-law, John, for their love, my sister, Dada, for her patience, help, and love, and my brother, Walid, for his love and moral support.

TABLE OF CONTENTS

LIST OF TABLES

LIST OF FIGURES

NOMENCLATURE

A_{cb}	- surface area of copper bar
AAPD	- average absolute percent deviation
C_p	- specific heat of fluid
DEA	- diethanolamine
d	- test section diameter
G	- mass velocity of the fluid
Gr	-Grashof number, $d_i^3 \rho^2 g\beta(\bar{T}_{w_i} - T_b)/\mu^2$
g	- gravitational acceleration
H_1	- peripheral average heat transfer coefficient, defined by Equation (6.1)
H_2	- peripheral average heat transfer coefficient, defined by Equation (6.2)
$\bar{h}$	- peripheral average heat transfer coefficient
h_c	- convective heat transfer coefficient
h_i	- local inside heat transfer coefficient
h_{nc}	- convective heat transfer coefficient from plane surfaces
I	- current in test section
k	- thermal conductivity
k_{ss}	- thermal conductivity of stainless steel
L	- total heated length
L_{ent}	- entrance length of test section
$\dot{m}$	- mass flow rate of fluid

Nu - Nusselt number, $\bar{h}\, d_i/k$

Pr - Prandtl number, $C_p \mu/k$

$\dot{q}/_A$ - heat flux rate

Re - Reynolds number, $d_i\, G/_\mu$

r - test section radius

T_b - bulk fluid temperature

T_I - temperature at outside surface of insulation

T_{w_o} - outside wall temperature

T_{w_i} - inside wall temperature

$T_{w_{in}}$ - outside wall temperature for inlet test section

$T_{w_{out}}$ - outside wall temperature for outlet test section

$\bar{T}_{w_{in}}$ - peripheral average inside wall temperature

t - tube wall thickness

V - fluid velocity; voltage drop in test section

X - axial location of thermocouple stations

X^* - dimensionless axial distance, $\pi/_{(4Gr)}$

$\frac{X}{d_i}$ - dimensionless distance from the inlet of test section

Greek Letters

β - coefficient of volume expansion of the fluid

μ - fluid viscosity

ρ - fluid density

θ - angular position

Subscripts

b	- bulk fluid
cb	- copper bar
DB	- Dittus-Boelter
F	- film
i	- inside tube surface
in	- test section inlet
ins	- insulation
o	- outside tube surface
out	- test section outlet
PK	- Petukhov
ST	- Sieder-Tate
ss	- stainless steel

CHAPTER I

INTRODUCTION

Physical properties are essential in the design and development of heat and mass transfer equipment. Accurate physical properties are important in developing empirical, semi-empirical or theoretical predictions. Since these data will be used in the form of dimensionless groups it is important to test available sets of properties in such groups.

The primary purpose of this work is to try and establish the effect well-defined physical properties for pure components and/or mixtures have on estimates of the heat transfer coefficient. An experimental apparatus was built with a horizontal straight test section geometry such that we can most easily measure the variables needed to evaluate the local heat transfer coefficient. Most of the experimental runs were in the turbulent flow regime where better correlations are available for estimating the heat transfer coefficient than in laminar flow. The apparatus was designed to use the widest possible range of fluids with vastly different properties.

Experimental studies were made with water, methanol, toluene, 85 wt % ethylene glycol-water mixture, 50 wt % ethylene glycol-water mixture, heavy oil coker, 30 wt % diethanolamine-water mixture, and n-octane in turbulent flow in an electrical-resistance-heated

tube. For the heavy oil coker system, runs were also taken in laminar flow for the thermally developing region.

The apparatus was in the form of a closed piping loop constructed so that in the test section, Reynolds number and Prandtl number of the circulating fluids could be held at desired levels. The loop contained a pump, an entrance section, a test section, a flow meter, a fluid cylinder, and a heat exchanger. The test section was made of 0.43 in. i.d. stainless steel tube and was insulated from the piping system electrically and thermally. The test section was heated by a DC current through two copper bars silver soldered to the tube. Thermocouples were attached to the outer surface of the tubes. Inner surface temperatures and local heat fluxes were calculated from the outside surface temperature using a numerical solution. Local heat transfer coefficients were obtained around the periphery of the tube. Experimental heat transfer coefficients were compared with those predicted using different sets of physical property data and the following heat transfer correlations in the turbulent flow region:

1. Sieder-Tate (1) equation
2. Dittus-Boelter (2) equation
3. Petukhov (3) correlation.

Experimental data in the laminar flow region were compared with the Morcos-Bergles correlation (4). For the thermal entrance region, data were compared with equations developed by Shah (5), Grigull and Tratz (6) and Churchill and Ozoe (7). The study covered Reynolds numbers from 52 to 60, 500 and Prandtl numbers 5.3 to 1570.

CHAPTER II

LITERATURE SURVEY

Up to the present date numerous heat transfer measurements have been made for fluids in turbulent flow. However, little consideration has been given to the effects of property inaccuracies on the prediction of the heat transfer coefficient and other areas of chemical engineering interest. This chapter presents a summary of these investigations.

Nangia and Taborek (8) have related the importance of thermal conductivity of liquids in all heat transfer applications and the relatively high exponents (0.65-1.0) under which it appears in equations. They also showed that despite the importance of thermal conductivity, experimental data even at ordinary temperature levels are scarce, particularly for liquids. Contrary to gases, the theory of liquids is not developed to a significant degree to permit a satisfactory theoretical analysis for the prediction of this property; consequently, large errors are frequently encountered by using the present heat transfer correlations for industrial design purposes.

Nangia and Taborek (9) selected four of the most important properties -- thermal conductivity, specific heat, viscosity, and density to demonstrate the probable errors incountered in industrial applications. They reported the following conclusions:

1. Data and predictive methods for liquids are badly lacking due to measurement difficulties and the present poor understanding of intermolecular relations in the liquid state.

2. Wide variations in the predicted values can have significant effect on the size and utility of heat transfer equipment designed using these physical property values.

McCoy, Mathur and Maddox (10) extended the consideration of physical property variations to many areas of chemical engineering interest, mainly pressure drop calculations, boiling heat transfer coefficient calculations, and distillation column sizing. The following conclusions were reported:

1. Errors of the order of 50-100% in physical property predictions are not uncommon. These errors generate substantial errors in process and design calculations, unnecessary expenditures for equipment, unsatisfactory equipment operation and inefficient plants.

2. More data need to be taken on both pure components and mixtures, particularly data taken under conditions of temperature, pressure and liquid-vapor contact that can be expected to be encountered in day-to-day plant operation.

3. Good predictive and correlative procedures can only be developed based on sound, accurate and precise experimental data.

Squires and Orchard (11) showed the following effects of data error on pressure drop and reboiler duties:

1. A 20% error in viscosity causes a 4% error in pressure drop calculation.

2. A 20% error in thermal conductivity causes an error of 9.2% in the boiling coefficients in reboilers.

3. A 20% error in density causes an error in pressure drop calculations of 18%. The same error causes an error of 10% in reboiler boiling coefficient.

4. The cumulative effects of data error result in a one for one loss in accuracy in pressure drop design and in reboiler boiling coefficient calculations.

5. Errors in the order of 50 to 100% in physical properties predictions are not uncommon. The errors result in unnecessary expenditures for equipment, unsatisfactory equipment operation and inefficient plants.

Williams and Albright (12) related the ability to effectively save energy in petroleum processes to the accuracy of the physical and thermodynamic data available. They reported that values of thermal conductivity of many petroleum components have been found to be 20 to 200% different than was reported 10 years ago. That improved data necessary for tighter design of heat exchange equipment are not available for all the compounds and materials found in the petroleum business. Uncertainties in data led to gasoline plant designs with excess compressor horsepower for refrigeration, relatively large temperature approaches in heat exchange equipment, fractionators with excess reboiler and condenser equipment.

Zudkevitch (13) pointed out that computer techniques, although essential in correlating data, can often lead to problems in delivering

reliable data in the form that a designer can use. The expanding scope of computer design programs creates a strong pressure for the use of "well-behaved" data correlations in the interest of overall efficiency of computer program operation. Care must be taken that this does not result in the misuse of a generalized correlation outside its region of validity.

Gray and Zudkevitch (14) investigated the specific features of LNG plant design which lead to relatively unique data problems. They reported the following conclusions:

1. There is a need for highly accurate prediction of enthalpy as a function of temperature, pressure, and composition in vapor, liquid and two-phase regions to minimize irreversible losses in exchanges.

2. Extremely accurate liquid density predictions are required to convert the known volume of LNG to a known mass in order to calculate the total heating values, which determine the selling price.

3. Reliable data at cryogenic conditions are difficult and expensive to obtain. Data development efforts should be concentrated where the economic impact is greatest.

4. The relative magnitude and impact of errors in data predictions at various conditions may be strongly dependent on process variations.

5. Phase equilibria and enthalpy calculations are identified as the most important thermodynamic properties in LNG facility. However, inaccuracies in less available transport properties cannot be ignored. For example, the effect of the coefficient of thermal conductivity on the heat transfer coefficients of a fluid is a direct function of the exponent, which varies between 0.65 and 1.0. Since the accuracy of

thermal conductivity data is not high, even with an exponent of 0.65 the effect on heat exchanger sizing can be serious.

Nani and Venart (15) obtained data on the thermal conductivity of gaseous and liquid methane measured within the conditions range of a liquefaction operation and compared the results with data from other publications. They reported discrepancies of up to 18%. A discrepancy of 18% raised to a power of 0.7 corresponds to an uncertainty of 12.3% in the heat transfer coefficient.

Nangia and Taborek (8) reported that an uncertainty of this magnitude may be significant for expensive cryogenic exchangers, particularly since the inability of an undersized exchanger to meet design temperatures may make it necessary to lower the mass flow rate, making the heat transfer coefficient even smaller. The alternative of raising coolant mass flow rate to raise the heat transfer coefficient may be precluded by pressure drop limitations.

Albright (16) showed that the effects of discrepancies in data on the economics of the entire LNG plant are not direct but also depend on whether an additional cascade stage is required or an additional load on one stage is partly compensated by a reduced load on the downstream equipment. Baker (17) estimated the effect of errors in enthalpy predictions on investment for cryogenic facilities. By updating Baker's estimates, the designer may make a rough estimate of the effect data errors have on investment in liquefication plants.

Recently, Streich and Kistenmacher (18) showed the influence of property inaccuracies in low temperature designs. They presented three examples to illustrate the severity of bad predictions.

1. For the C_2 and C_3 splitter in olefin plants, inaccuracy in equilibrium constant values results in excess trays and/or excess reflux.

2. Accurate enthalpy calculations are needed in the processing chain in which ammonia is produced. Using the standard available methods results in poor estimates because of excessive extrapolation.

3. In natural gas liquefaction plants, inaccuracies in vapor-liquid-equilibrium constant values change the vapor-liquid-ratio of the recycle stream, and this would change the heat load on the exchanger.

In recent years there have been three major search efforts of the literature for correlative and predictive techniques. The American Petroleum Institute (19) has published a data book containing recommended procedures to be used for predicting physical properties of petroleum derived constituents. The American Institute of Chemical Engineers (20) has published a computer package containing recommended procedures for physical properties data predictions. A recent evaluation of the available methods for thermal conductivity prediction made during the revision of Chapter 7, "Thermal Properties," of the API Data Book (19) indicates that uncertainties on the order of 25-30% can readily be encountered. Fluid Properties Research, Inc. (FPRI) has a body of experimental data both from the literature and by measurements-collected on thermal conductivity, viscosity, heat capacity, density and interfacial tension. Present efforts are directed toward extending this to include all transport and thermal properties of importance to industrial process design. To augument experimental

data measurements and aid the predictive-correlative work, FPRI maintains an up-to-date computer file of literature on physical properties and their measurement.

CHAPTER III

EXPERIMENTAL SYSTEM

An experimental apparatus has been designed, constructed, and equipped with instruments to measure the variables needed to evaluate the local heat transfer coefficients in laminar and turbulent flow in a uniformly-heated straight tube using distilled water, methanol, toluene, 85 wt % ethylene glycol-water, 50 wt % ethylene glycol-water, heavy oil coker, 30 wt % diethanolamine-water, and n-octane. A sketch of the experimental set up is shown in Figure 1. The DC power source, operating procedures, and the way the thermocouples were fabricated and placed on the tube wall along the test section was essentially the same as that used by Farukhi (21), Singh (22) and Moshfeghian (23). Some parts of this chapter and the following chapters are taken directly from their Doctor of Philosophy thesis (23) (22) (21).

Description of Apparatus

Test Section

The test section is fabricated from a Gibson tube ASTM-A269, (½ in.) o.d. x (0.035 in.) wall thickness. It is isolated electrically from upstream and downstream sections by means of two teflon bushings that could take temperatures up to 450°F and pressures up

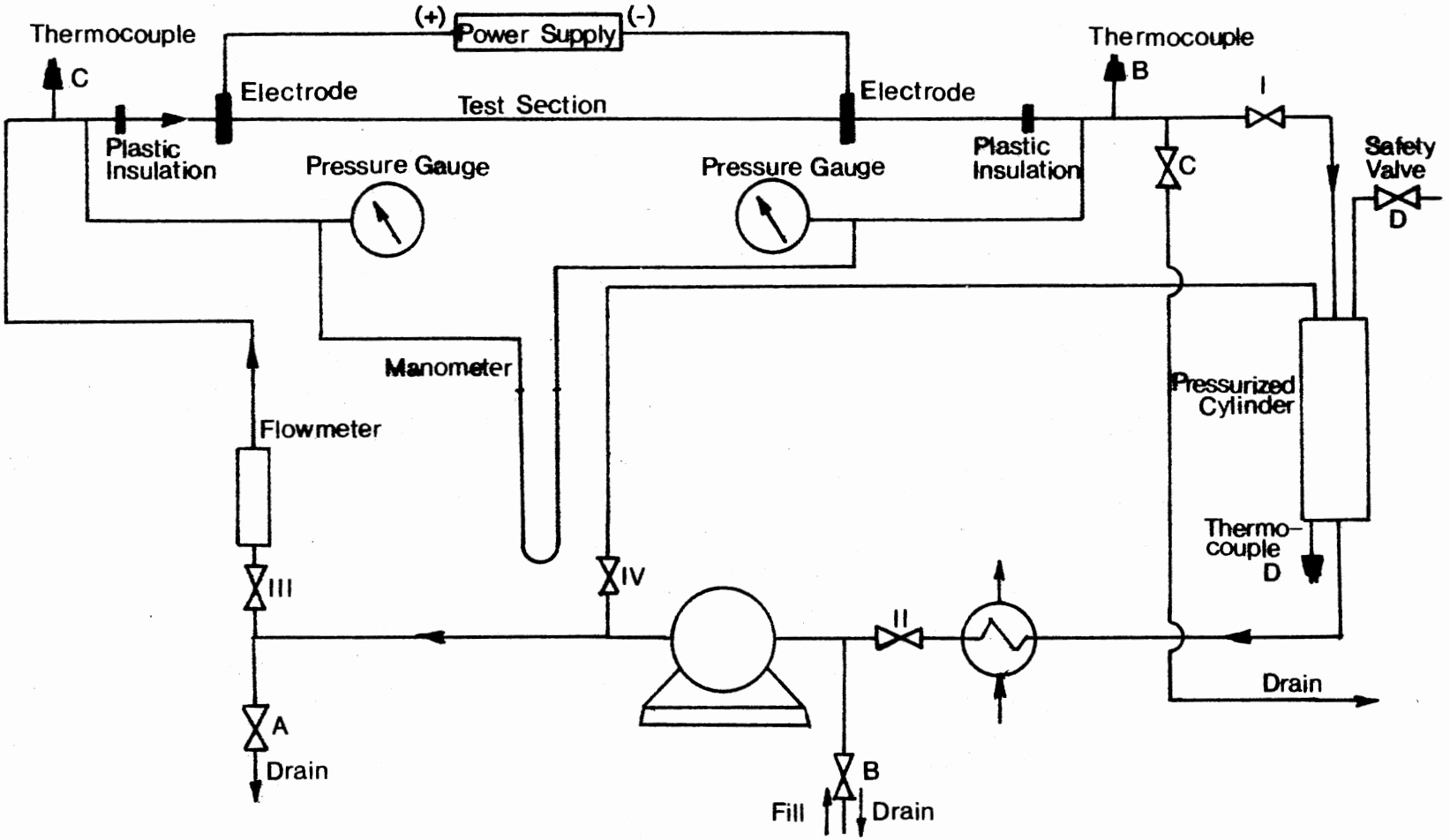

Figure 1. Schematic of Heat Transfer Loop

to 1000 psia. A direct current is supplied to the test section by means of two copper bars silver-soldered at each end. The electric current flows axially through the tube wall generating heat at a uniform rate which is removed by the circulating water in the heat exchanger. The test section is thermally insulated by first wrapping several layers of bonded fiberglass tape, then by using 1½ in. thickness of rigid white hydrous calcium silicate insulation wrapped with aluminum foil.

An entrance length of 3 ft. is maintained to allow essential completion of hydrodynamic development.

Dimensions of the test section with thermocouple locations are given in Figure 2.

Fluid Cylinder

A pressurized fluid cylinder of capacity 0.8 gal. is used. The cylinder is surrounded by a gasket where water could flow and be used for cooling the fluid. The top cover of the cylinder, which could be removed, is connected to the main loop and the recycle line. At the bottom an iron constantan thermocouple (OMEGA J type) is inserted to measure the fluid temperature in the cylinder.

Heat Exchanger

A one shell-pass-multi-tube heat exchanger was used to cool the test fluid from the test section. The test fluids pass in the tubes while water, used as a cooling fluid, passes in the shell side.

DC Power Source

In order to generate the DC current to be supplied to the test

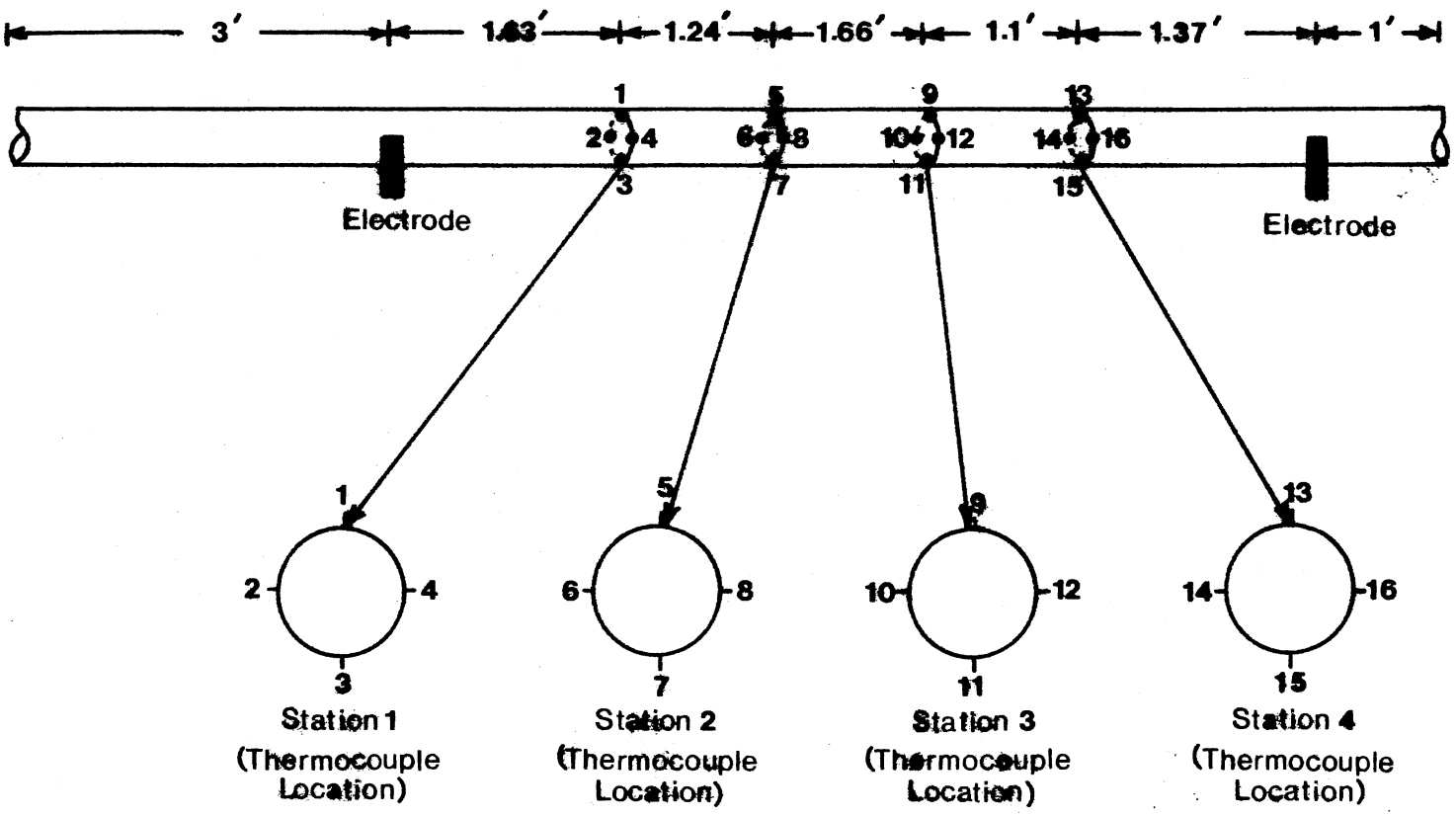

Figure 2. Dimensions of Test Section with Thermocouple Locations

section through two copper bars silver soldered to the tube, a Lincoln-weld SA-750 AC motor driven DC generator is used. This DC power generator has a maximum rated output power of 30 KW. The passage of the DC current through the wall provided a constant heat source to the fluid.

Pump

An adjustable speed drive pump was used to pump the fluid through the test section. The pump was manufactured by Rose Equipment Company and has the following specifications: 1 Roper FIG. I H5 Spec. 5 connected through a Lovejoy coupling to a 2 HP, 3 phase adjustable speed gear head motor with a range of 190 RPM to 1900 RPM. The complete unit is mounted on a common base including a coupling guard. Maximum pressure is 300 psi and maximum temperature is 400^{o}F.

Instrumentation

Thermocouples

Temperatures were measured using two different types of iron-constantan thermocouples connected to a thermocouple indicator through a switch box selector.

1. Iron constantan thermocouples (OMEGA J type) to measure inlet and outlet bulk fluid temperatures.

2. Insulated wire thermocouples "Iron-Constantan" to measure the outside wall temperature of the test section tube.

This pair of dissimilar metals has a sensitivity of 30 microvolts per degree Fahrenheit, higher than any other thermocouple type for the temperature range of interest.

OMEGA "J Type" Thermocouples

Two Iron-Constantan J Type thermocouples with a positive iron wire and a negative constantan wire, manufactured by Omega Corporation, were used to measure the bulk fluid temperature at the inlet and outlet of the test section. A third thermocouple was inserted at the bottom of the fluid cylinder. This type of sheathed ungrounded thermocouple was used because (23):

"1. The sheath protects the thermocouple from corrosion by the fluid.

2. The ungrounded thermocouples are immune to any stray emfs that may be produced by the DC heating."

Thermocouples were calibrated using a Leeds and Northrup standard platinum resistance thermometer as a reference. Details of the calibration procedure are presented in Chapter IV.

Insulated Wire Thermocouples

Thermocouples made from fiber glass-insulated, 30 B&S gauge Iron-constantan thermocouple wire were used to measure the outside wall temperatures of the test section tube. A thermocouple welder was used to fabricate the thermocouples. The hot junctions of the thermocouples were placed at four stations on the tube wall along the test section. At each station four thermocouples were placed 90 degrees apart on the tube periphery. The position of each station and the thermocouple layout is shown in Figure 2 and Table I.

To insulate the thermocouple leads electrically from the heating current, a thin layer of sauereisen cement was first placed at the

TABLE I

PRINCIPAL THERMOCOUPLE LOCATIONS

Thermocouple No.	Description
A	Room Temperature
B	Bulk Fluid Outlet Temperature
C	Bulk Fluid Inlet Temperature
D	Fluid Bath Temperature

Location of Test Section Thermocouples

No.	$\frac{X}{d_i}$	No.	$\frac{X}{d_i}$
1	45.5	9	127.0
2	45.5	10	127.0
3	45.5	11	127.0
4	45.5	12	127.0
5	80.2	13	157.0
6	80.2	14	157.0
7	80.2	15	157.0
8	80.2	16	157.0

intended thermocouple location and allowed to set before cementing the thermocouple leads to its intended location. The thermocouple wires from the thermocouple beads were held in place about ½ in. from the thermocouple beads by means of a layer of asbestos paper tape and a flexible hose clamp. The asbestos paper tape was placed between the clamp and the thermocouple wire to prevent any accidental short-circuiting of the thermocouple wires due to the sharp edges of the metal hoseclamp. The thermocouple wires were then placed along the test section for about two inches and clamped again to the tube before being led off to a switch box, where a master switch is connected to a thermocouple indicator. All thermocouples were calibrated using a platinum resistance thermometer as a reference. Details of the calibration procedure are presented in Chapter IV.

Test Gauges

The two pressure gauges used were connected by 1/8 in. stainless steel tubing to the inlet and outlet of the test section as shown in Figure 1. They have 2 psi subdivisions and could read up to 400 psi. The two gauges were calibrated against a Ruska "2400 Model Dead Weight Gauge". The pressure of the reference gauge was plotted against that of the two test gauges and working equations were developed to correct the pressure at the inlet and outlet of the test section. Results of the calibration procedure are presented in Appendix B. A U type manometer was connected to indicate the pressure drop across the test section. The U type manometer was manufactured by the Meriam Instrument Co. and has the following specifications: Model 10AA25WM, 36 inches range with 0.1 in. subdivisions.

Rotameters

A Brooks rotameter and a Fischer and Porter flow indicator were used to indicate and measure the flow rates of the different fluids tested. Their specifications are given in Table II.

TABLE II

FLOWMETER SPECIFICATIONS

Item	Rotameter 1	Rotameter 2
Rotameter model number	10-110-10	7807F
Rotameter tube number	R-10M-25-3	0051F-1
Float number	10-RV-64	--
Maximum water flow rate, gpm	6.28	1.25

Calibration tables are presented in Appendix B

Digital Multi Meter (DMM)

The power input to the test section was measured by means of a digital multimeter manufactured by John Fluke Manufacturing Company, Inc. The model is 8000A with 3½ digit display. Push-button controls allow the selection of five AC or DC voltage ranges, five AC or DC current ranges, and six resistance ranges. Only the DCV function and voltage range were used.

The current flowing through the test section was measured by pushing the DCV function and the millivolt range (MV) in conjunction with a 50 millivolt shunt (see Figure 3).

The 50 millivolt shunt was connected in the line carrying the current to the test section. When the push button is on (MV), the digital multimeter is connected across the shunt and the corresponding millivolt reading corresponds to the current flowing. The shunt is rated such that 50 millivolt reading corresponds to 750 AMPS.

The voltage drop across the test section was measured by pushing the DCV function and the 20 volt range with connections to the two copper bars. The 200 volt range was pushed first. For more accurate readings the 20 volt range was then used.

Multipoint T/C Selection

The multipoint selector used is a switching unit having the capability of accepting the outputs of several thermocouples; selecting one or more of them and feeding the signals into the thermocouple indicator.

The front panel of the selector consists of a series of push button switches (12 in a row) which select the desired thermocouple. The thermocouples were wired to the multipoint selector by using the procedure noted below:

1. Remove the four screws securing the rear panel; remove the two screws from the top and bottom of the instrument and slide the circuit board out.

2. Remove the shield by removing the six screws securing it to the board.

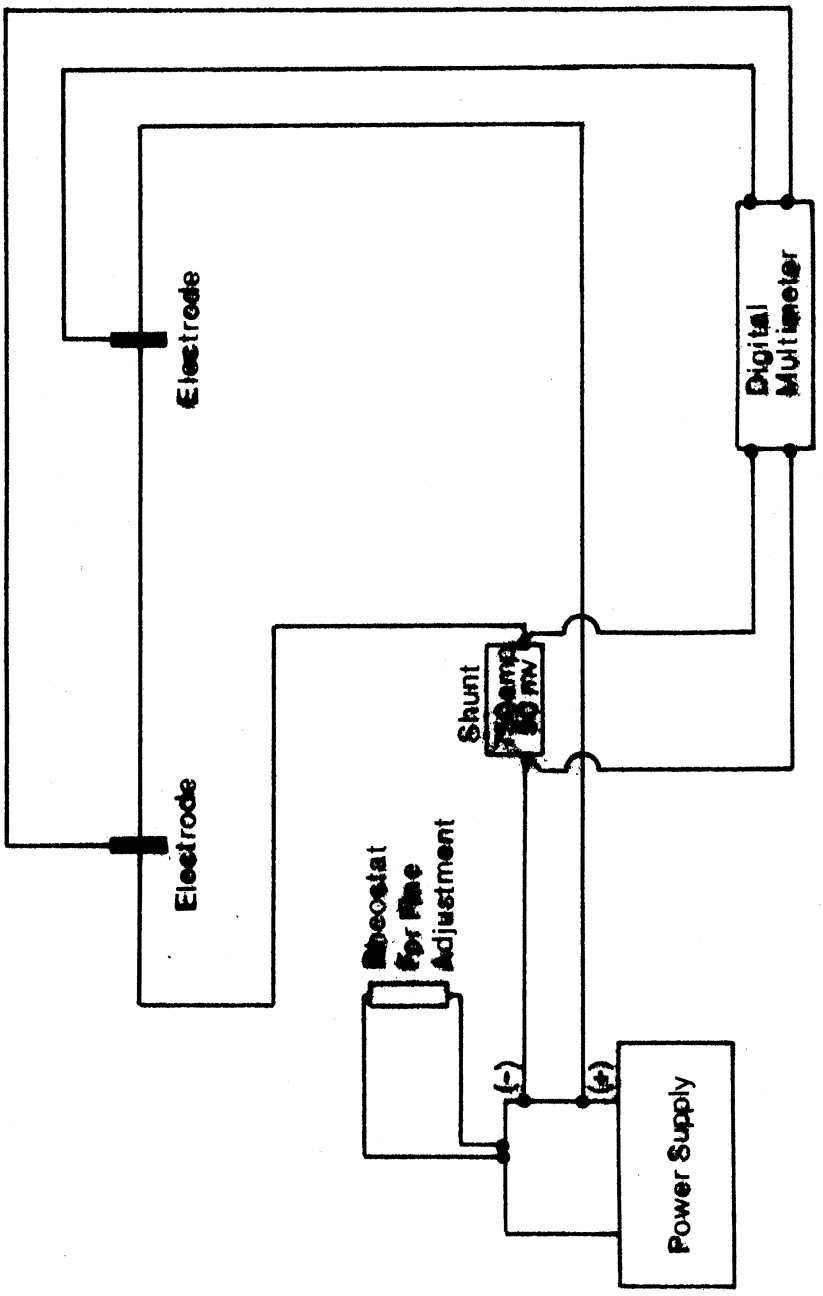

Figure 3. Electric Loop

3. Route the thermocouple wires to the appropriate terminals. (HI=TC+:LO=TC-) switch numbers on the bottom board to correspond to front panel switches viewed left to right. (SI- the first push button on the left.)

CAUTION: Because the second board is mounted upside down, the wiring is reversed. S12 corresponds to the first switch on the left, S11 to the second switch and so on until S1 corresponds to the last switch on the right.

4. Run thermocouple wire from the HI, LO and GD terminals on the board. These three wires attach to the respective thermocouple inputs of the thermocouple indicator.

5. Replace the shield; slide the boards back into the housing.

Digital Thermocouple Indicator

The thermocouple indicator is a Doric Scientific DS350 type J (Iron-Constantan) with a stated accuracy $\pm$ 0.27% for the -32.0^{o}F to +800.0^{o}F temperature range. The thermocouple indicator used converts the thermocouple emf fed to the instrument into its corresponding temperature reading which is displayed directly in degrees Fahrenheit on the digital readout panel of the indicator. Further details may be obtained from the Digital Thermocouple Indicator Manual (24).

Auxiliary Equipment

All the measuring devices used were calibrated, except for the 8000 A Digital Multimeter where similar units used by the Electrical

Engineering Department at Oklahoma State University were all found to be in the accuracy range guaranteed by the manufacturer. The description of the auxiliary equipment consists of three sections:

1. Flow indicator calibration and fluid flow rate measurement equipment.

2. Digital thermocouple indicator equipment.

3. Pressure gauge calibration equipment.

Rate Measurement Equipment

The fluid flow measurement equipment consisted of the following:

1. Weighing Equipment: A set of calibrated weights was used in conjunction with a five kilogram capacity Ohaus Pan Balance to weigh the amount of fluid collected for weights that are above 1200 grams. The balance has a sensitivity of 0.5 grams.

For weights of the collected fluid that were less than 1200 grams, a Mettler P1210 balance was used. The balance has a sensitivity of 0.01 grams.

2. Fluid Collecting Vessels: The vessels used consisted of different capacity beakers and cylindrical metallic jars. The fluid was collected for a recorded interval of time, so that the mass flow rate could be recorded.

3. Stop Watch: A 10 minute stop watch with a main dial range of 10 seconds was used to time the fluid flow rate. The stop watch has a precision of 0.1 seconds.

Digital Thermocouple Indicator Calibration Equipment

A Leeds and Northrup model 8687 Volt Potentiometer was used for the calibration of the digital thermocouple indicator. The potentiometer used has a maximum stated accuracy of ± (0.03% of reading + 30 microvolts) (25).

Test Gauge Calibration Equipment

A Dead Weight Gauge model 2400 was used in the calibration of the two test gauges in conjunction with a Ruska Pump installed in the line between the Dead Weight Gauge and the test gauge. The Dead Weight Gauge used was calibrated by the manufacturer by direct intercomparison with a Dead Weight Gauge calibrated by the National Bureau of Standards. The Dead Weight Gauge used has a maximum stated accuracy of ± (0.01% of reading) (26).

CHAPTER IV

EXPERIMENTAL PROCEDURE

This chapter includes the following sections: (1) Calibration Procedure; (2) Loop Operating and Data Gathering Procedure.

Calibration Procedure

Thermocouple Calibration

1. Calibration Equipment Specifications:

   A. Variable Temperature Oil Bath

      Model 910 AB
      Instruction Manual No. 1684
      Rosemount, Inc.

   B. Platinum Resistance Thermometer:

      Series 8163-QB
      Serial No. 1827669
      Leeds and Northrup Company

   C. Muller Temperature Bridge:

      Serial No. 8069B
      Leeds and Northrup Company

2. Calibration Procedure:

All thermocouples were calibrated, before being installed in the test section, using a standard platinum resistance thermometer. A Muller Bridge was used to measure the resistance of the standard platinum thermometer. Both the standard resistance thermometer and the thermocouples were immersed in a constant temperature oil bath.

temperature of the bath was measured by noting the resistance of the platinum thermometer, which was read twice in the N (Normal position and twice in the R (Reverse) position, and taking the reading of the thermocouples which were connected to the Multipoint Selector which in turn was connected to the digital thermocouple indicator.

The average of the N and R position readings was taken and corresponding Standard temperatures were read from IPTS-68 table for the resistance thermometer (Serial No. 1761202).

A zero reading in the Muller Bridge was found to correspond to zero ohm resistance. R_o, the resistance of the platinum resistance thermometer at 0^oC was found to be 25.5770. Five readings were taken to cover the temperature range of interest (60^oF - 400^oF).

The converted temperature readings of the standard platinum resistance thermocouple were plotted vs the temperature readings of the thermocouples, and working equations were developed to correct the thermocouple readings. Thermocouple calibration data are presented in Appendix B.

Flow Meter Calibration

Calibration procedures were used for distilled water, methanol, and toluene systems. Data were taken with the flow rate increasing up to the maximum and then decreasing to the minimum flow rate.

The calibration procedure consisted of the following steps:

1. The fluid flow rate was adjusted to the desired float setting or percent maximum flow on the flow meter. This was done by either changing the recycle flow rate or adjusting the speed of the pump.

2. A previously weighed empty container was used to collect the fluid flowing in the system for a measured time interval. This was after the flow indicator was steady on a given flow setting.

3. Temperature readings were taken using the thermocouple inserted from the bottom of the cylinder.

4. The sample collected was weighed and then returned to the vessel.

The above procedure was repeated two times for each flow setting on the indicator.

For 50 wt % ethylene glycol-water, 85 wt % ethylene glycol-water, heavy coker oil, 30 wt % diethanolamine-water, and n-octane systems the flow rate was measured by repeating the above procedure for each run.

Calibration data are presented in Appendix B.

Digital Thermocouple Indicator Calibration

The Digital Thermocouple Indicator was calibrated periodically. The calibration procedure is detailed in Section IV of the Owners Manual (23).

Manometer Calibration

The reading of the U-type Manometer was set to zero when there was no fluid flow in the test section. Liquid mercury was used as the indicator fluid in the manometer.

Test Gauges Calibration

The test gauges were calibrated against a Dead Weight Gauge

model 2400. The following procedure was followed:

1. The Read Out and the pressure gauge which were connected on both sides of the diaphragm of the differential pressure were at equilibrium (Zero Reading).

2. The system was closed off to atmosphere and weights of nonmagnetic stainless steel were placed on the interchangeable piston cylinder-weight table assembly.

3. Pressure was applied from the gas cylinder to pressurize the pressure gauge. The pressure was built slowly until the needle indicated a zero reading which corresponded to equal pressures on both sides of the differential pressure indicator.

4. Steps 2 and 3 were repeated by incrementing the weights to obtain the maximum anticipated pressure.

5. Readings were also taken when the pressure was reduced.

Loop Operating and Data Gathering Procedure

Start-Up Procedure

After the experimental loop was constructed, and all measuring devices were installed, the fluid flow loop was tested for possible leaks by flowing water at an anticipated maximum pressure and flow rate. Any leaks detected were eliminated. The fluid flow loop was then insulated and prepared for obtaining experimental data.

The following steps were followed to gather data for each run:

1. The DC generator was started. Main switch on "ON" position and the green button pushed. The polarity switch was kept on the "OFF" position to allow the generator to warm up for about 30 minutes.

2. Cooling water was started to the heat exchanger located down stream of the test section.

3. The digital thermocouple indicator was activated.

4. The pump was started and the fluid was allowed to circulate in the recycle line.

5. The test section was pressurized by regulating Valve I (Figure 1) in conjunction with the recycle control Valve IV.

6. The polarity switch was moved from the "OFF" position to either the "Electrode Negative" or "Electrode Positive" position, allowing the DC current to flow through the test section.

7. The digital Multimeter was activated.

Data Recording Process

Before any data were recorded the following steps were followed:

1. Control valves I and IV (Figure 1) were adjusted to give the desired flow rate.

2. The DC current was adjusted by varying the output control switch on the control box of the generator. Fine control adjustment of the current was made by a variable rheostat connected to the generator.

3. Flow rate of the cooling water to the heat exchanger was adjusted so that the fluid temperature in the cylinder and at the inlet of the test section remained constant.

4. The experimental set up was then allowed to operate to achieve steady state. If necessary, minor adjustments were made to cooling water rate, current, and fluid flow rate, before any readings were taken.

5. After about two hours of operation coupled with checking for temperature approach to steady state the following experimental data were taken:

   a. The inlet and outlet bulk fluid temperature.

   b. The test section surface temperature.

   c. The voltage drop across the test section and the DC current flowing through the test section.

   d. The room and cylinder temperature.

   e. The pressure in the system as indicated by the pressure gauges.

   f. The flow rate of the system.

6. Step 5 was repeated after about half an hour to ascertain if steady state had been achieved.

7. Steady state was deemed to have been achieved if the two sets of temperature measurements agreed within $\pm$ 0.3^{o}F.

If steady state had not been achieved, steps 5 and 6 were repeated after about half an hour of continued operation where a steady state was achieved for most of the runs.

The fluid flow rate and/or the current and/or the cooling water flow rate was changed to a new set of conditions and the entire data recording process was repeated for the new set of input conditions. For each of the 50 wt % ethylene glycol-water, 85 wt % ethylene glycol-water, heavy oil coker, and 30 wt % diethanolamine-water runs, the mass flow rate of the fluid was measured, after obtaining the temperature and pressure data as indicated in steps 5 and 6 of the Data Recording Process section.

Shut-Down Procedure

The following steps were followed to shut down the system:

1. The polarity switch of the DC Generator was turned to the "OFF" position and the red button was pushed to turn down the generator. The main switch was turned to "OFF" position.

2. The Digital Multimeter was deactivated.

3. After the fluid temperature was close to room temperature the pump was stopped and cooling water was shut off the heat exchanger.

4. The system was depressurized. All valves were opened except the drainage valves.

Each time the fluid was changed, the fluid flow loop was cleaned with acetone or water. After draining the system, air was blown in the fluid flow loop.

CHAPTER V

ANALYSIS OF DATA

Experimental measurements for the variables needed to evaluate the local heat transfer coefficients for fluid flow in a horizontal test tube were taken using the following working fluids: distilled water, methanol, toluene, 85 wt % ethylene glycol-water, 50 wt % ethylene glycol-water, heavy oil coker, 30 wt % diethanolamine-water and n-octane. A total of 159 runs were made: 6 runs with distilled water; 26 runs with methanol; 24 runs with toluene; 7 runs with 85 wt % ethylene glycol-water; 18 runs with 50 wt % ethylene glycol-water; 42 runs with heavy oil coker of which the first 7 runs were dropped out for inconsistency in the heat balance results; 23 runs with 30 wt % diethanolamine-water; and 13 runs with n-octane. The experimental data are presented in Appendix A. Computer programs which were originally written by Farukhi (20) and modified by Moshfeghian (27) were modified and used to reduce the experimental data using the IBM 370/158 computer.

All the variables measured for each experimental run are listed under item 5 of Data Recording Process in Chapter IV. The outside surface temperatures were measured at 16 locations along the length of the test section. Thermocouple locations are given in Table I in Chapter III.

Fluid physical property data were evaluated at the bulk fluid temperature and at the film fluid temperature at each thermocouple location. The viscosity was also evaluated at the inside wall temperature at each thermocouple location and at the average inside wall temperature. The bulk fluid temperature was assumed to increase linearly along the axial length of the test section, starting from the inlet electrode.

Average bulk fluid temperature for the entire test section for each data run was taken to be the arithmetic average of the inlet and outlet bulk fluid temperatures.

Different sets of physical property data, for each of the fluids run, were tested using available literature correlations which predict the local heat transfer coefficient for the flow of a fluid in horizontal tubes. Regression correlations were developed for each set of the experimental physical property data tested. Thermal conductivity and electrical resistivity regression correlations of stainless steel used were developed by Singh (22). Appendix C gives a listing of the regression correlations. The correlations were incorporated into the computer programs used for the data reduction.

Data reduction consisted of the following steps:

1. Calculation of the percentage error in heat balance.
2. Calculation of the local inside wall temperature and the inside wall radial heat flux.
3. Calculation of the local heat transfer coefficient.
4. Calculation of the relevant dimensionless numbers for each of the different sets of physical property data used.

Details regarding each of the above steps follow.

Calculation of the Percentage Error in Heat Balance

Heat losses were important in so far as they affected the calculations of the local bulk temperature and the local heat input. The percentage error in the heat balance for each data run was calculated as follows:

$$\dot{q}_{input} = (V)(I) - \dot{q}_{loss} \tag{5.1}$$

where

$\dot{q}_{input}$ = heat input rate, Joules/sec

V = voltage drop across test section, volts;

I = current in test section, amperes;

$\dot{q}_{loss}$ = heat loss, Joules/sec (calculated from Appendix H).

$$\dot{q}_{output} = (\dot{m})(c_p)[T_{b_{out}} - T_{b_{in}}] \tag{5.2}$$

where

$\dot{q}_{output}$ = heat output rate, Joules/sec;

$\dot{m}$ = mass flow rate of fluid flowing through test section, kg/sec;

c_p = heat capacity of the fluid, Joules/(kg.K);

$(T_b)_i$ = bulk fluid temperature at the test section inlet, K;

$$\text{\% error in heat balance} = \left(\frac{\dot{q}_{input} - \dot{q}_{output}}{\dot{q}_{input}}\right) \times 100 \tag{5.3}$$

The inlet and outlet temperatures were corrected based on the thermocouple calibration procedure given in Appendix B. Typical error in the heat balance is given in Appendix F.

Calculation of the Local Inside Wall Temperature and the Inside Wall Radial Heat Flux

Computer programs originally written by Owhadi (28) and Crain (29) and modified by Farukhi (21) and Moshfeghian (27) were modified to compute the inside wall temperatures from the measured outside wall temperatures after being corrected based on the calibration procedure given in Appendix B. The inside wall temperatures were computed by a trial and error solution. Equations used for the numerical solution of the wall temperature gradient with internal heat generation along with their derivations are presented in Appendix D. The program also computes the inside wall radial heat flux at each thermocouple location on the test section. Details regarding the computer program are given in Moshfeghian's thesis (27).

Calculation of the Local Heat Transfer Coefficient

The local convection heat transfer coefficients were calculated using the inside wall temperature, the rate of heat flow per unit inside surface area and the bulk fluid temperature. That is, in principle:

$$h_i = \frac{(\dot{q}/A)_i}{[(T_w)_i - T_b]} \tag{5.4}$$

where

h_i = local inside heat transfer coefficient, $(J/m^2 \cdot s \cdot K)$;

$(\dot{q}/A)_i$ = local inside wall heat flux, $(J/m^2 \cdot s)$;

$(T_w)_i$ = local inside wall temperature, K;

T_b = bulk fluid temperature at the thermocouple station, K.

Calculation of the Relevant Dimensionless Numbers

Reynolds and Prandtl numbers were calculated at the bulk fluid temperature and average film temperature at each station. The Nusselt number was also calculated for each station using the circumferentially-averaged local heat transfer coefficient at each station. Grashof number was calculated for each station using the circumferentially-averaged inside wall temperature and the bulk fluid temperature at each station. Dimensionless numbers were recalculated whenever a new set of physical property data was tested. For the thermally developing runs a dimensionless axial distance was introduced. The definitions of the dimensionless numbers evaluated are given in Table III.

All the experimental data gathered were reduced using the above procedures. Sample calculations for one data run are given in Appendix F.

The inside wall heat transfer coefficients were calculated for each thermocouple location along the test section and were digitally plotted for the four thermocouple locations on the tube periphery for each data run.

TABLE III

DEFINITION OF THE DIMENSIONLESS NUMBERS EVALUATED

Dimensionless Number	Symbol	Definition
Reynolds	Re	$\frac{(d_i)(G)}{\mu}$ where $G = \frac{\dot{m}}{\frac{\pi}{4}(d_i)^2}$
Prandtl	Pr	$\frac{(C_p)(\mu)}{k}$
Nusselt	Nu	$\frac{(d_i)^3(\rho)^2(g)(\beta)(\bar{T}_w - T_b)}{\mu^2}$
Dimensionless Axial Distance	X*	$\frac{\pi}{4\ (GZ)}$
Graetz	GZ	$(Re)(Pr)(\frac{d_i}{L})$

CHAPTER VI

EXPERIMENTAL RESULTS AND DISCUSSION

Experimental data were gathered for Reynolds numbers ranging from 52 to 60,500 and Prandtl numbers ranging from 5.3 to 1,570 in a straight horizontal (0.5 in.) o.d. x (0.035 in.) wall thickness test section. The test fluids were distilled water, toluene, methanol, 85 wt % ethylene glycol-water, 50 wt % ethylene glycol-water, heavy premium coker, 30 wt % diethanolamine-water and n-octane. All the experimental runs were conducted under approximately constant wall heat flux conditions. Results of this study together with a discussion of the results are presented in this chapter.

Correlations Used to Predict the Turbulent Heat Transfer for Constant and Variable Property Fluids

Many correlations exist for predicting the heat transfer coefficient in the turbulent flow regime. To compare the experimental heat transfer coefficient at each station along the test section, an arbitrary choice of the following equations was made because of their wide usage in heat transfer calculations, mainly for industrial applications.

Sieder-Tate(1); Re > 2100

$$Nu = 0.023\ Re_b^{0.8}\ Pr_b^{1/3}\ (\mu_b/\mu_w)^{0.14} \qquad (6.1)$$

where the subscripts b and w indicate that the relevant physical properties are evaluated at the bulk and wall temperatures respectively.

Equation (6.1) is intended to apply only to fully developed coefficients and to variable property fluids (high heating rates). Moshfeghian (23) reported a mean absolute deviation for equation (6.1) of 10% (water and Re > 10,000). Sleicher and Rouse (30) reported an average deviation of 23% for equation (6.1) for data with μ_b/μ_w ranging from 1.43 to 2.88.

Dittus-Boelter (2); Re > 2100

$$Nu = 0.023\ Re^{0.8}\ Pr^{0.4} \tag{6.2}$$

Moshfeghian (23) reported a root-mean-square error for Equation (6.2) of 16.66% (3.16 < Pr < 10 and 10,000 < Re < 32,000).

Sleicher and Rouse (30) reported an average deviation for the constant property data of 40% for Equation (6.2) at intermediate Prandtl numbers and high Reynolds number.

Most of the heat-transfer coefficients upon which Equation (6.2) was based and all the coefficients upon which Equation (6.1) was based are coefficients that are averages over the length of an exchanger.

Petukhov Correlation

$$Nu = \frac{RePr(f/8)}{1.07+12.7(Pr^{2/3}-1)\sqrt{f/8}} \tag{6.3}$$

for

$0.5 < Pr < 2000$;

and

$10^4 < Re < 5 \times 10^6$

where

$$f = (1.82 \log Re - 1.64)^{-2}$$

The heat transfer coefficients upon which Equation (6.3) was based are point (or local) coefficients. Petukhov recommends a Seider-Tate type correction $(\mu_b/\mu_w)^{0.11}$ to Equation (6.3) for variable property fluids

Eagle-Ferguson (31) (for water only); Re ≥ 2100

$$h = c\ (1.75\ T_b + 160)\ V^{0.80} \tag{6.4a}$$

where

$$c = 0.9109 - 0.4292 \log (d_i). \tag{6.4b}$$

Appendix G presents the comparison between the experimental and predicted heat transfer coefficient at each station along the test section for the experimental runs.

Laminar Flow Regime Correlations

A limited number of correlations exist that adequately predict the laminar flow heat transfer coefficient. The Morcos-Bergles correlation (4) was used because it takes into account the effect of natural convection in the laminar flow region.

$$Nu = \left\{ (4.63)^2 + \left[0.055 \left(\frac{Gr\ Pr^{1.35}}{P_w^{0.25}} \right)^{0.4} \right]^2 \right\}^{\frac{1}{2}} \tag{6.5}$$

for

$$Re < 1200;$$

$$3 \times 10^4 < Ra < 10^6;$$

$$4 < Pr < 175;$$

and

$$2 < P_w < 66$$

where

$$P_w = \frac{h\, d_i^2}{K_w\, I}$$

t = tube wall thickness; and

K_w = thermal conductivity of tube wall.

Thermal Entrance Correlations

The peripheral average heat transfer coefficient at each thermocouple station along the test section was compared with the following equations developed by Shah (5), Grigull and Tratz (6), and Churchill and Ozoe (7) for the thermal entrance region. The approximate equations (6.6) and (6.7) are recommended by Shah (5) and Equation (6.8) by Grigull and Tratz (6) for the range of X^* indicated:

$$Nu = \begin{cases} 1.302(X^*)^{-\frac{1}{3}} - 1 & \text{for } X^* \leq 0.00005 \quad (6.6) \\ 1.302(X^*)^{-\frac{1}{3}} - 0.5 & 0.00005 \leq X^* \leq 0.0015 \quad (6.7) \\ 4.364 + 8.68(10^3 X^*)^{-0.506}\, e^{-41X^*} & \text{for } X^* \geq 0.0015 \quad (6.8) \end{cases}$$

The dimensionless distance X^* in the flow direction for thermal entrance region heat transfer is specified for a circular tube as

$$X^* = \pi/(4GZ) \qquad (6.9)$$

where GZ is the Graetz number defined in Table III.

Churchill and Ozoe (7) proposed the following single relation for the entire range of X^*.

$$\frac{Nu + 1}{5.364} = \left[1 + \frac{220}{\pi} X^* \right]^{-\frac{10}{9}}^{\frac{3}{10}} \qquad (6.10)$$

Impact of Data Uncertainties on the Heat Transfer Coefficient

A sensitivity analysis was undertaken to study the influence of data on the heat transfer coefficient calculated from the Sieder-Tate, Dittus-Boelter, and Petukhov equations. The specific physical properties considered are viscosity, heat capacity, thermal conductivity and density. Large errors can occur in experimental values of physical properties data, not to mention the wide variations in value for specific physical properties predicted by different correlations available in the literature. Errors in density measurements not only have a direct effect on the prediction of the heat transfer coefficient but also have an effect on viscosity, which normally is measured as kinematic viscosity and then changed to absolute viscosity by the use of liquid densities. The same is true for heat capacity, where an error in heat capacity will cause an error of the same magnitude in heat balances.

Uncertainties exist and are still to be found in the subject of liquid thermal conductivities. Ziebland (50) suggested that toluene might serve as a thermal conductivity standard. Touloukian (37) indicated that further papers containing data greater by 5 percent on the thermal conductivity of toluene have appeared since Ziebland proposed his equation.

The effect of specific data errors on the Sieder-Tate, Dittus-Boelter, and Petukhov heat transfer coefficients are presented in Figures 4 to 8.

Figure 4 shows the effect of errors in thermal conductivity on the predicted heat transfer coefficients. The errors created in the three equations are essentially linear. A positive error of 50% in thermal conductivity gives respectively errors of 37%, 33%, and 32% in Sieder-Tate, Dittus-Boelter, and Petukhov coefficients, while a negative error of 50% results in a 31% error in Sieder-Tate coefficient, 26.5% error in Dittus-Boelter coefficient, and 31% in Petukhov coefficient.

Figure 5 shows the effects of viscosity errors on the heat transfer coefficient. A 50% smaller than actual viscosity, yields approximately 38% error in Sieder-Tate coefficient, 35% error in Petukhov coefficient, and 32% error in Dittus-Boelter coefficient, while a 50% greater liquid viscosity will give approximately 15% error in Dittus-Boelter coefficient, 16.5% error in Petukhov coefficient, and 17% error in Sieder-Tate coefficient.

Figure 6 shows the effect of liquid density on the calculated heat transfer coefficient. 50% error in density results in a heat transfer coefficient 38-42% too large or too small.

Figure 7 shows the effect of heat capacity errors on heat transfer coefficient. A 50% error in heat capacity results in a heat transfer coefficient 11-24% too large or too small. A 50% error in heat capacity will also cause an equal size error in the heat balance.

Figure 8 shows the effect of cumulative errors in physical properties on the heat transfer coefficient. If errors are to add in the

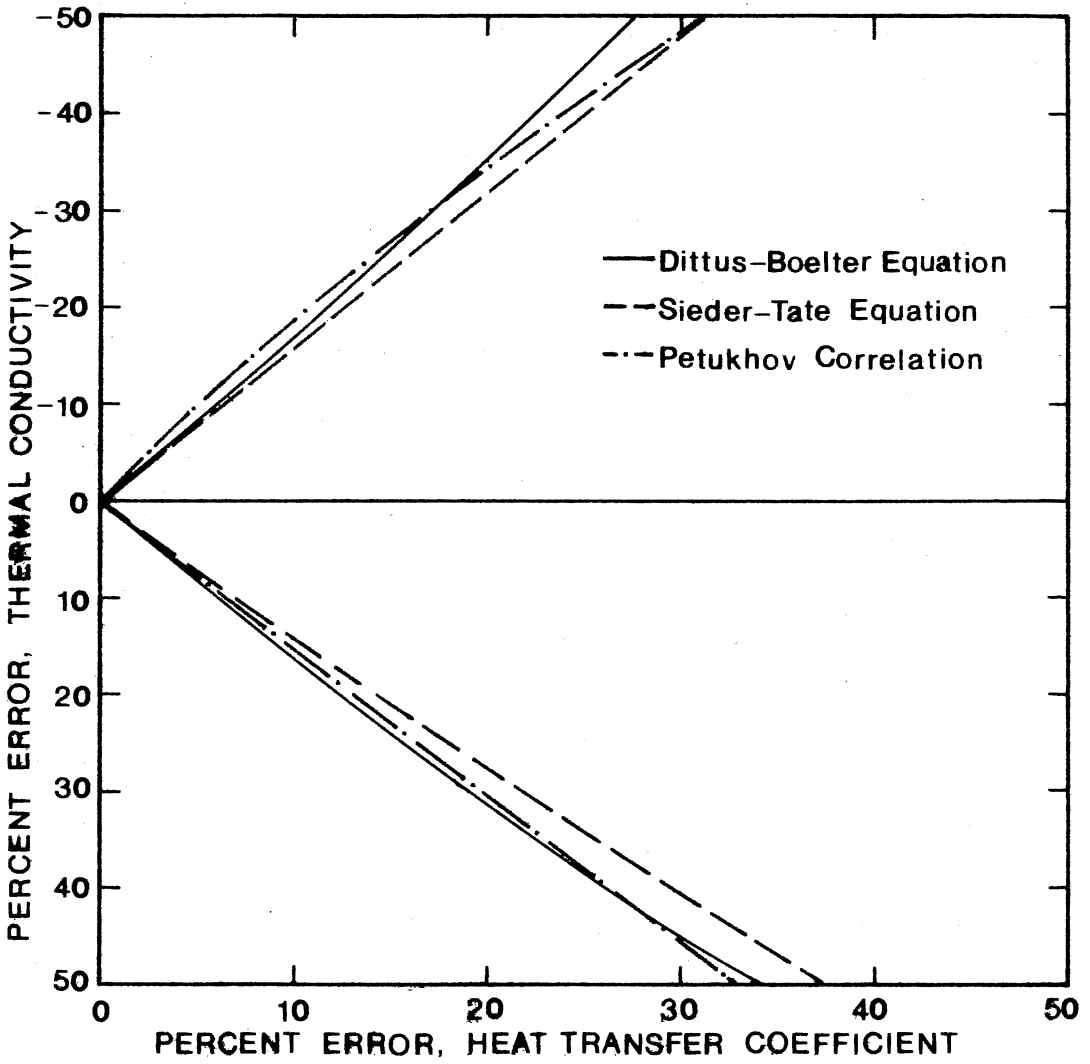

Figure 4. Influence of Thermal Conductivity Error on Heat Transfer Coefficient

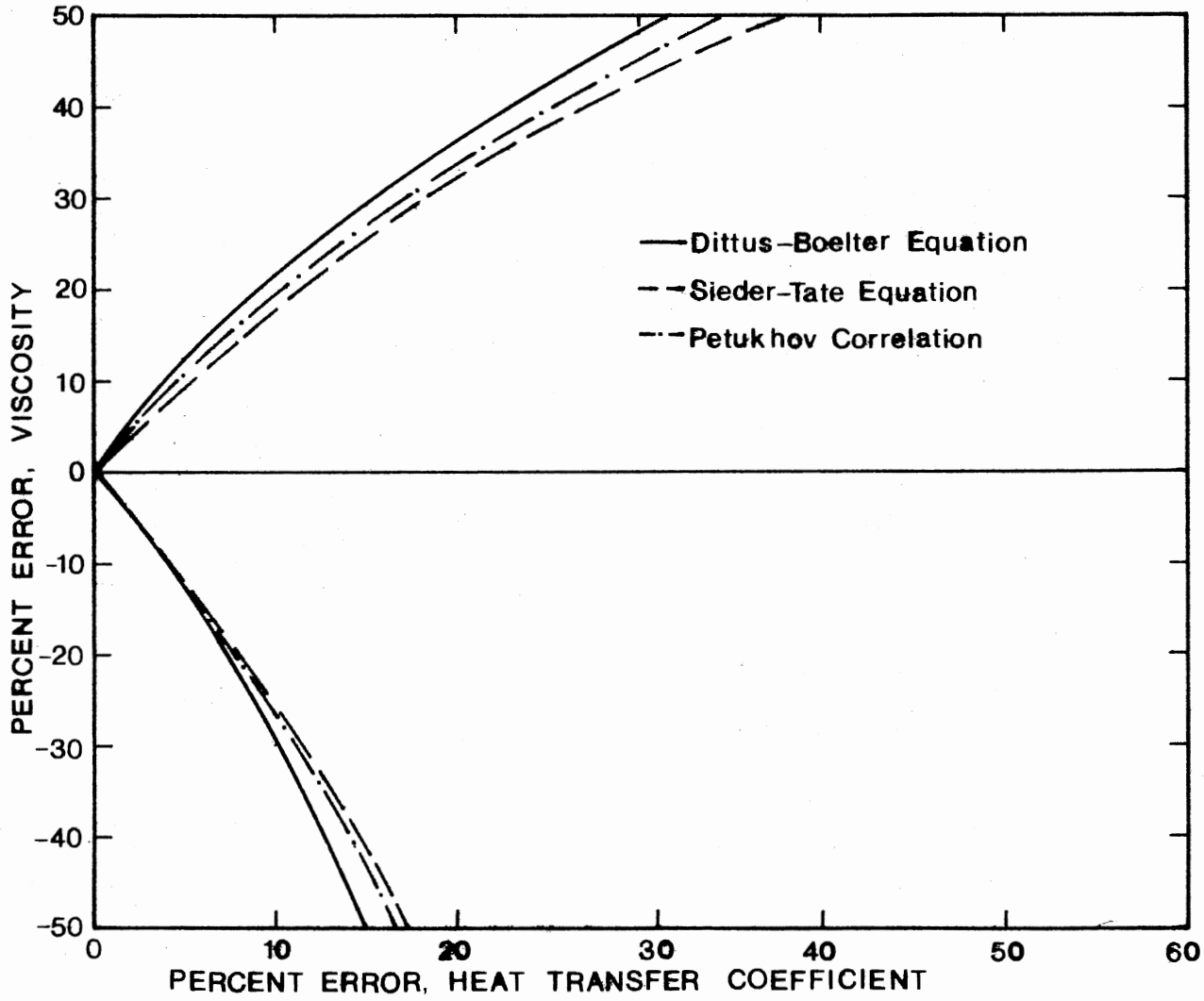

Figure 5. Influence of Viscosity Error on Heat Transfer Coefficient

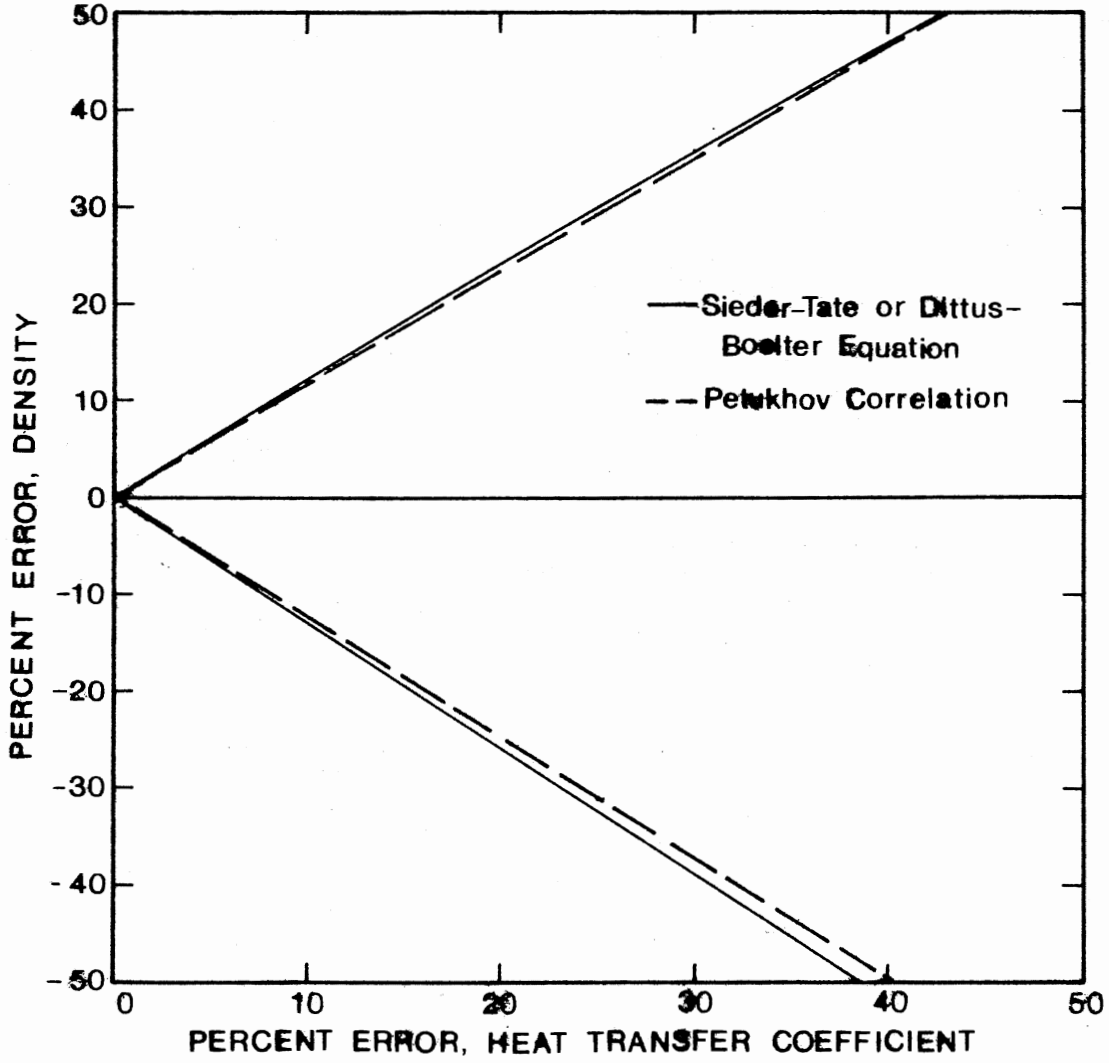

Figure 6. Influence of Density Error on Heat Transfer Coefficient

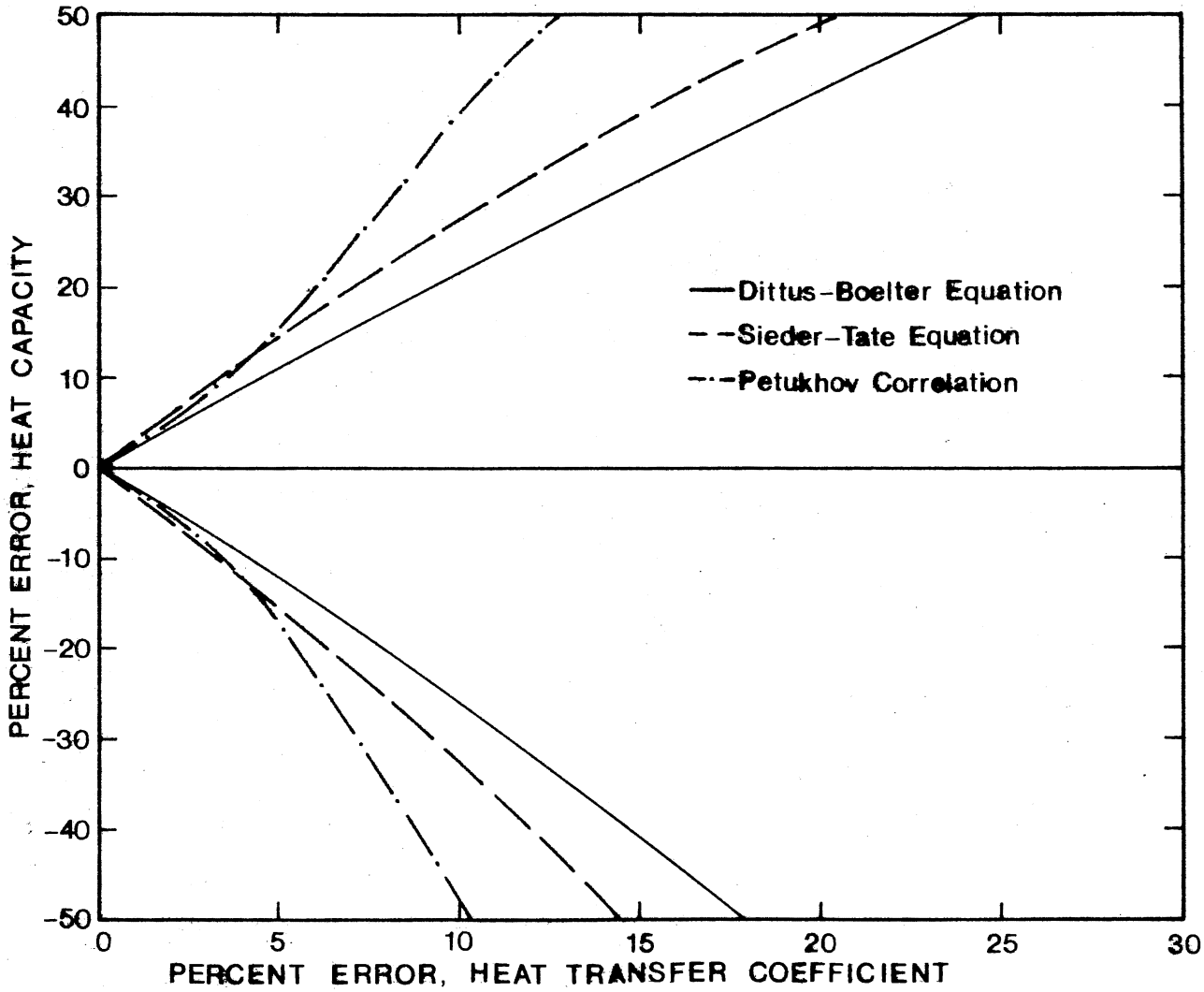

Figure 7. Influence of Heat Capacity Error on Heat Transfer Coefficient

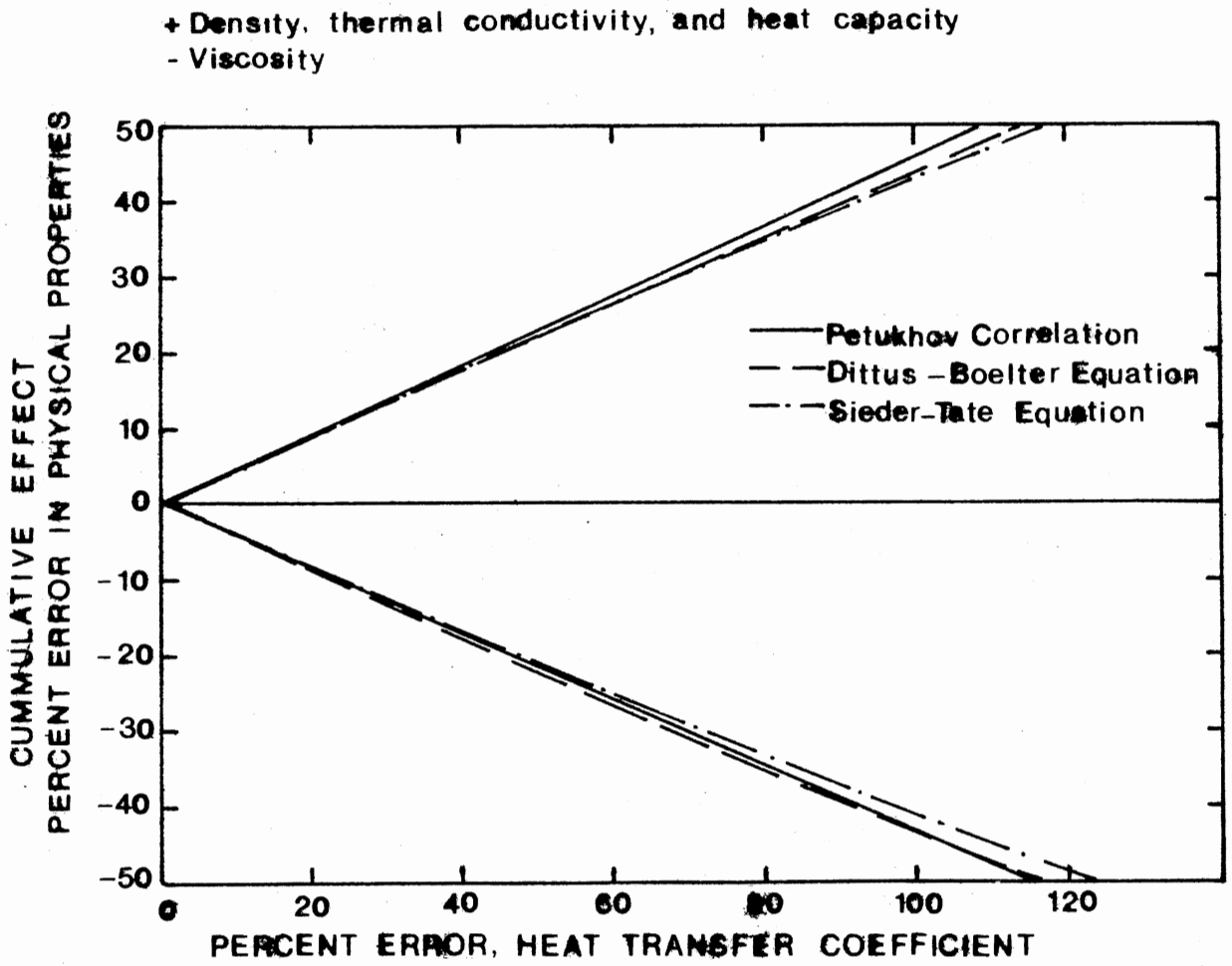

Figure 8. Effect of Cummulative Error in Density, Thermal Conductivity, Heat Capacity and Viscosity on Heat Transfer Coefficients

same direction, then a 30% accumulative change in physical properties would result in a heat transfer coefficient 65% too large or 70% too small.

Calculation of Heat Transfer Coefficients from Experimental Data

Values of the Reynolds and Prandtl numbers, average values of the heat flux and the heat transfer coefficient for the inside wall were computed for each thermocouple location along the test section for each data run. These values are summarized in Appendix G for all the experimental data runs used in the discussion.

The average heat transfer coefficient at each of the four thermocouple stations along the test section was defined as follows:

$$H_1 = \begin{matrix}\text{average heat} \\ \text{transfer coefficient}\end{matrix} = \frac{1}{4} \sum_{i=1}^{4} \left[\frac{(\dot{q}/A)_i}{(T_w)_i - T_b} \right] \qquad (6.11)$$

where i indicates the peripheral location on the tube cross section at a thermocouple location. The average heat transfer coefficient obtained from Equation (6.11) was then used to determine the average Nusselt number for the thermocouple station. The different sets of physical properties of the fluid used in determination of the Reynolds, Prandtl and Nusselt numbers were evaluated at the bulk fluid temperature at the thermocouple station, T_b, calculated by a heat balance based upon the inlet and outlet bulk fluid temperatures and the heat input.

In addition to Equation (6.11) the average heat transfer coefficient at a thermocouple station was also computed as follows:

$$H_2 = \begin{matrix}\text{average heat} \\ \text{transfer coefficient}\end{matrix} = \frac{(\bar{\dot{q}}/A)}{\bar{T}_w - T_b} \qquad (6.12)$$

where i indicates the peripheral location on the tube cross section at a given thermocouple station. In Appendix G, H_1 and H_2 represent the average heat transfer coefficient using Equations (6.11) and (6.12) respectively. For the runs in the turbulent flow region where the peripheral distribution of inside wall temperatures is uniform, H_1 and H_2 become equal; however, for a nonuniform distribution of inside wall temperatures H_1 becomes larger than H_2.

The peripheral distribution of heat transfer coefficients in the turbulent flow regime is fairly uniform. Natural convection effects are negligible due to the increased mixing of the fluid due to turbulent flow.

Figure 9 presents the peripheral distribution of heat transfer coefficients for Run 612. The average Reynolds number for this run was 22,000, and the average heat flux was 27,800 Btu/hr-ft^2 (87,698 W/m^2).

Physical Property Data Sources

The main literature sources from which physical properties of the test fluids were taken were API (19), TEMA (42), and Gallant (39). The author also had access to proprietary FPRI (35) measured values. Physical property data from the above sources is commonly used in engineering calculations. A comparison between the different physical property data sources is presented to exemplify to some extent the wide choice available for a practicing process or design engineer. The wide range of variations found between these sources is typical of other physical property data obtained from literature sources. Unless otherwise mentioned, all of the physical property data equations

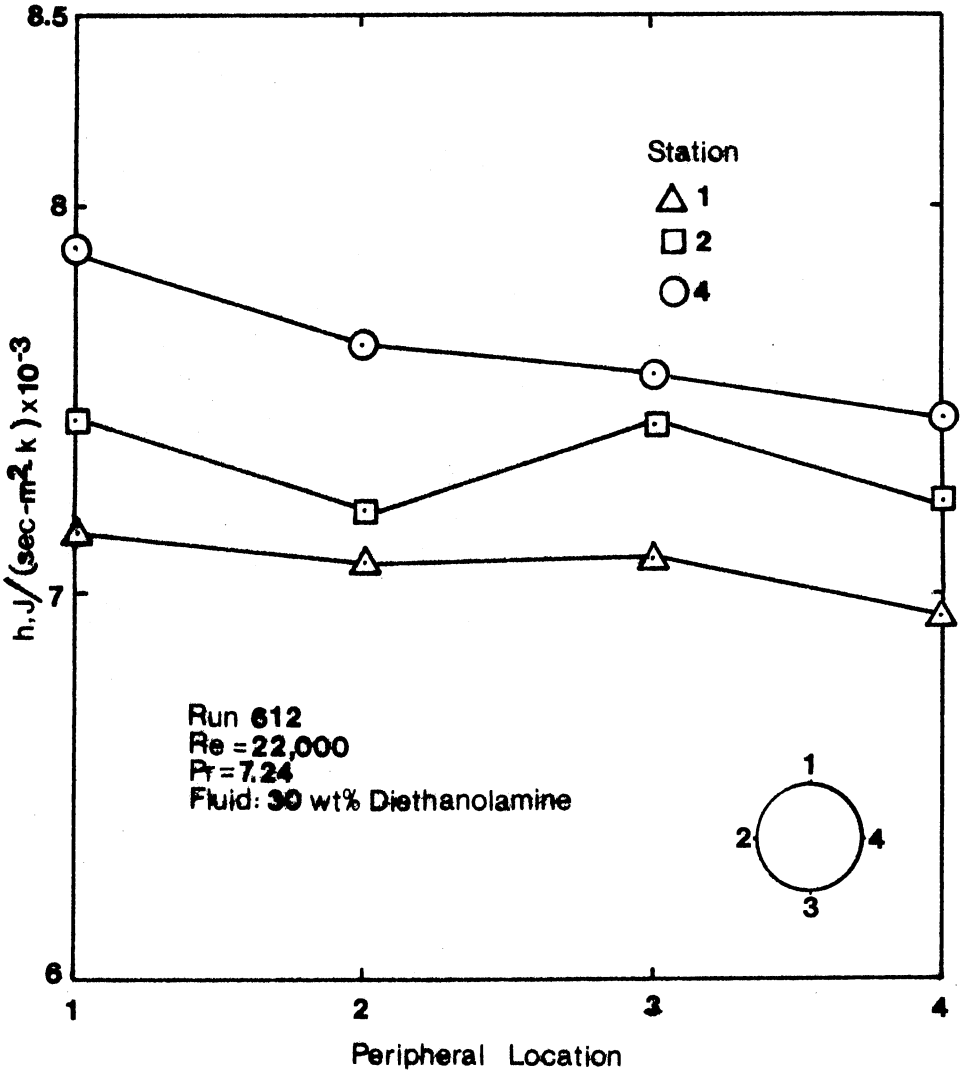

Figure 9. Peripheral Distribution of Heat Transfer Coefficients

are developed based on experimental data reported in literature or from proprietary sources.

Figure 10 shows that the Smith (34) equation predicts a 24.6% higher thermal conductivity value for toluene than the prediction of the FPRI (35) equation.

Figure 11 shows the scatter in thermal conductivity data of methanol. Yaws (36) equation predicts a thermal conducitvity value at 365 K of 0.1652 J/m.S.K compared to a value of 0.2035 predicted by Touloukian (37). This represents an uncertainty of 18.8% in the experimental value of thermal conductivity.

Errors in liquid heat capacity data will cause equal size errors in heat balance calculations. The degree of confidence in the measurable data depends on the expenditure of care and the refinement of technique used. Large errors in heat capacity predictions can occur if a situation such as shown in Table IV is encountered, where a correlation or predictive technique is used outside the range of its application. The Tyagi (38) procedure for estimating the heat capacity of organic liquids is compared with experimental heat capacity values for methanol and toluene taken from Gallant (39), Touloukian (40) and Pachaiyappan (41). The Tyagi procedure works satisfactorily in estimating heat capacity for toluene, but gives errors as high as 60% for methanol.

Physical properties measurements for the oil sample were made in the FPRI Laboratories over a temperature range of 100-500^{o}F. Density estimates by the API recommended procedure (19) fall 5-10% below FPRI values. No comparison was made with TEMA (42) because the density was beyond the range of the TEMA charts.

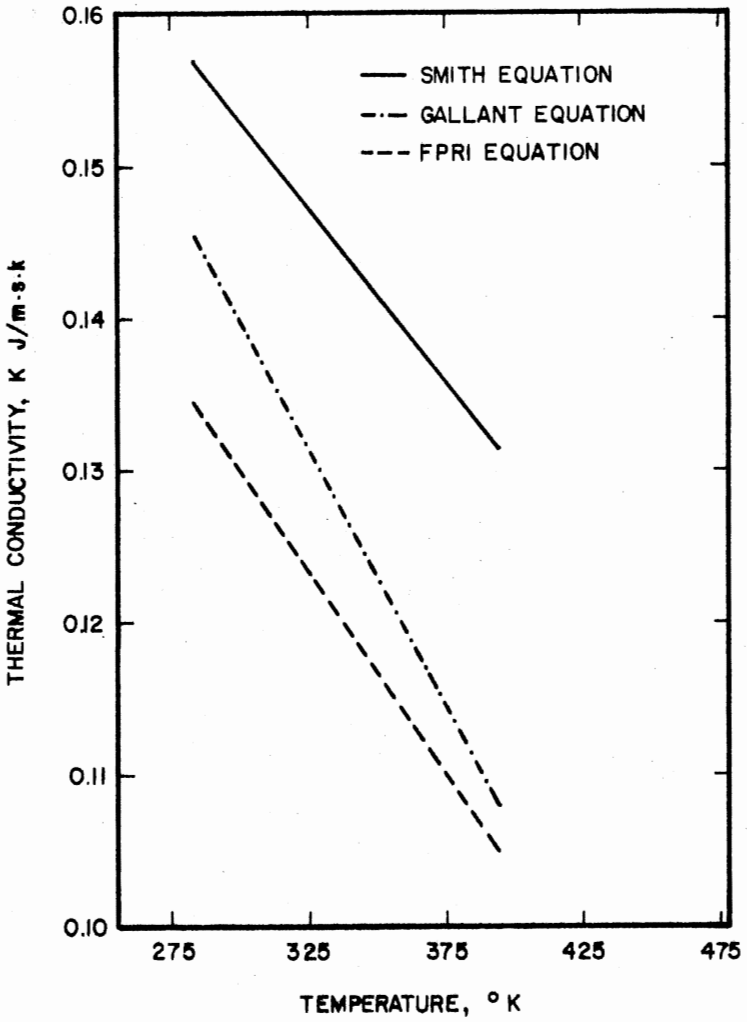

Figure 10. Liquid Thermal Conductivity of Toluene

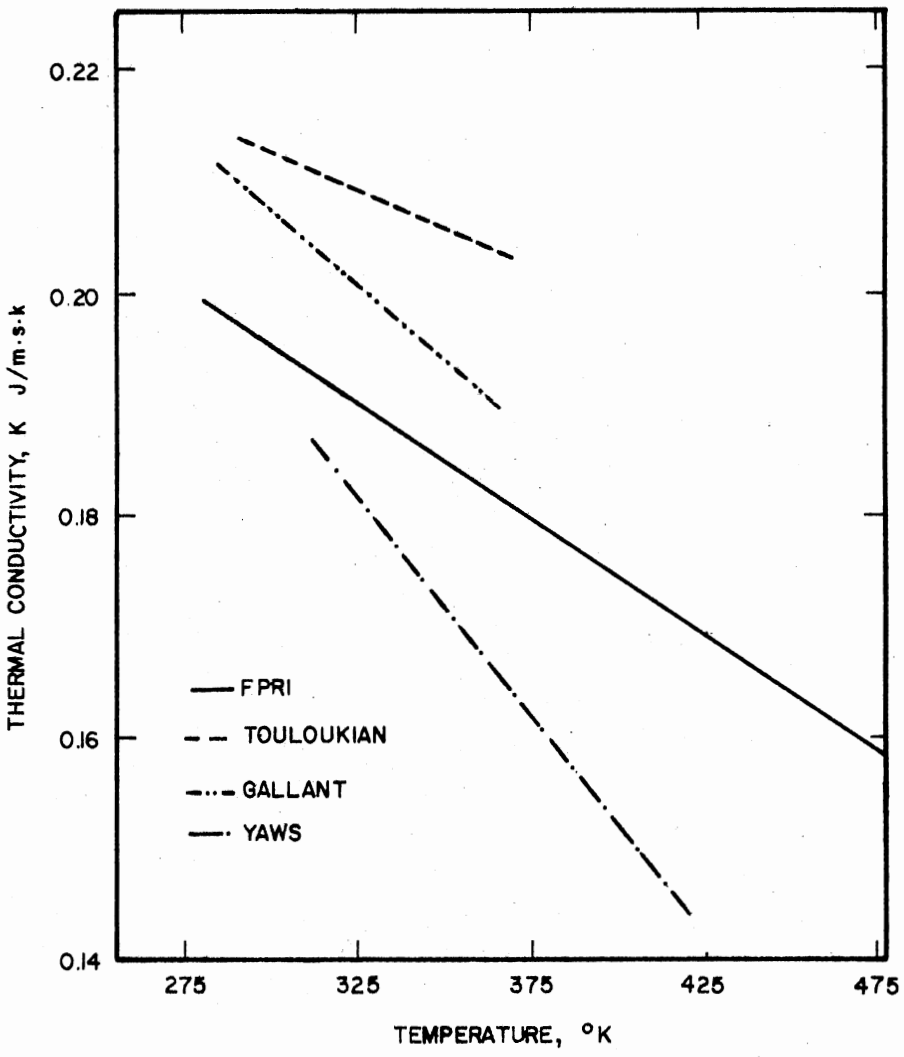

Figure 11. Liquid Thermal Conductivity of Methanol

TABLE IV

COMPARISON BETWEEN EXPERIMENTAL AND CALCULATED HEAT CAPACITIES FOR METHANOL AND TOLUENE
(Values in Cal/gm^{o}C)

Compound	Temperature ^{o}F	Experimental Value	Method 1 (38)	% Error[a]
Toluene[b]	80	0.4114	0.4142	- 0.68
	120	0.4291	0.4323	- 0.76
	200	0.4655	0.4683	- 0.60
	280	0.5000	0.5066	- 1.31
Methanol[c]	104	0.6010	0.9884	-64.50
	176	0.7700	1.0337	-34.25
	248	0.9075	1.1060	-21.87

[a] % Error = [Experimental Value-Literature Value/Experimental Value] x 100

[b] Experimental Value from Gallant

[c] Experimental Value from Pachaiyappan

FPRI thermal conductivity measurements for the heavy premium coker sample were compared with API (19) and TEMA (42) values. Thermal conductivity estimates by TEMA fall 3-14% below FPRI values, while API thermal conductivity values were 9-11% below FPRI values. TEMA (42) heat capacity estimates were up to 11.2% above FPRI values. Heat capacity estimates by the API recommended procedure fall up to 13% below FPRI values.

Kinematic viscosity estimates by the API recommended procedure were transformed to absolute viscosity using the API density equation which was based on density estimates which fall up to 10% below FPRI values. There were wide variations between the estimated absolute viscosity values and FPRI experimental data.

Figures 12 and 13 show a comparison of calculated mixture density using mole fraction and weight fraction averages of pure components with experimental data from FPRI (35), Dow (43) and Gallant. Figure 13 shows that Gallant density data for glycol mixtures compares favorably with the values computed by using the weight fraction average of pure components. Figure 12 shows that Dow's data extrapolated above 350 K deviate considerably from FPRI density measurements. The deviations increase with increasing temperature.

Figure 14 shows a comparison of Gallant (39) and Dow (43) specific heat data for the 85 wt % ethylene glycol mixture. Specific heat data computed using a weight fraction average compares favorably with Gallant data. Values computed using a mole fraction average over predict Dow data by up to 13%.

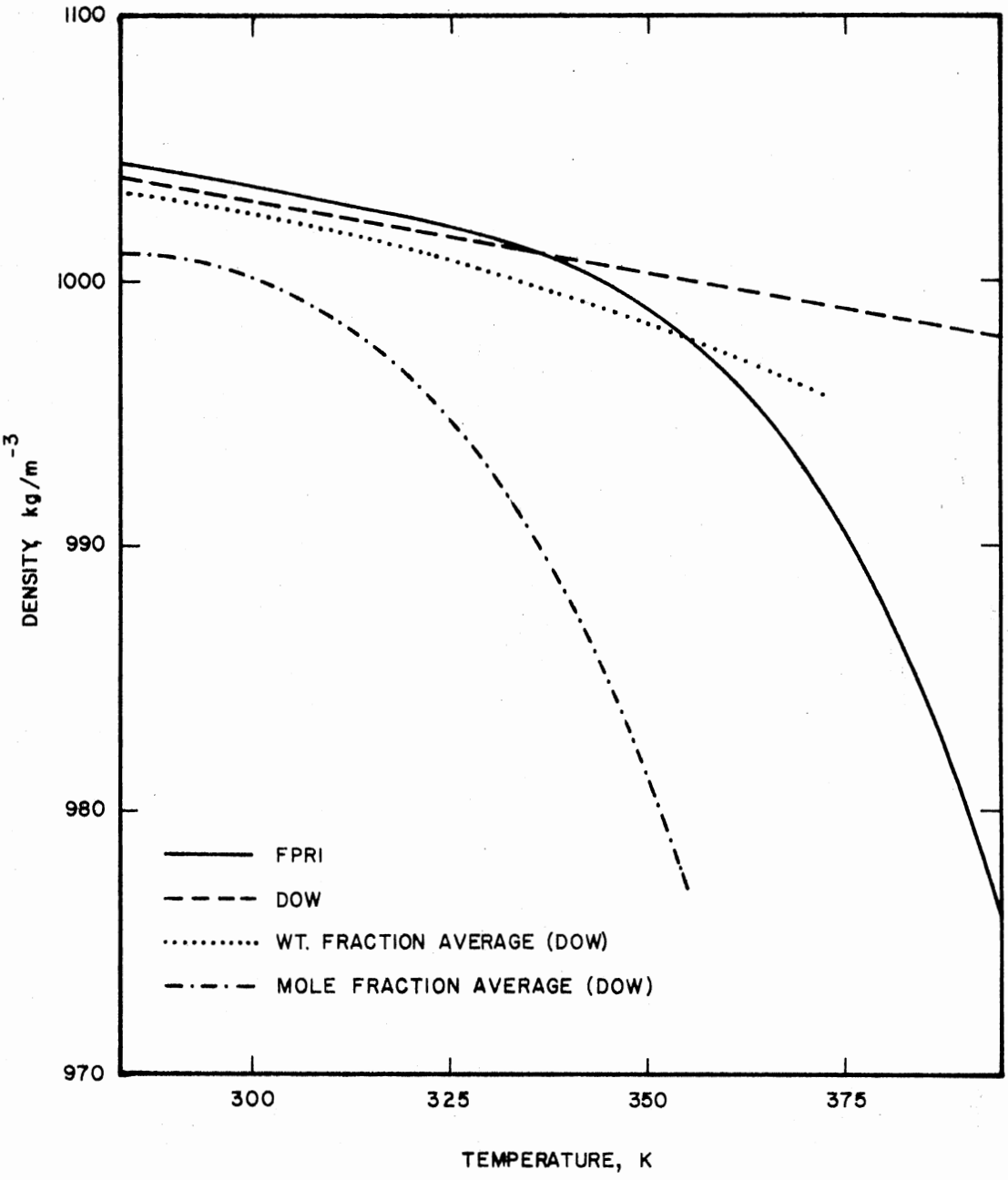

Figure 12. Density of 30 wt % Diethanolamine-Water Solution

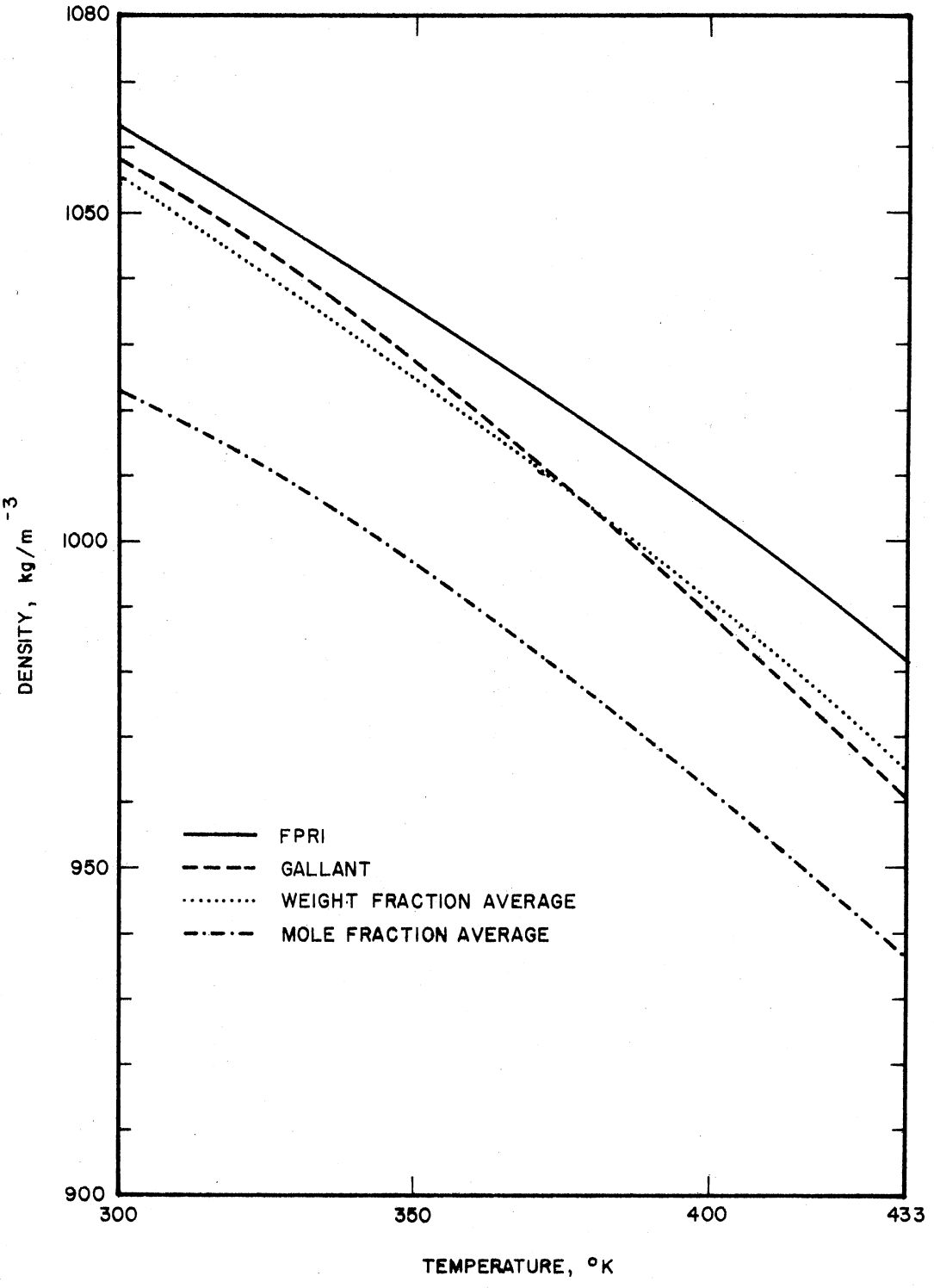

Figure 13. Density of 50 wt % Ethylene Glycol-Water Solution

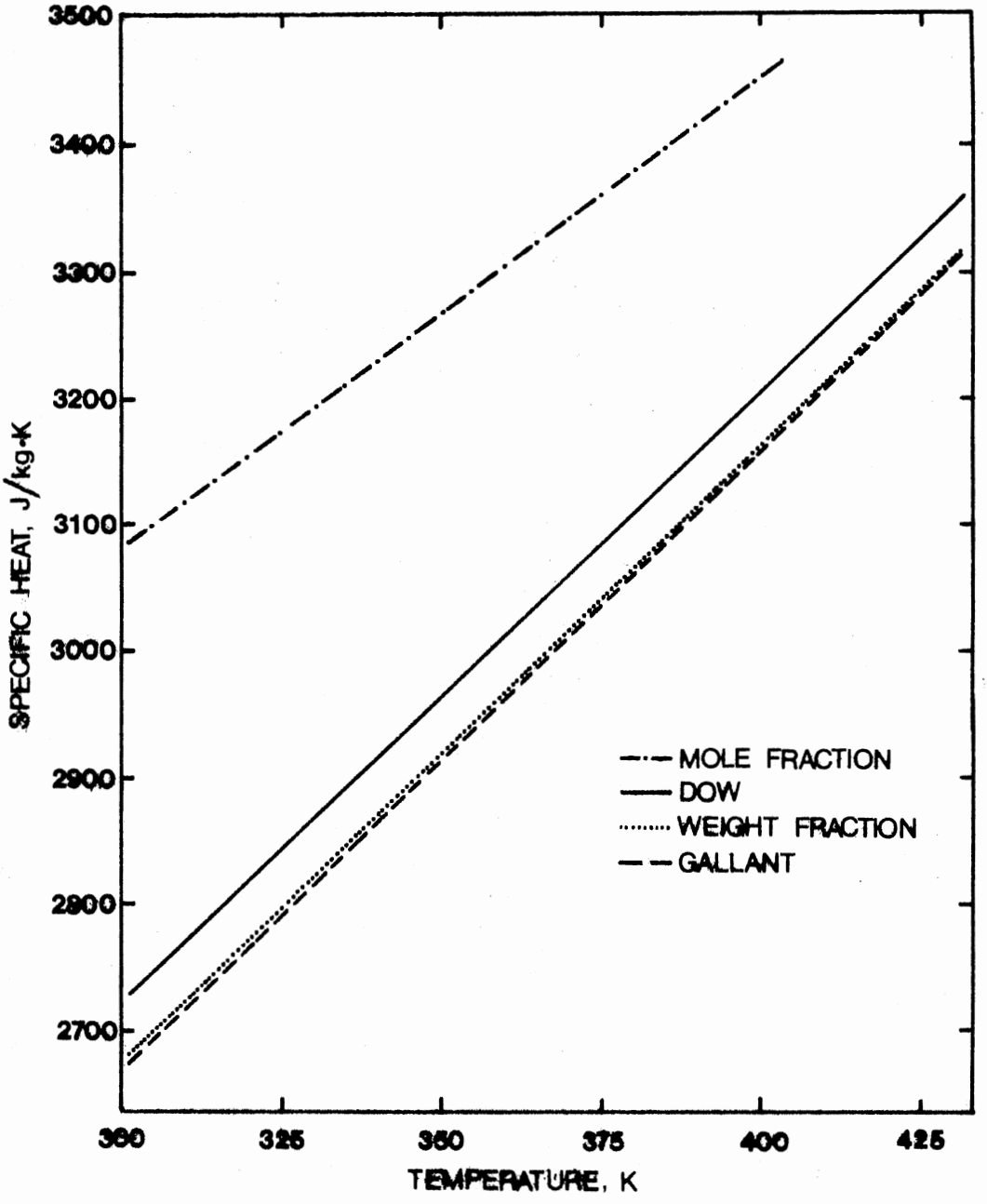

Figure 14. Specific Heat of 85 wt % Ethylene Glycol-Water Solution

Figure 15 shows viscosity data from FPRI (36) and Dow (43) for the 30 wt % diethanolamine-water solution. There is considerable variation in the mixture property data depending on whether a mole fraction average or a weight fraction average of the pure components is used.

Figure 16 shows that there is considerable disagreement between Gallant (39) and ESDU (44) experimental thermal conductivity data on ethylene glycol mixtures. Values computed by using a mole fraction/ weight fraction average of the pure components over predict the thermal conductivity data by up to 90%.

Comparisons of Experimental Data for Pure Components

The average heat transfer coefficient at each of the four thermocouple stations along the test section was calculated according to Equations (6.11) and (6.12) for all the test fluids. Preliminary measurements with distilled water were taken to check the performance of the experimental system. Correlations developed to compute the physical properties of water are given in Appendix C. Runs were taken for a Reynolds number range of 11,800 to 23,100 and Prandtl numbers of 2.54 to 5.11.

Table V presents the average absolute percent deviation (AAPD) for all water runs. The Eagle-Ferguson equation shows a 2.1% average deviation with a 9.0% maximum deviation. The average absolute percent deviation for the Sieder-Tate equation is 8.1 with a maximum deviation of 11.1%. The results for the distilled water system are within the reported accuracy of the literature equations and are in agreement with Malina and Aparrow (32) and Allen and Eckert (33) results.

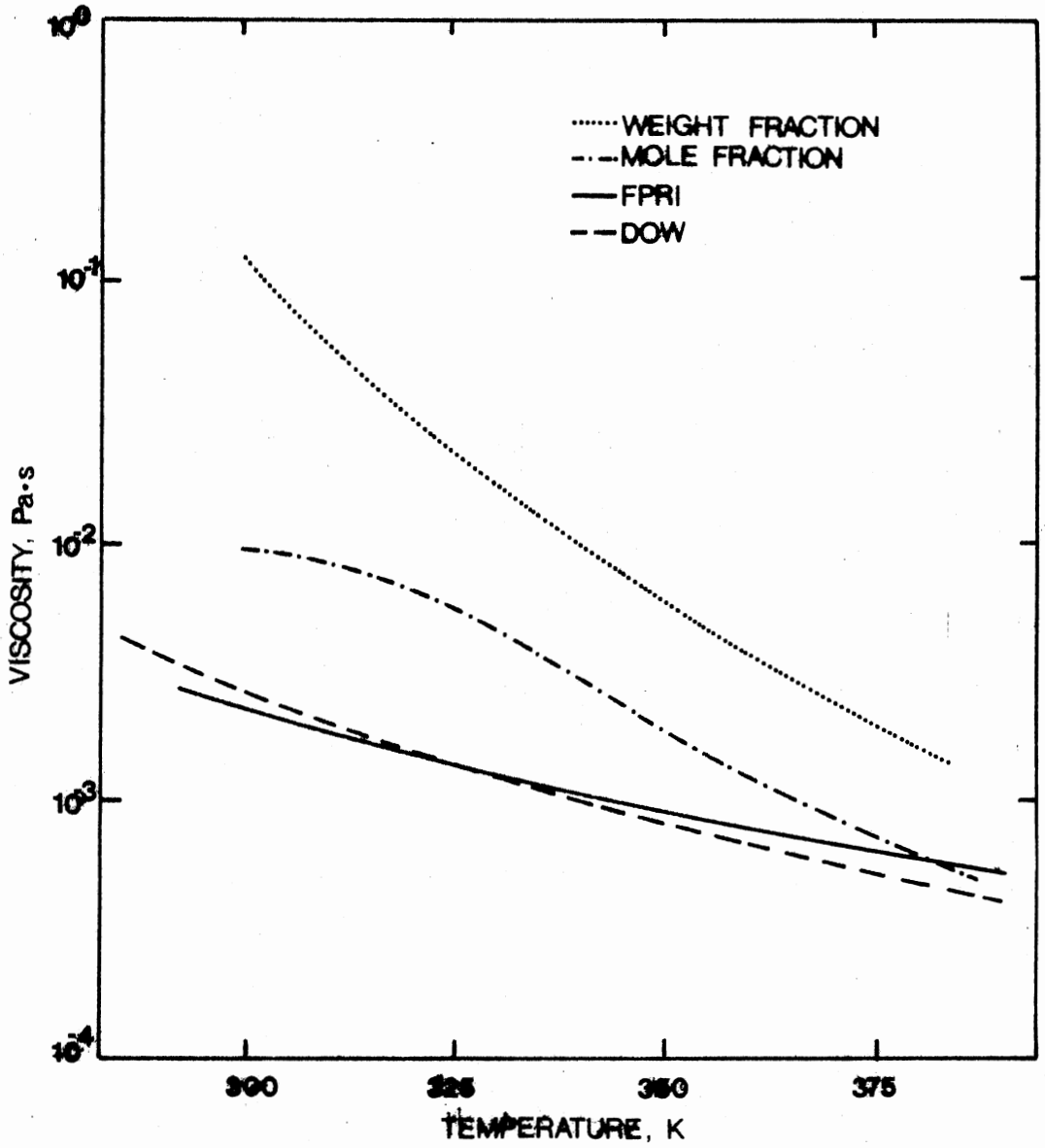

Figure 15. Viscosity of 30 wt % Diethanolamine-Water Solution

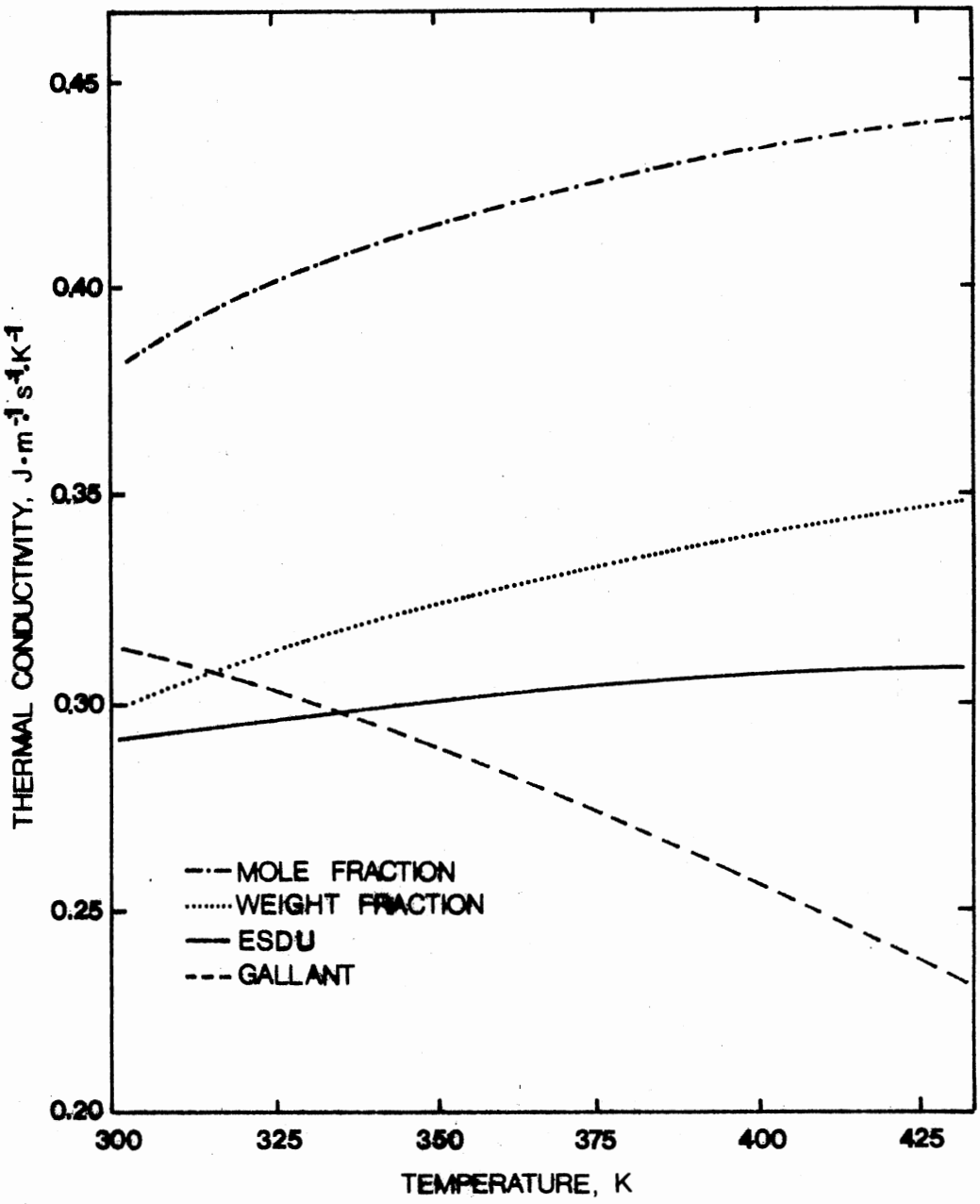

Figure 16. Thermal Conductivity of 85 wt % Ethylene Glycol-Water Solution

TABLE V

DISTILLED WATER EXPERIMENTAL RESULTS COMPARED WITH LITERATURE PREDICTIONS

	Average Absolute Percent Deviation	Max -	Max +
Sieder-Tate	8.1	16.7	-
Eagle-Ferguson	2.1	8.3	6.4
Dittus-Boelter	4.8	13.0	-

For methanol and toluene, experimental heat transfer coefficient data in the turbulent flow region were taken in the heat transfer loop used by Moshfeghian (23). The test section was a U-bend with eleven thermocouple stations, each of which had eight thermocouples installed on the outer surface of the test section. Experimental data were taken for stations 9, 10, and 11 and analyzed for station 11. As reported by Moshfeghian (23), the secondary flow effect caused by the U-bend is carried to the straight section downstream of the bend causing higher heat transfer coefficients than those predicted for a straight tube which is not preceded by a 180^{o} bend. At station 11 Moshfeghian (23) reported excellent agreement between the experimental heat transfer coefficient and the predicted heat transfer coefficient due to the decay of the secondary flow effect. Experimental data taken from station 11 were used to compare the effect of specific data errors on Sieder-Tate, Dittus-Boelter and Petukhov heat transfer coefficients.

Figure 17 compares the peripheral average heat transfer coefficient with that predicted from the Dittus-Boelter equation for toluene using FPRI (35) and Smith (34) thermal conductivity data. Using FPRI thermal conductivity data improves the prediction of the heat transfer coefficient by 9%.

Tables VI and VII present a sensitivity analysis using FPRI and Smith thermal conductivity data on the Sieder-Tate, and Petukhov heat transfer coefficients. The AAPD using Smith k-values and the Sieder-Tate equation is 14.9 compared with an AAPD of 3.3 using FPRI data, an improvement of 11.6% in the prediction of the heat transfer coefficient. Using the Petukhov correlation and Smith conductivity data the AAPD is 41.9 compared to an AAPD of 26.8, or 15.1% improvement in the prediction of the heat transfer coefficient.

Table VIII presents the effects of heat capacity errors on heat balances, and on the prediction of the heat transfer coefficient. For run 101 the heat balance error is 80%, while the error in Sieder-Tate coefficient is 78.6%. The error in the Petukhov coefficient is 132.6% . Table IX shows the effect of using improved heat capacity data on the calculations of the heat transfer coefficient. The error in the heat balance is reduced to -4.3%. The error in the Sieder-Tate coefficient is only 7.2%, a 72.4% improvement over the prediction using Tyagi heat capacities.

The effects of cumulative errors in physical properties on the heat transfer coefficient for methanol and toluene systems are studied using data taken from Gallant (39), Touloukian (40), TEMA (42), and FPRI (35). Table X compares the AAPD of the heat transfer coefficient

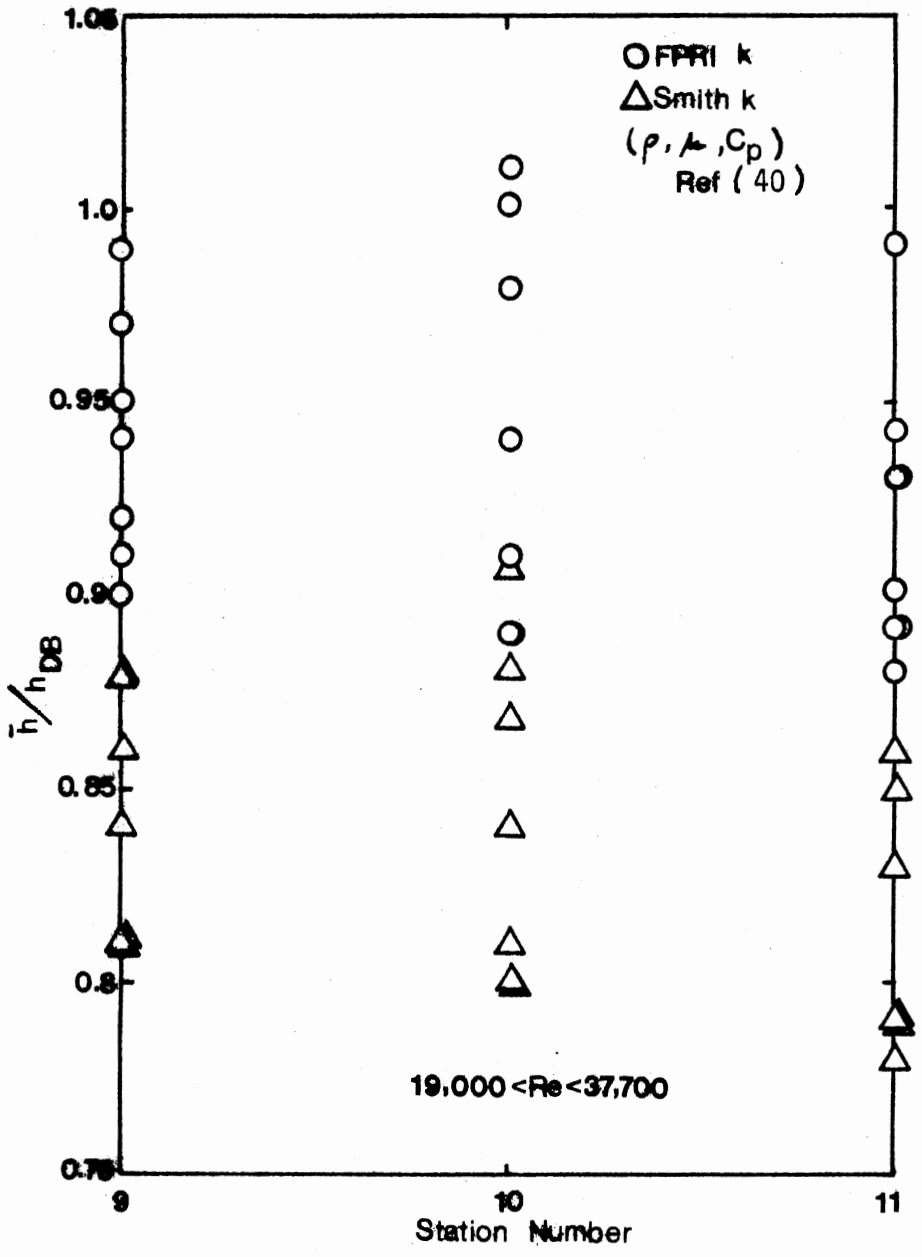

Figure 17. Effect of Improved Thermal Conductivity Data on Dittus-Boelter Heat Transfer Coefficient for Toluene

TABLE VI

EFFECT OF IMPROVED THERMAL CONDUCTIVITY DATA FOR TOLUENE ON COEFFICIENT CALCULATED FROM SIEDER-TATE EQUATION

Run Number	Reynolds Number	FPRI* Deviation %	Smith Deviation %
204	20,900	3.85	12.3
205	22,900	1.01	13.6
206	23,900	1.01	13.6
213	29,500	2.00	16.3
214	30,700	4.00	8.7
217	32,900	9.90	25.0
221	36,600	1.01	14.9

*$\%\ \text{Deviation} = \left(\frac{\text{Experimental Value} - \text{Literature Value}}{\text{Experimental Value}}\right) \times 100$

TABLE VII

EFFECT OF IMPROVED THERMAL CONDUCTIVITY DATA FOR TOLUENE ON COEFFICIENT CALCULATED FROM PETUKHOV'S EQUATION

Run Number	Reynolds Number	FPRI* Deviation %	Smith Deviation %
204	20,900	21.9	40.8
205	22,900	26.5	40.8
206	23,900	26.5	40.8
213	29,500	28.2	42.8
214	30,700	20.5	33.3
217	32,900	27.0	53.8
221	36,600	26.6	40.8

*$\%\ \text{Deviation} = \left(\frac{\text{Experimental Value} - \text{Literature Value}}{\text{Experimental Value}}\right) \times 100$

TABLE VIII

INFLUENCE OF HEAT CAPACITY ERROR ON HEAT BALANCE CALCULATIONS FOR METHANOL

Run Number	Reynolds Number	Heat Balance Error %	Heat Transfer Coefficient Error %		
			h^{*}	h^{**}	h^{***}
101	18,000	-80.2	-78.6	-108.3	-132.6
109	19,700	-74.2	-66.7	- 96.1	-117.4
117	21,100	-75.1	-78.6	-108.3	-132.6
119	23,600	-66.3	-66.7	- 92.3	-117.4
124	28,400	-58.6	-58.7	- 81.8	-104.1

*Evaluated using Sieder-Tate equation and Tyagi heat capacity procedure

**Evaluated using Dittus-Boelter equation and Tyagi heat capacity procedure

***Evaluated using Petukhov correlation and Tyagi heat capacity procedure

TABLE IX

INFLUENCE OF IMPROVED HEAT CAPACITY DATA ON HEAT BALANCE CALCULATIONS FOR METHANOL[a]

Run Number	Heat Balance Error	Heat Transfer Coefficient Error %		
		h^b	h^c	h^d
101	-8.80	-4.2	-19.1	-31.6
109	-5.40	5.7	- 7.5	-19.0
117	-6.10	-6.4	-20.5	-33.3
119	-1.30	-6.6	4.2	16.3
124	.33	+13.0	2.9	7.5

[a]Literature value of physical properties data from Pachaiyappan

[b]Evaluated using Sieder-Tate equation and Pachaiyappan data

[c]Evaluated using Dittus-Boelter equation and Pachaiyappan data

[d]Evaluated using Petukhov correlation and Pachaiyappan data

TABLE X

COMPARISON OF HEAT TRANSFER COEFFICIENTS FOR METHANOL AND TOLUENE RUNS

	Dittus-Boelter								
	FPRI			Gallant			TEMA		
	(Max +)	(AAPD)	(Max-)	(Max +)	(AAPD)	(Max-)	(Max +)	(AAPD)	(Max-)
Toluene	7.4	4.9	13.6	-	11.7	25.0	2.9	11.0	26.6
Methanol	14.5	4.5	17.6	1.0	14.7	26.6	9.0	8.9	22.0
	Petukhov								
	FPRI			Gallant			TEMA		
	(Max +)	(AAPD)	(Max-)	(Max +)	(AAPD)	(Max-)	(Max +)	(AAPD)	(Max-)
Toluene	-	14.7	29.8	-	20.8	38.9	-	20.2	40.8
Methanol	4.8	14.1	31.6	-	22.9	40.8	-	17.8	35.2

predicted using Dittus-Boelter equation and Petukhov correlation with physical properties data taken from FPRI, Gallant, and TEMA. Using FPRI physical properties data improves the prediction of Dittus-Boelter heat transfer coefficient for toluene by 6.8% and that of methanol by 10.2%. The improvement in the prediction of the heat transfer coefficient for toluene using Petukhov correlation is 6.1 and for methanol is 8.8%.

Heat transfer tests were made using a heavy premium coker sample for both the laminar and turbulent regions. Using FPRI and API physical properties data, heat transfer coefficients predicted using Sieder-Tate equation, Dittus-Boelter equation, and Petukhov correlation were compared with experimental data. The average absolute percent deviation ranged from 7.2 using FPRI data and Sieder-Tate equation to 53.8 using API data and Petukhov correlation. The heat transfer coefficients obtained using FPRI data were consistently better than API values. Comparisons are presented as an average absolute percent deviation in Table XI. Using FPRI physical properties data improves the prediction of Petukhov heat transfer coefficient by 33.3%.

N-octane heat transfer runs were taken for Reynolds numbers ranging from 19,800 to 60,500. The Prandtl number range was 6.1-9.0. Physical properties data from Gallant (39), FPRI (35), and TEMA were used to predict the heat transfer coefficients. Table XII shows that the AAPD ranged from 5.8 using Petukhov correlation to 17.6 using Sieder-Tate equation. Heat transfer coefficient predicted using Gallant and TEMA data were in agreement with FPRI predictions. The maximum deviation was less than 2%. The results indicate that n-octane is a well investigated material.

TABLE XI

COMPARISON OF HEAT TRANSFER COEFFICIENTS
FOR HEAVY PREMIUM COKER RUNS

	API			FPRI		
	(Max +)	(Max -)	(AAPD)	(Max +)	(Max -)	(AAPD)
Sieder-Tate	-	35.1	17.7	10.7	13.6	7.4
Dittus-Boelter	-	51.5	31.6	-	33.3	7.5
Petukhov	-	69.5	53.8	-	42.9	20.5

TABLE XII

COMPARISON OF HEAT TRANSFER COEFFICIENTS FOR N-OCTANE RUNS

	Gallant			TEMA			FPRI*		
	(Max +)	(Max -)	(AAPD)	(Max +)	(Max -)	(AAPD)	(Max +)	(Max -)	(AAPD)
Sieder-Tate	20.6	-	16.06	22.5	-	17.55	22.5	-	17.46
Dittus-Boelter	9.91	4.17	5.80	11.5	3.1	7.10	11.5	3.1	6.95
Petukhov	-	16.3	7.57	-	14.9	5.76	-	14.9	6.14

*Heat capacity values from Gallant

Local Heat Transfer Tests for Mixtures

Experiments were performed to determine heat transfer coefficients around the circumference and along the heated length of the test tube for aqueous solutions of 50 and 85 wt % ethylene glycol and 30 wt % diethanolamine (DEA). Mixture physical properties data of aqueous ethylene glycol have been extensively studied due to their application in wet gas treatment.

Tables XIII through XV compare the AAPD of the heat transfer coefficient for the 50 wt % ethylene glycol-water mixture, predicted using Petukhov correlation, Sieder-Tate equation, and Dittus-Boelter equation with physical properties data taken from Dow, Gallant and FPRI. Using FPRI physical properties data improves the prediction of the Petukhov heat transfer coefficient by 22.8% as compared to the heat transfer coefficient obtained using Gallant data. FPRI data improve the prediction of the heat transfer coefficient using Sieder-Tate equation by 36.3% and that using Dittus-Boelter equation by 28.0%.

The observations for the 85 wt % ethylene glycol-water mixture are similar to those of the 50 wt % ethylene glycol-water mixture as seen in Table XVI.

Table XVII shows comparison for 30 wt % diethanolamine-water solution. Mixture data obtained from Dow and computed by a weight/mole fraction average method were used. The comparison shows that the estimated heat transfer coefficient using Dow data is more reliable than that obtained by using the mixing rules (based on mole and weight fraction methods).

TABLE XIII

COMPARISON OF HEAT TRANSFER COEFFICIENTS FOR
50 WT % ETHYLENE GLYCOL-WATER MIXTURE WITH
DITTUS-BOELTER EQUATION

Run No.	Dow	Gallant	FPRI*	Weight Fraction Average
402	16.8	29.0	6.5	54.5
403	17.8	33.0	8.0	51.5
404	18.8	36.0	9.0	49.3
405	24.0	45.5	15.0	57.5
406	26.5	51.3	18.5	63.5
407	22.0	47.8	15.3	58.2

*Thermal conductivity data taken from ESDU

TABLE XIV

COMPARISON OF HEAT TRANSFER COEFFICIENTS FOR 50 WT % ETHYLENE GLYCOL-WATER MIXTURE WITH PETUKHOV CORRELATION

Run No.	Dow	Gallant	FPRI*	Weight Fraction Average
402	5.3	18.0	4.5	40.7
403	5.8	20.8	3.8	36.2
404	6.0	22.5	2.8	34.3
405	11.0	31.5	3.25	42.5
406	13.5	36.5	6.8	47.8
407	9.5	33.3	4.3	39.5

* Thermal conductivity data taken from ESDU

TABLE XV

COMPARISON OF HEAT TRANSFER COEFFICIENTS FOR 50 WT % ETHYLENE GLYCOL-WATER MIXTURE WITH SIEDER-TATE EQUATION

Run No.	Dow	Gallant	FPRI*	Weight Fraction Average
402	33.0	49.8	20.0	77.0
403	33.3	53.3	20.8	71.0
404	32.8	55.5	20.8	67.5
405	33.0	66.3	27.0	77.0
406	39.0	71.0	29.8	80.5
407	32.5	65.0	24.8	68.0

*Thermal conductivity data taken from ESDU

TABLE XVI

COMPARISON OF HEAT TRANSFER COEFFICIENTS FOR 85 WT % ETHYLENE GLYCOL-WATER RUNS

	FPRI			Dow			Gallant		
	(Max +)	(Max -)	(AAPD)	(Max +)	(Max -)	(AAPD)	(Max +)	(Max -)	(AAPD)
Sieder-Tate	25.4	-	20.6	28.1	-	26.7	62.5	-	49.1
Dittus-Boelter	14.6	-	10.4	16.7	-	12.6	40.1	-	29.8
Petukhov	4.8	7.6	5.0	7.4	7.5	8.5	27.0	-	16.8

TABLE XVII

COMPARISON OF HEAT TRANSFER COEFFICIENTS FOR 30 WT % DIETHANOLAMINE-WATER RUNS

	Dow			Weight Fraction Average		
	(Max +)	(Max -)	(AAPD)	(Max +)	(Max -)	(AAPD
Sieder-Tate	82.1	-	20.4	70.2	-	56.2
Dittus-Boelter	16.7	7.5	8.9	51.2	-	40.0
Petukhov	8.3	20.5	6.1	-	69.5	24.0

The results obtained using the mole fraction mixing rule are not reported because the Reynolds number is outside the range of applicability of the correlations. Tables XIII to XV show that heat transfer predictions using the weight fraction average are comparable in magnitude to Gallants predictions.

Thermal Entrance Tests

A brief examination of the thermal entrance region was made with heavy premium coker (oil) system. A series of 18 test runs was taken for Reynolds numbers from 52 to 1860 and Prandtl numbers ranging from 108 to 1570. The peripheral average heat transfer coefficient at each thermocouple station along the test section was calculated using Equations (6.11) and (6.12) and was compared with the equations developed by Shah (5), Grigull and Tartz (6), and Churchill and Ozoe (7) for the thermal entrance problem. The approximate equations (6.6) and (6.7) are recommended by Shah (5) and equation (6.8) by Grigull and Tartz (6) for the range of X^* defined by Equation (6.9).

Figure 18 presents the peripheral distribution of heat transfer coefficient for run 508. The average Reynolds number for this run was 205, the average Prandtl number was 578 and the average heat flux was 3,300 Btu/hr-ft^2 (10,505 W/m^2).

Figure 18 indicates that as the fluid moves along the test section the difference between the heat transfer coefficients at the top and the bottom of the tube increases. This behavior was observed by Moshfeghian (23) and explained by the fact that during heating the fluid near the wall is warmer and, therefore, the heavier fluid near the center of the tube flows downward. The effect of this natural convection

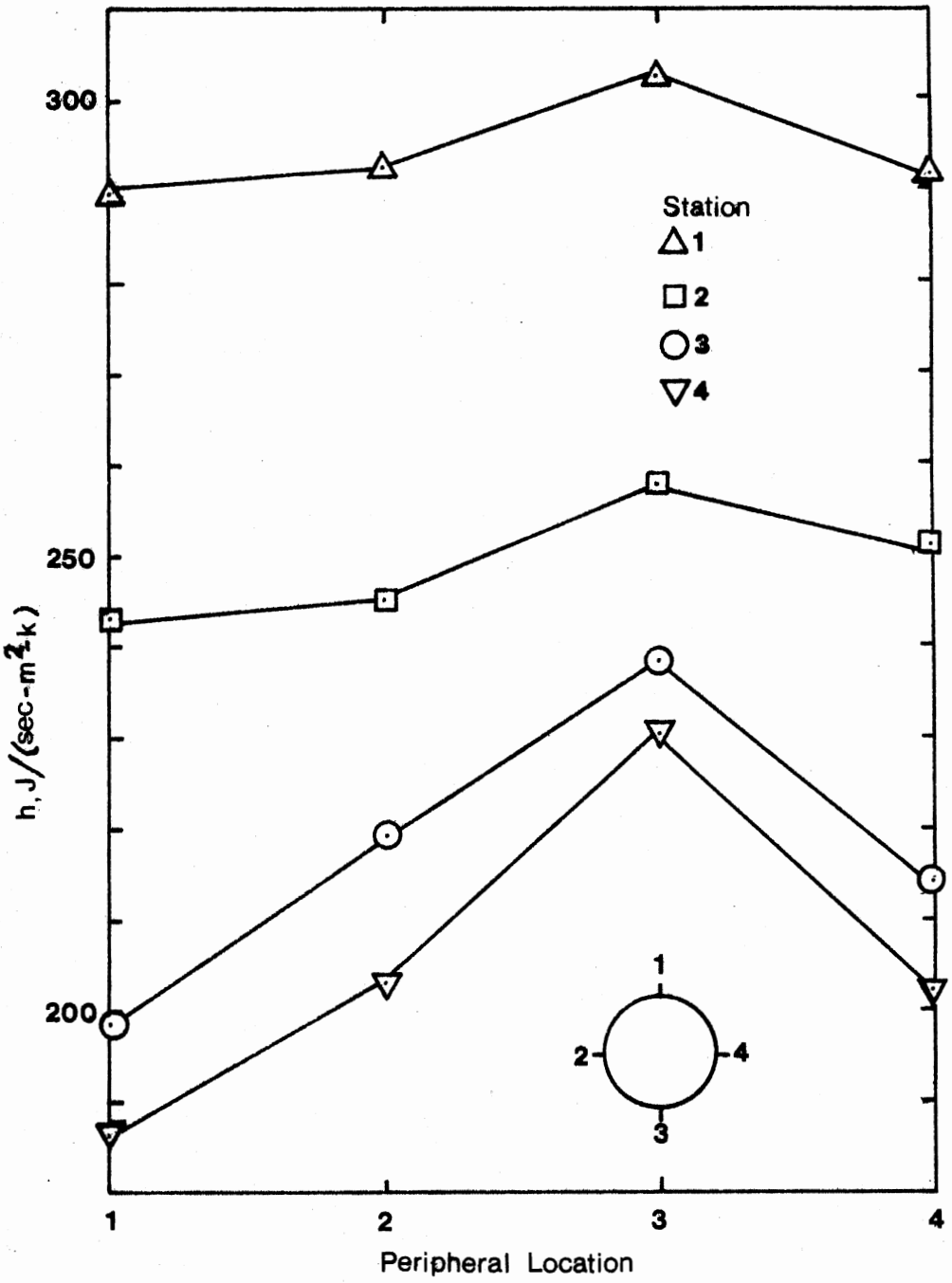

Figure 18. Peripheral Distribution of Heat Transfer Coefficients, Run 508

flow as indicated by Figure 18 is to cause the heat transfer coefficient to be higher at the bottom than at the top of the tube.

Figure 19 shows values of the local Nusselt number along the test section for run 516. The Nusselt number is higher near the start of heating and the profile flattens out along the test section. The experimental results are compared with those predicted by Equations (6.6) to (6.8) and Equation (6.10). The same profile for Nusselt number along the test section is predicted, but Nusselt number predicted by Shah's equation is 30% lower than the experimental value. This may be interpreted as due to the fact that the basic idealization made in developing the thermal entrance analytical results is that the fluid properties are constant. The fluid properties of the heavy oil system, mainly the viscosity, are heavily temperature dependent. For run 516, ($\bar{T}_w - T_b = 116.4^{\circ}F$) at $\frac{X}{d_i} = 45$, the ratio of wall to bulk viscosity $\left(\frac{\mu_w}{\mu_b}\right) = 0.11$. Such variations in fluid properties distort the velocity profile, which in turn affects the temperature profile.

Figure 20 shows value of the local Nusselt number along the test section for run 513 where $\left(\frac{\mu_w}{\mu_b}\right) = 0.31$ at $\frac{X}{d_i} = 45$. Shah's equation predicts a Nusselt number of 22.7, 14.7% less than the experimental value.

Large temperature differences between the wall and bulk fluid temperature were encountered in the heavy oil runs. Shah (5) and Ozoe (6) solutions deviate substantially from experimental results. A limited number of solutions for such temperature dependent fluids have appeared in the literature. Kays (45) and Kays and London (46) suggested that, for engineering applications, it is convenient to employ constant property analytical solutions, or experimental data obtained

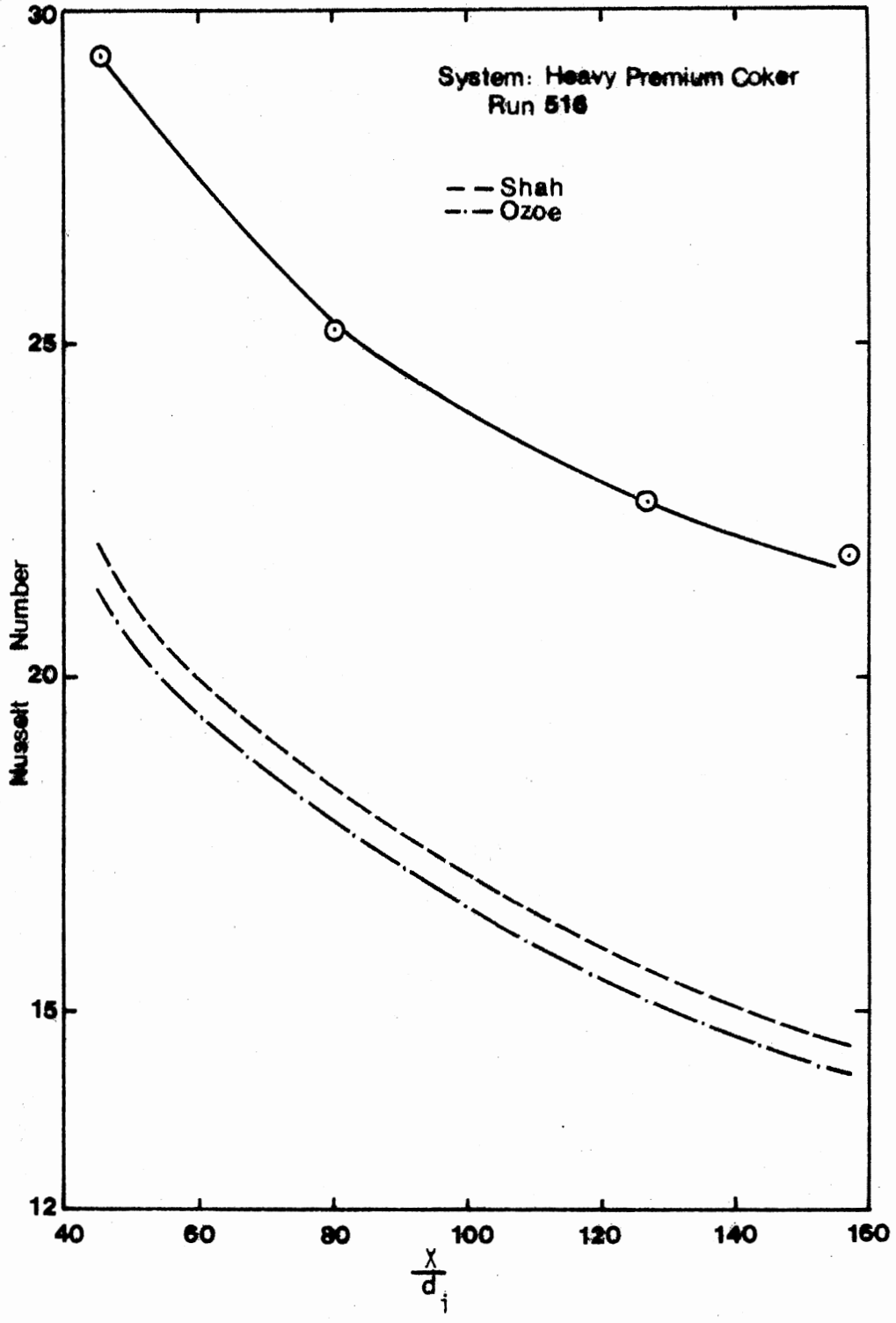

Figure 19. Nusselt Number as a Function of Dimensionless Distance for Run 516

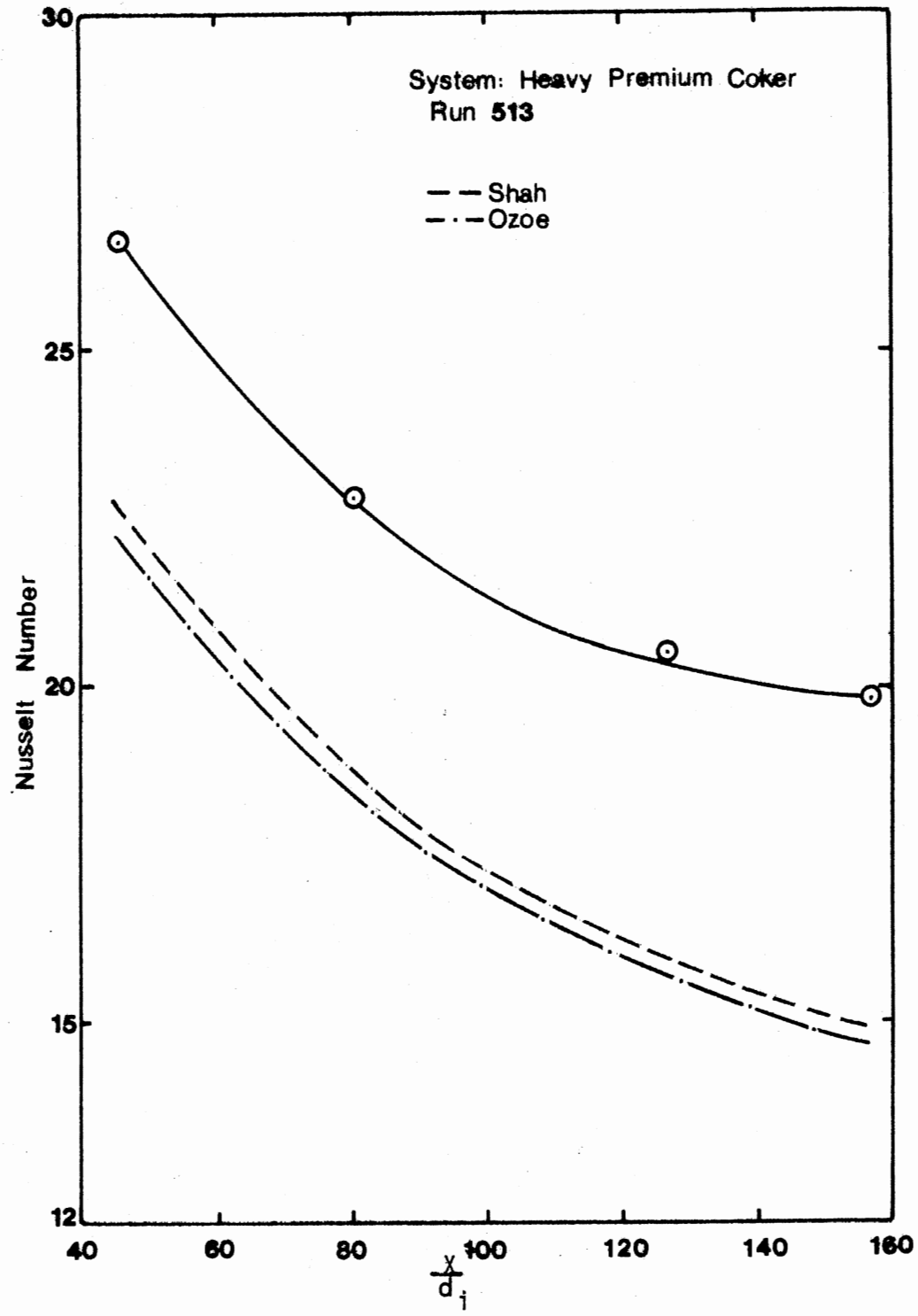

Figure 20. Nusselt Number as a Function of Dimensionless Distance for Run 513

with small temperature differences with a correlation to account for property variations. A property ratio correction for viscosity, $\left(\frac{\mu_w}{\mu_b}\right)^{0.14}$, is recommended by Kays and Perkins (47) for developed and developing laminar flow through a circular tube. The viscosity correction was applied to Equation (6.6), (6.7) and (6.9). The corrected equations predict a heat transfer coefficient that agrees within 13% of the calculated average heat transfer coefficient for the thermal entrance test runs.

Laminar Flow Regime

Experimental data taken by Moshfeghian (23) for ethylene glycol in the laminar flow region was used to study the effects of physical property data on the prediction of the heat transfer coefficient. The peripheral average heat transfer coefficient at thermocouple station number 3 on the straight section upstream of the bend was calculated using Equation (6.12), and was compared to the results predicted by the correlation (Equation (6.5)) developed by Morcos and Bergles (4).

The Morcos-Bergles correlation takes into account the effect of natural convection in the laminar flow region. The agreement between the experimental data at station Number 3 and Morcos-Bergles correlation was reported by Moshfeghian (23) to be excellent for Reynolds numbers less than 1000.

Table XVIII shows the experimental heat transfer coefficient (H_2) for runs 258-362. Also shown is the deviation of the heat transfer coefficient from experimental data as predicted by the Morcos-Bergles correlation for two sets of physical property data taken from Moshfeghian (23) and Campbell (48).

TABLE XVIII

COMPARISON OF HEAT TRANSFER COEFFICIENTS DATA FOR ETHYLENE GLYCOL

Run No	Re*	Re**	$h_{(expt)}$ ($J/m^2.S.K$)	Deviation* %	Deviation** %
352	95.1	102	214.6	11.1	16.3
353	129	139	227.1	16.3	20.5
351	35.4	59.8	186.8	8.7	16.3
354	180	197	223.2	23.5	29.9
355	220	239	239.1	17.6	25.0
356	263	289	252.7	16.3	23.5
359	290	324	225.4	17.6	25.0
357	342	387	265.7	14.9	23.5
361	398	451	223.7	25.0	35.2
362	467	534	236.8	17.6	26.6
260	284	345	274.8	1.0	7.6
258	393	478	283.3	1.0	9.9

$$\% \text{ Deviation} = \frac{h_{expt} - h_{lit}}{h_{expt}} \times 100$$

*$h_{(lit)}$ is evaluated using Morcos and Bergles correlation with Moshfeghian physical property data

**$h_{(lit)}$ is evaluated using Morcos and Bergles correlation with Campbell physical property data.

Using the physical property data reported in Moshfeghian (23), the average deviation of the predicted heat transfer coefficient is 14.2%. Using Campbell's physical property data, the heat transfer coefficient is predicted with a 21.6% average deviation from the experimental value. FPRI data (35) were found to predict a heat transfer coefficient that agrees within 2% of the data from Moshfeghian.

Development of Correlation for Thermal Entrance Region

Experimental data in the thermal entrance region gathered using heavy coker oil were used to develop a correlation that accounts for the effects of physical property variations on the peripherally-averaged heat transfer coefficient. A correlation similar to the literature correlation with a viscosity ratio correction for variable property effects was assumed as follows:

$$Nu = [a(X^{*e})-c] \left(\frac{\mu_b}{\mu_w}\right)^d \tag{6.15}$$

where $X^* = \left(\frac{\pi}{4GZ}\right)$.

Computer programs developed by Chandler (49) were used to fit the experimental data to the above equation and estimate the parameters.

The following correlation with an AAPD of 4.7 was obtained using FPRI (35) physical properties data.

$$Nu = [1.085\ (X^*)^{-0.343} + 3.513] \left(\frac{\mu_b}{\mu_w}\right)^{0.065} \tag{6.16}$$

with $52 \leq Re \leq 1{,}890$, $0.0001 \leq X^* \leq .002$, and $2.8 \leq \left(\frac{\mu_b}{\mu_w}\right) \leq 16.7$.

To study the effects of uncertainties in physical properties data on the parameters of the proposed correlation, experimental data were again fitted using API (19) physical property data. The following correlation with an AAPD of 5.1 was obtained.

$$Nu = [4.017(X^*)^{-0.243} - 5.992] \left(\frac{\mu_b}{\mu_w}\right)^{0.059} \qquad (6.17)$$

Equation (6.16) was used with FPRI physical properties and compared to experimental data to show the magnitude of the error involved in correlations developed on inaccurate physical property data. The AAPD of the predicted heat transfer coefficient was 15.8%.

CHAPTER VII

CONCLUSIONS AND RECOMMENDATIONS

Experimental measurements of the heat transfer coefficients for laminar and turbulent flow inside a horizontal straight tube were made. Eight fluids, methanol, toluene, distilled water, 85 wt % ethylene glycol-water mixture, 50 wt % ethylene glycol-water mixture, heavy premium coker, 30 wt % diethanolamine-water mixture, and n-octane were studied. Literature correlations for straight tubes were tested using well defined physical properties to determine how well they could predict the experimental result.

The following conclusions were arrived at as a result of the total study:

1. Regardless of the equation used, the accuracy of prediction of a heat transfer coefficient is tied with the availability of accurate physical properties data. Significant improvements in the predictions of the heat transfer coefficient were consistently observed when reliable and accurate physical properties data were used. Inaccurate physical properties data can be a major cause of error in heat transfer coefficient predictions using any of the predictive or correlative methods.

2. In the case of mixtures, the problem of predicting accurate heat transfer coefficients is compounded by the nonavailability of

universal mixing rules. This conclusion is based on the wide deviations that were observed when predicted properties computed by commonly used mixing rules were used in the predictions of the heat transfer coefficient. Generally pure component heat transfer coefficient predictions are significantly better than heat transfer coefficient predictions in the case of mixtures.

3. Any predictive correlation has an inherent error depending on the physical properties used to develop that correlation. Some errors in the heat transfer coefficient predictions are bound to crop up when a different set of physical properties data sources are used. The uncertainty in heat transfer coefficient prediction made by using the same correlation is different in magnitude for different fluids investigated. Due to the reasons outlined above all existing correlations need to be used with caution.

4. A correlation has been developed to predict the local Nusselt number for the thermal entrance region for variable property fluid.

5. The investigation clearly indicates that wide differences exist in the experimental physical properties data reported by different sources. The errors are further magnified when predictive methods for physical properties are used.

6. Errors in individual physical properties translate into errors in the predicted heat transfer coefficient. A sensitivity analysis indicating the magnitude of these errors was made.

The following recommendations are made, based on the results of this study for future research in the area:

1. The conclusions made above indicate that several of the existing correlations, especially those that were developed when

sufficiently accurate data were not available, need to be looked at closely. If need be, improvement in their predictive capability can be made by proper modifications or recalculation of the coefficients based on more accurate or recent data.

2. Equation (6.16) for the thermal entrance region was developed for $0.0001 \leq X^* \leq 0.002$. This equation can be properly modified to extend its range of applicability and to make it more general.

3. A similar type of study needs to be undertaken with pure vapor and vapor mixtures to provide a complete understanding of the magnitude of the problems and conclusions made here.

4. An accurate method of measuring pressure drop needs to be incorporated in the experimental setup.

BIBLIOGRAPHY

1. Sieder, E. N. and C. E. Tate, "Heat Transfer and Pressure Drop of Liquids in Tubes," Ind. Eng. Chem., 28, (1963), p. 1429

2. Dittus, F. W. and L. M. Boelter, Univ. of Calif. (Berkeley) Eng. Pub., 2, (1930), p. 443.

3. Petukhov, B. S., "Heat Transfer and Friction in Turbulent Pipe Flow with Variable Properties," Adv. Heat Transf., 6, (1970), p. 503.

4. Morcos, S. H. and A. E. Bergles, "Combined Forced and Free Laminar Convection in Horizontal Tubes," Transactions of ASME, Journal of Heat Transfer, 97, (1975), 212.

5. Shah, R. K., "Thermal Entry Length Solutions for the Circular Tube and Parallel Plates," Proc. Natl. Heat Mass Transfer Conf., 3rd Indian Inst. Technol., Bombay, Vol. I, Pap. No. NMT-11-75 (1975).

6. Grigull, U. and H. Tratz, "Thermischer Linlauf in Ausgebildeter Laminarer Rohrstramung. Int." Int. J. Heat Mass Transfer, 8, (1965), p. 699.

7. Churchill, S. W. and H. Ozoe, "Correlations for Laminar Forced Convection with Uniform Heating in Flow Over a Plate and in Developing and Fully Developed Flow in a Tube," J. Heat Transfer, 95, (1973), p. 78-84.

8. Nangia, K. K. and J. Taborek, "Thermal Conductivity of Liwuids-Critical Evaluation of Data Sources and Predictive Methods," Presented at 11th International Conference on Thermal Conductivity, Albuquerque, New Mexico, October 1, 1971.

9. Nangia, K. K. and J. Taborek, "Physical Properties of Liquids-Status of Present Knowledge and Importance in Design Methods for Heat Transfer and Fluid Flow," Presented at 13th National Heat Transfer Conference, Denver, Colorado, August 6-9, 1972.

10. McCoy, D. D., V. K. Mathur and R. N. Maddox, "Effect of Physical Properties on Chemical Engineering Design and Calculations," Proceedings of Silver Jubilee Meeting, Indian Institute of Chemical Engineers, New Delhi, India, December 2-6, 1972.

11. Squires, E. W. and J. C. Orchard, "Comparison of Design Versus Performance of Gas Plants," Proceedings, GPA Annual Convention, March, 1968.

12. Williams, C. C. and M. A. Albright, "Better Data Saves Energy," Hydrocarbon Processing, (1976), p. 115.

13. Zudkevitch, D., J. Joffe, and G. M. Schroeder, in: Proceedings Intern. Symposium on Distillation, London: Hodgson and Sons, (1969), p. 141.

14. Zudkevitch, D. and R. D. Gray, Cryogenic Eng., 20, (1975), p. 103.

15. Nani, P. and J. E. S. Venart, in: Advances in Cryogenic Engineering, 18, New York: Plenum Press, (1973), p. 280.

16. Albright, M. A., "Design Implications of the NGPA Research Programs," presented at 49th NGPA Annual Convention, Denver, Colorado, March 17-19, 1970.

17. Baker, O, "The Value of Enthalpy Research to the Petroleum Industry," presented at 39th NGPA Annual Convention, Houston, Texas, 1960.

18. Streich, M. and H. Kistenmacher, "Property Inaccuracies Influence Low Temperature Designs," Hydrocarbon Processing, (May, 1979), p. 237-241.

19. American Petroleum Institute Technical Data Book, Washington, D.C.: Petroleum Refining, 2nd Edition (1970).

20. A.I.Ch.E. Physical Property Estimation System, General Descriptive Manual, Cambridge: Arthur D. Little, Inc., (September, 1965).

21. Farukhi, M. N., "An Experimental Investigation of Forced Convective Boiling at High Qualities Inside Tubes Preceded by 180 Degree Bends," Ph.D. Thesis, Oklahoma State University, Stillwater, Oklahoma (1974).

22. Singh, S. P., "Liquid Phase Heat Transfer in Helically Coiled Tubes," Ph.D. Thesis, Oklahoma State University, Stillwater, Oklahoma (1973).

23. Moshfeghian, M., "Fluid Flow and Heat Transfer in U-Bends," Ph.D. Thesis, Oklahoma State University, Stillwater, Oklahoma (1978).

24. Digital Thermocouple Indicator Manual, Manual No. 350-4490-03. California: Doric Co. (January, 1979).

25. Directions for 8687 Volt Potentiometer, Manual No. 177126, Issue 5, Pennsylvania: Leeds & Northrup Company (September, 1975).

26. Dead Weight Gauge Manual, Manual No. 8-61-3M, Texas: Ruska Instrument Company, (September, 1975).

27. Moshfeghian, M., "The Effect of a 180^{o} Bend on Turbulent Heat Transfer Coefficient in a Pipe," M.S. Thesis, Oklahoma State University, Stillwater, Oklahoma (1975).

28. Owhadi, A., K. J. Bell and B. Crain, Jr., "Forced Convection Boiling Inside Helically Coiled Tubes," Int. J. of Heat and Mass Transfer, 11, (1968), p. 1779.

29. Crain, Berry, Jr., "Forced Convection Heat Transfer to a Two-Phase Mixture of Water and Steam in a Helical Coil," Ph.D. Thesis, Oklahoma State University, Stillwater, Oklahoma (1973).

30. Sleicher, C. A. and M. W. Rouse, "A Convenient Correlation for Heat Transfer to Constant and Variable Property Fluids in Turbulent Pipe Flow," Int. Journal of Heat and Mass Transfer, 18, (1975), p. 677.

31. Eagle, A. and R. M. Ferguson, Inst. Mech. Engrs., London, 2, (1930), p. 985.

32. Malina, J. A. and E. M. Sparrow, "Variable-Property, Constant Property and Entrance Region Heat-Transfer Results for Turbulent Flow of Water and Oil in a Circular Tube," Chem. Engr. Sci., 19, (1964), p. 953-962.

33. Allen, R. W. and E. R. G. Eckert, "Friction and Heat Transfer Measurements to Turbulent Pipe Flow of Water (Pr = 7 and 8) at Uniform Wall Heat Flux," J. Heat Transfer, 86, (1964), p. 301-310.

34. Smith, J. F, "Thermal Conductivity of Liquid," Industrial Engineering Chemistry, 22, (1930), p. 1249.

35. FPRI, Fluid Properties Research, Inc., Measured Values, Oklahoma State University, (1979).

36. Yaws, C. L., "Physical Properties," Chem. Engr., New York: McGraw-Hill, (1977).

37. Touloukian, Y. S. and S. Saxema, "Thermophysical Properties of Matter," 3, Thermal Conductivity of Non Metallic Liquids and Gases, New York, (1971).

38. Tayagi, K. P., Estimation of Saturated Liquid Heat Capacities, Mechanical Engineering Department, Birla Institute of Technology and Sciences, Pilani, India.

39. Gallant, R. W., Physical Properties of Hydrocarbon, Houston: Gulf Publishing Company, (1970).

40. Touloukian, Y. S. and T. Makita, "Thermophysical Properties of Matter," 6, Specific Heat, Non Metallic Liquids and Gases, New York: IFI/Plenum, (1971).

41. Pachaiyappan, R. Britt, Chem. Eng., 16, (1971), p. 382.

42. Standards for Tubular Exchanger Manufacturers Association, 5th ed., (1968).

43. _____, Gas Conditioning Fact Book, Midland, Michigan: Dow, The Dow Chemical Company, (1962).

44. _____, "Thermal Conductivity of Liquid Glycols, Glycerol and Their Aqueous Solution," Engineering Sciences Data, Item No. 70004, London, (1970).

45. Kays, W. M., Convective Heat and Mass Transfer, New York: McGraw-Hill, (1966).

46. Kays, W. M. and A. L. London, Compact Heat Exchangers, 2nd Ed., New York: McGraw-Hill, (1964).

47. Kays, W. M. and H. C. Perkins, "Forced Convection, Internal Flows in Ducts," in: Handbook of Heat Transfer (W. M. Rohsenow and J. P. Hartnett, eds.), New York: McGraw-Hill, (1973), p. 193.

48. Campbell, John, Gas Conditioning and Processing, 2, Campbell Petroleum Series, (1978).

49. Chandler, J. P., MARQ 2.3 A.N.S.I. Standard Fortran, Department of Computing and Information Sciences, Oklahoma State University, Stillwater, Oklahoma, (1975).

50. Ziebland, H. and J. T. Burton, J. Chem. Eng. Data, 6, (1961) p. 579-583.

51. McLaughlin, E., "Heat Transfer in Coiled Pipes," M.S. Thesis, University of California, (1958).

52. McAdams, W. H., Heat Transmission, 2nd Ed., New York: McGraw-Hill Book Company, Inc., (1942), p. 237-246.

APPENDIX A

EXPERIMENTAL DATA

Run Number	Test Fluid
1 - 6	Distilled Water
101 - 126	Methanol
201 - 224	Toluene
301 - 307	85 wt % Ethylene Glycol-Water Mixture
401 - 418	50 wt % Ethylene Glycol-Water Mixture
501 - 542	Heavy Premium Coker
601 - 623	30 wt % Diethanolamine-Water Mixture
701 - 713	n-octane

Only sample runs are presented here. The rest of the experimental data are available at:

School of Chemical Engineering
Oklahoma State University
Stillwater, Oklahoma 74074
USA

Att: Dr. R. N. Maddox

RUN NUMBER 702

FLUID FLOW RATE	=	716.07	LBM/HOUR
CURRENT TO TUBE	=	141.00	AMPS
VOLTAGE DROP IN TUBE	=	6.49	VOLTS
ROOM TEMPERATURE	=	79.70	DEGREES F
UNCORRECTED INLET TEMPERATURE	=	69.90	DEGREES F
UNCORRECTED OUTLET TEMPERATURE	=	78.10	DEGREES F

OUTSIDE SURFACE TEMPERATURES - DEGREES F

	1	2	3	4
1	84.0	85.3	87.3	88.4
2	84.0	85.2	87.2	88.5
3	84.0	85.2	87.2	88.5
4	84.1	85.3	87.4	88.6

RUN NUMBER 705

FLUID FLOW RATE	=	980.03	LBM/HOUR
CURRENT TO TUBE	=	221.25	AMPS
VOLTAGE DROP IN TUBE	=	10.43	VOLTS
ROOM TEMPERATURE	=	81.20	DEGREES F
UNCORRECTED INLET TEMPERATURE	=	86.10	DEGREES F
UNCORRECTED OUTLET TEMPERATURE	=	101.00	DEGREES F

OUTSIDE SURFACE TEMPERATURES - DEGREES F

	1	2	3	4
1	112.5	114.7	118.4	120.3
2	112.6	114.9	118.0	120.4
3	112.5	114.4	117.8	120.6
4	112.8	115.0	118.4	120.8

RUN NUMBER 710

FLUID FLOW RATE	= 1116.80	LBM/HOUR
CURRENT TO TUBE	= 435.00	AMPS
VOLTAGE DROP IN TUBE	= 22.00	VOLTS
ROOM TEMPERATURE	= 85.00	DEGREES F
UNCORRECTED INLET TEMPERATURE	= 155.10	DEGREES F
UNCORRECTED OUTLET TEMPERATURE	= 204.70	DEGREES F

OUTSIDE SURFACE TEMPERATURES - DEGREES F

	1	2	3	4
1	241.7	248.2	260.5	266.4
2	241.2	248.5	259.0	267.0
3	240.4	247.9	258.1	266.5
4	242.0	249.2	260.6	267.6

RUN NUMBER 708

FLUID FLOW RATE	= 1129.70	LBM/HOUR
CURRENT TO TUBE	= 321.00	AMPS
VOLTAGE DROP IN TUBE	= 15.52	VOLTS
ROOM TEMPERATURE	= 84.60	DEGREES F
UNCORRECTED INLET TEMPERATURE	= 112.90	DEGREES F
UNCORRECTED OUTLET TEMPERATURE	= 139.80	DEGREES F

OUTSIDE SURFACE TEMPERATURES - DEGREES F

	1	2	3	4
1	160.8	164.4	171.1	174.5
2	160.5	164.7	170.5	175.0
3	160.3	164.3	170.2	174.9
4	160.9	165.0	171.4	175.4

RUN NUMBER 606

FLUID FLOW RATE	=	1410.44	LBM/HOUR
CURRENT TO TUBE	=	195.00	AMPS
VOLTAGE DROP IN TUBE	=	9.33	VOLTS
ROOM TEMPERATURE	=	83.70	DEGREES F
UNCORRECTED INLET TEMPERATURE	=	130.70	DEGREES F
UNCORRECTED OUTLET TEMPERATURE	=	135.20	DEGREES F

OUTSIDE SURFACE TEMPERATURES - DEGREES F

	1	2	3	4
1	139.0	139.5	141.1	141.2
2	139.1	139.8	140.8	141.6
3	138.9	139.7	140.6	141.6
4	139.4	139.8	141.3	141.9

RUN NUMBER 607

FLUID FLOW RATE	=	1412.30	LBM/HOUR
CURRENT TO TUBE	=	232.50	AMPS
VOLTAGE DROP IN TUBE	=	11.14	VOLTS
ROOM TEMPERATURE	=	84.60	DEGREES F
UNCORRECTED INLET TEMPERATURE	=	133.70	DEGREES F
UNCORRECTED OUTLET TEMPERATURE	=	140.20	DEGREES F

OUTSIDE SURFACE TEMPERATURES - DEGREES F

	1	2	3	4
1	145.7	146.4	148.5	148.8
2	145.7	146.7	148.0	149.2
3	145.5	146.5	147.8	149.2
4	146.1	146.8	148.5	149.6

RUN NUMBER 613

FLUID FLOW RATE	= 1333.85	LBM/HOUR
CURRENT TO TUBE	= 363.00	AMPS
VOLTAGE DROP IN TUBE	= 17.90	VOLTS
ROOM TEMPERATURE	= 88.20	DEGREES F
UNCORRECTED INLET TEMPERATURE	= 169.70	DEGREES F
UNCORRECTED OUTLET TEMPERATURE	= 187.10	DEGREES F

OUTSIDE SURFACE TEMPERATURES - DEGREES F

	1	2	3	4
1	197.7	199.8	204.4	206.1
2	197.7	200.5	204.0	206.8
3	197.5	200.2	203.8	206.9
4	198.5	200.7	205.1	207.3

RUN NUMBER 616

FLUID FLOW RATE	= 1236.20	LBM/HOUR
CURRENT TO TUBE	= 448.50	AMPS
VOLTAGE DROP IN TUBE	= 22.30	VOLTS
ROOM TEMPERATURE	= 88.40	DEGREES F
UNCORRECTED INLET TEMPERATURE	= 160.70	DEGREES F
UNCORRECTED OUTLET TEMPERATURE	= 191.50	DEGREES F

OUTSIDE SURFACE TEMPERATURES - DEGREES F

	1	2	3	4
1	210.7	214.2	221.5	224.5
2	210.8	214.8	221.4	225.5
3	210.6	213.3	220.6	225.7
4	211.7	215.2	222.2	226.2

RUN NUMBER 619

FLUID FLOW RATE	=	1218.00	LBM/HOUR
CURRENT TO TUBE	=	186.00	AMPS
VOLTAGE DROP IN TUBE	=	8.83	VOLTS
ROOM TEMPERATURE	=	83.90	DEGREES F
UNCORRECTED INLET TEMPERATURE	=	109.80	DEGREES F
UNCORRECTED OUTLET TEMPERATURE	=	114.80	DEGREES F

OUTSIDE SURFACE TEMPERATURES - DEGREES F

	1	2	3	4
1	120.6	121.3	122.7	123.0
2	120.8	121.4	122.6	123.3
3	120.6	121.1	122.5	123.3
4	120.9	121.5	122.9	123.4

RUN NUMBER 623

FLUID FLOW RATE	=	1107.83	LBM/HOUR
CURRENT TO TUBE	=	384.00	AMPS
VOLTAGE DROP IN TUBE	=	19.10	VOLTS
ROOM TEMPERATURE	=	88.50	DEGREES F
UNCORRECTED INLET TEMPERATURE	=	170.60	DEGREES F
UNCORRECTED OUTLET TEMPERATURE	=	194.30	DEGREES F

OUTSIDE SURFACE TEMPERATURES - DEGREES F

	1	2	3	4
1	208.5	211.3	217.5	219.7
2	208.4	211.7	216.7	220.5
3	207.9	210.4	216.1	220.4
4	208.9	211.8	217.8	220.8

RUN NUMBER 509

FLUID FLOW RATE	=	1438.80	LBM/HOUR
CURRENT TO TUBE	=	132.00	AMPS
VOLTAGE DROP IN TUBE	=	6.51	VOLTS
ROOM TEMPERATURE	=	87.30	DEGREES F
UNCORRECTED INLET TEMPERATURE	=	121.90	DEGREES F
UNCORRECTED OUTLET TEMPERATURE	=	126.60	DEGREES F

OUTSIDE SURFACE TEMPERATURES - DEGREES F

	1	2	3	4
1	183.0	194.0	204.7	209.2
2	181.5	192.3	201.6	206.1
3	179.7	191.5	202.6	208.5
4	181.6	193.3	206.9	213.6

RUN NUMBER 510

FLUID FLOW RATE	=	1449.30	LBM/HOUR
CURRENT TO TUBE	=	150.75	AMPS
VOLTAGE DROP IN TUBE	=	7.54	VOLTS
ROOM TEMPERATURE	=	90.70	DEGREES F
UNCORRECTED INLET TEMPERATURE	=	129.10	DEGREES F
UNCORRECTED OUTLET TEMPERATURE	=	135.20	DEGREES F

OUTSIDE SURFACE TEMPERATURES - DEGREES F

	1	2	3	4
1	208.5	223.0	236.8	244.3
2	205.5	219.5	231.0	236.8
3	202.5	217.6	231.7	239.0
4	205.7	220.8	238.8	247.5

RUN NUMBER 516

FLUID FLOW RATE	=	1022.20	LBM/HOUR
CURRENT TO TUBE	=	184.50	AMPS
VOLTAGE DROP IN TUBE	=	9.47	VOLTS
ROOM TEMPERATURE	=	91.40	DEGREES F
UNCORRECTED INLET TEMPERATURE	=	124.00	DEGREES F
UNCORRECTED OUTLET TEMPERATURE	=	137.00	DEGREES F

OUTSIDE SURFACE TEMPERATURES - DEGREES F

	1	2	3	4
1	247.2	272.4	299.0	308.6
2	244.1	268.1	287.1	296.4
3	240.8	263.4	281.8	289.7
4	244.0	267.3	291.3	300.6

RUN NUMBER 513

FLUID FLOW RATE	=	1070.93	LBM/HOUR
CURRENT TO TUBE	=	134.25	AMPS
VOLTAGE DROP IN TUBE	=	6.78	VOLTS
ROOM TEMPERATURE	=	91.20	DEGREES F
UNCORRECTED INLET TEMPERATURE	=	155.90	DEGREES F
UNCORRECTED OUTLET TEMPERATURE	=	163.10	DEGREES F

OUTSIDE SURFACE TEMPERATURES - DEGREES F

	1	2	3	4
1	232.7	246.4	258.8	264.6
2	228.3	241.2	250.1	253.8
3	224.3	237.8	249.3	254.0
4	228.5	242.1	257.8	263.5

RUN NUMBER 518

FLUID FLOW RATE	=	873.30	LBM/HOUR
CURRENT TO TUBE	=	133.50	AMPS
VOLTAGE DROP IN TUBE	=	6.50	VOLTS
ROOM TEMPERATURE	=	87.60	DEGREES F
UNCORRECTED INLET TEMPERATURE	=	92.40	DEGREES F
UNCORRECTED OUTLET TEMPERATURE	=	100.20	DEGREES F

OUTSIDE SURFACE TEMPERATURES - DEGREES F

	1	2	3	4
1	158.7	170.4	179.9	185.3
2	159.1	171.3	182.6	188.6
3	159.2	172.5	184.4	191.2
4	159.6	172.5	185.0	191.4

RUN NUMBER 519

FLUID FLOW RATE	=	829.20	LBM/HOUR
CURRENT TO TUBE	=	106.50	AMPS
VOLTAGE DROP IN TUBE	=	5.10	VOLTS
ROOM TEMPERATURE	=	79.60	DEGREES F
UNCORRECTED INLET TEMPERATURE	=	82.50	DEGREES F
UNCORRECTED OUTLET TEMPERATURE	=	87.90	DEGREES F

OUTSIDE SURFACE TEMPERATURES - DEGREES F

	1	2	3	4
1	129.6	138.3	146.4	150.6
2	129.7	138.9	147.3	152.3
3	129.5	139.1	147.6	152.9
4	129.9	139.1	148.4	153.4

RUN NUMBER 540

FLUID FLOW RATE	= 1540.55	LBM/HOUR
CURRENT TO TUBE	= 315.00	AMPS
VOLTAGE DROP IN TUBE	= 16.93	VOLTS
ROOM TEMPERATURE	= 89.10	DEGREES F
UNCORRECTED INLET TEMPERATURE	= 269.40	DEGREES F
UNCORRECTED OUTLET TEMPERATURE	= 294.20	DEGREES F

OUTSIDE SURFACE TEMPERATURES - DEGREES F

	1	2	3	4
1	359.5	360.5	365.9	366.1
2	359.3	361.3	364.5	367.9
3	359.1	359.5	364.0	367.9
4	360.6	361.5	366.2	368.5

RUN NUMBER 541

FLUID FLOW RATE	= 1616.94	LBM/HOUR
CURRENT TO TUBE	= 313.50	AMPS
VOLTAGE DROP IN TUBE	= 16.81	VOLTS
ROOM TEMPERATURE	= 89.40	DEGREES F
UNCORRECTED INLET TEMPERATURE	= 271.50	DEGREES F
UNCORRECTED OUTLET TEMPERATURE	= 295.20	DEGREES F

OUTSIDE SURFACE TEMPERATURES - DEGREES F

	1	2	3	4
1	357.6	358.6	364.0	364.2
2	357.5	359.2	362.7	366.0
3	357.2	357.3	362.1	366.4
4	358.8	359.3	364.2	366.7

RUN NUMBER 415

FLUID FLOW RATE	= 1544.90	LBM/HOUR
CURRENT TO TUBE	= 246.00	AMPS
VOLTAGE DROP IN TUBE	= 11.87	VOLTS
ROOM TEMPERATURE	= 78.90	DEGREES F
UNCORRECTED INLET TEMPERATURE	= 138.40	DEGREES F
UNCORRECTED OUTLET TEMPERATURE	= 145.50	DEGREES F

OUTSIDE SURFACE TEMPERATURES - DEGREES F

	1	2	3	4
1	152.3	153.0	155.1	155.4
2	152.4	153.5	154.7	155.8
3	152.0	153.6	154.8	156.1
4	152.7	153.6	155.1	156.3

RUN NUMBER 416

FLUID FLOW RATE	= 1462.00	LBM/HOUR
CURRENT TO TUBE	= 249.00	AMPS
VOLTAGE DROP IN TUBE	= 12.00	VOLTS
ROOM TEMPERATURE	= 83.50	DEGREES F
UNCORRECTED INLET TEMPERATURE	= 140.30	DEGREES F
UNCORRECTED OUTLET TEMPERATURE	= 147.40	DEGREES F

OUTSIDE SURFACE TEMPERATURES - DEGREES F

	1	2	3	4
1	154.3	154.9	157.2	157.8
2	154.4	155.4	156.9	158.2
3	154.1	155.7	157.0	158.4
4	154.6	155.6	157.5	158.7

RUN NUMBER 417

FLUID FLOW RATE	= 1462.00	LBM/HOUR
CURRENT TO TUBE	= 310.50	AMPS
VOLTAGE DROP IN TUBE	= 15.36	VOLTS
ROOM TEMPERATURE	= 84.20	DEGREES F
UNCORRECTED INLET TEMPERATURE	= 175.20	DEGREES F
UNCORRECTED OUTLET TEMPERATURE	= 188.10	DEGREES F

OUTSIDE SURFACE TEMPERATURES - DEGREES F

	1	2	3	4
1	196.8	197.8	201.8	202.8
2	196.9	198.6	201.2	203.5
3	196.4	199.0	201.4	203.9
4	197.3	198.9	202.2	204.2

RUN NUMBER 418

FLUID FLOW RATE	= 1100.00	LBM/HOUR
CURRENT TO TUBE	= 348.00	AMPS
VOLTAGE DROP IN TUBE	= 17.53	VOLTS
ROOM TEMPERATURE	= 84.90	DEGREES F
UNCORRECTED INLET TEMPERATURE	= 198.60	DEGREES F
UNCORRECTED OUTLET TEMPERATURE	= 218.00	DEGREES F

OUTSIDE SURFACE TEMPERATURES - DEGREES F

	1	2	3	4
1	228.2	230.0	235.6	237.3
2	228.3	231.2	235.0	238.0
3	227.9	231.9	235.3	238.7
4	228.9	231.7	236.1	239.0

APPENDIX B

CALIBRATION DATA

TABLE XIX

CALIBRATION DATA FOR ROTAMETER 1 FOR METHANOL

Rotameter Setting % Maximum Flow	Mass Flow Rate, kg/sec x 10^3
20	65.5
30	107.8
35	122.9
40	145.1
50	182.7
60	218.0
70	253.4

The flow rate was also measured for each individual data run and checked with the calibration data for any deviation.

TABLE XX

CALIBRATION DATA FOR ROTAMETER 1 FOR TOLUENE

Rotameter Setting % Maximum Flow	Mass Flow Rate, kg/sec x 10^3
15	53.6
25	81.7
35	128.9
40	146.0
45	165.8
60	220.8

Experimental data runs were taken for rotameter settings between 35 and 40% maximum flow. The flow rate was also measured for each individual data run.

TABLE XXI

CALIBRATION DATA FOR ROTAMETER 2 FOR DISTILLED WATER

Flow Indicator % Maximum Flow	Mass Flow Rate, kg/sec x 10^{-3}
35	7.4
40	12.7
50	25.5
60	35.6
74	58.0
85	65.0
90	71.4
96	77.4

For distilled water, 85 wt % ethylene glycol, 50 wt % ethylene glycol, heavy oil coker, 30 wt % ethanolamine, and n-octane. The flow rate was measured for each individual data run. For most of the runs the flow indicator was set above the allowed % maximum flow and and was used merely as an indication of the flow rate.

TABLE XXII

CALIBRATION DATA FOR PRESSURE GAUGE 1*

Calibration Weight, psi	Pressure Gauge 1 Readings, psi
6	7
10	11
14	15
16	17
26	27.5
46	48
86	89
106	108
146	148
186	188
206	207
246	246
286	287
306	307
346	347
386	387

*Gauge 1 was used to measure the pressure at the inlet of the test section.

TABLE XXIII

CALIBRATION DATA FOR PRESSURE GAUGE 2*

Calibration Weight, psi	Pressure Gauge 2 Readings, psi
6	5
10	9
30	29.5
50	49
70	69
90	90
110	110
130	129.5
150	150
190	190
210	210
230	229
250	248.5
290	288
310	308
350	348
390	389

*Gauge 2 was used to measure the pressure at the exit of the test section.

TABLE XXIV

CALIBRATION DATA FOR OUTSIDE SURFACE THERMOCOUPLES

Thermocouple Number	Average Resistance of Platinum Thermometer (Ohms)	Thermocouple Temperature ^{o}F
1	28.2917	80.80
1	35.2088	201.38
1	40.8871	309.35
1	46.3682	410.65
2	28.2917	80.75
2	35.0277	201.45
2	40.8867	309.35
2	46.3683	410.65
3	28.2918	80.90
3	35.0280	201.55
3	40.8868	309.35
3	46.3691	410.75
4	28.2920	80.84
4	35.0273	201.55
4	40.8870	309.35
4	46.3659	410.65
5	28.2920	80.94
5	35.0273	201.55
5	40.8871	309.35
5	46.3687	410.85
6	28.2924	80.89
6	35.0272	201.65
6	40.8877	309.45
6	46.3674	410.95
7	28.2921	80.93
7	35.0267	201.60
7	40.8882	309.45
7	46.3673	410.85
8	28.2919	80.90
8	35.0264	201.70
8	40.8876	309.50
8	46.3687	310.95
9	28.2916	80.90
9	35.0256	201.65
9	40.8874	309.40
9	46.3675	410.95

TABLE XXIV (Continued)

Thermocouple Number	Average Resistance of Platinum Thermometer (Ohms)	Thermocouple Temperature °F
10	28.2910	80.90
10	35.0256	201.75
10	40.8871	309.40
10	46.3673	410.85
11	28.2912	80.80
11	35.0251	201.75
11	40.8870	309.45
11	46.3671	410.90
12	28.2910	80.95
12	35.0250	201.75
12	40.8869	309.40
12	46.3672	410.75
13	28.2907	80.95
13	35.0244	201.85
13	40.8867	309.55
13	46.3670	410.95
14	28.2907	80.95
14	35.0236	201.75
14	40.8861	309.35
14	46.3673	410.75
15	28.2906	80.98
15	35.0238	201.80
15	40.8866	309.50
15	48.3678	410.85
16	28.2901	80.90
16	40.8855	201.80
16	40.8861	309.40
16	40.3675	410.95

TABLE XXV

CALIBRATION DATA FOR INLET, OUTLET, TANK, AND ROOM TEMPERATURE THERMOCOUPLES

Thermocouple Number	Average Resistance of Platinum Thermometer (Ohms)	Thermocouple Temperature ^{o}F
A	27.9977	75.0
A	32.2385	151.3
A	36.8580	235.0
A	42.0804	331.6
A	45.9968	404.3
B	27.9957	75.0
B	32.2491	151.5
B	36.8449	233.6
B	42.0738	331.4
B	45.9908	404.3
C	27.9926	75.3
C	32.2582	151.7
C	36.8306	235.3
C	42.0694	332.1
C	45.9876	404.8
D	27.9898	74.7
D	32.2684	151.5
D	36.8300	235.1
D	42.0688	331.8
D	45.9873	404.9

The temperature readings that correspond to the platinum resistance thermocouple were plotted against the temperature readings of the thermocouples. A list of equations to correct each thermocouple reading is presented.

$Y \equiv$ corrected temperature (^{o}F)

$X \equiv$ thermocouple readings (^{o}F)

Thermocouple N^{o}	Correction Equation
1	$Y = 1.0020778X - 0.838071$
2	$Y = 1.0019837X - 0.822011$
3	$Y = 1.0022411X - 0.974183$
4	$Y = 1.0023455X - 0.962775$
5	$Y = 1.0020697X - 0.971310$
6	$Y = 1.0016284X - 0.918308$
7	$Y = 1.002012X - 0.989383$
8	$Y = 1.0045167X - 0.968263$
9	$Y = 1.0017766X - 0.960431$
10	$Y = 1.0021237X - 1.047469$
11	$Y = 1.00164135X - 0.931528$
12	$Y = 1.00254X - 1.146893$
13	$Y = 1.0019416X - 1.114510$
14	$Y = 1.0026209X - 1.164563$
15	$Y = 1.0022848X - 1.150480$
16	$Y = 1.0019399X - 1.056475$
A	$Y = 0.999003X - 0.213310$
B	$Y = 0.998805X + 0.051831$
C	$Y = 0.9974599X - 0.35678$
D	$Y = 0.9959433X - 0.251994$

APPENDIX C

PHYSICAL PROPERTIES

Physical property equation constants for the pure components and mixture test fluids are given in Tables XXVII to XXX. Table XXVI gives a list of pure components used as test fluids or for preparing mixture test fluids.

TABLE XXVI

LIST OF CHEMICALS

Chemical	Manufacturer	Purity or Label No.
Toluene	Mallinckrodt Company	Purified 8604
Methanol	Fisher Scientific Company	Purified 754325
Ethylene Glycol	Fisher Scientific Company	Purified 761607
Diethanolamine	Pfaltz & Bauer Company	Purified
N-Octane	Phillips Petroleum Company	99 Mole % Purity

TABLE XXVII

DENSITY EQUATION CONSTANTS FOR TEST FLUIDS

$$\rho = a + bT + cT^2 + dT^3$$

	Reference	ρ (Units)	T (Units)	a	b	c	d
Methanol	(41)	gm/cm^3	^oF	0.82762	-0.57059×10^{-3}	0.74493×10^{-6}	-0.22227×10^{-8}
Methanol	(42)	gm/cm^3	^oF	0.90227	-0.60215×10^{-3}	0.85140×10^{-7}	0
Methanol	(39)	gm/cm^3	^oF	0.84892	-0.13580×10^{-2}	0.92257×10^{-5}	-0.30368×10^{-7}
Methanol	(35)	gm/cm^3	^oF	0.82792	-0.45920×10^{-3}	0.33954×10^{-6}	-0.19874×10^{-8}
Toluene	(35)	gm/cm^3	^oF	0.90722	-0.67527×10^{-3}	0.17504×10^{-5}	-0.53136×10^{-8}
Toluene	(41)	gm/cm^3	^oF	0.94066	-0.67028×10^{-2}	0.24358×10^{-4}	-0.36033×10^{-7}
Toluene	(35)	gm/cm^3	^oF	0.88035	-0.21270×10^{-3}	0.55233×10^{-5}	0
85 wt % Ethylene Glycol	(43)	lbm/ft^3	^oF	70.8641	-0.23872×10^{-1}	0.46839×10^{-5}	0.53054×10^{-8}
85 wt % Ethylene Glycol	(35)	gm/cm^3	^oR	0.62554*	0.50098*	1053.6*	-
85 wt % Ethylene Glycol	(39)	gm/cm^3	^oR	0.59801*	0.45926*	1000.*	-
50 wt % Ethylene Glycol	(35)	gm/cm^3	^oR	0.71436*	0.60538*	948.8*	-
50 wt % Ethylene Glycol	(43)	gm/cm^3	^oR	0.73944*	0.61621*	875.0*	-
50 wt % Ethylene Glycol	(39)	gm/cm^3	^oR	0.62967*	0.5230*	1000.*	-

TABLE XXVII (Continued)

$\rho = a + bT = cT^2 + dT^3$

	Reference	(Units)	T (Units)	a	b	c	d
Heavy Premium Coker	(35)	kg/m^3	^oR	353.25*	0.29051*	900.17*	-
Heavy Premium Coker	(19)	gm/cm^3	^oR	0.38566*	0.31209*	1368.8*	-
30 wt % Diethanolamine	(35)	gm/cm^3	^oR	0.64997*	0.55926*	997.21*	-
30 wt % Diethanolamine	(51)	lbm/ft^3	^oF	65.3709	$-0.867/x10^{-2}$	$-0.37103x10^{-4}$	-
30 wt % Diethanolamine	(43)	lbm/ft^3	^oF	65.2316	$-0.68405x10^{-2}$	$-0.45737x10^{-4}$	0
n-Octane	(39)	lbm/ft^3	^oF	45.6214	$-0.25916x10^{-1}$	$-0.15823x10^{-4}$	0
n-Octane	(42)	lbm/ft^3	^oF	46.1618	$-0.34667x10^{-1}$	$0.5579x10^{-5}$	0
Water	(42)	kg/m^3	^oL	999.9886	$0.1890x10^{-1}$	$-0.5886x10^{-2}$	$0.1548x10^{-7}$

*Constants for $\rho = (axb)^{-(1-\frac{T}{C})^{2/7}}$

TABLE XXVIII

THERMAL CONDUCTIVITY EQUATION CONSTANTS FOR TEST FLUIDS

$$k_{(Btu/hr-ft-^oF)} = a_0 + a_1T + a_2T^2 + a_3T^3$$

	Reference	T (Units)	a_0	a_1	a_2
Methanol	(41)	^oF	0.12688	-0.16203×10^{-3}	0.26455×10^{-6}
Methanol	(42)	^oF	0.12954	-0.11801×10^{-3}	0
Methanol	(39)	^oF	0.13082	-0.12885×10^{-3}	0.63015×10^{-7}
Methanol	(35)	^oF	0.14188	-0.31719×10^{-4}	-0.81254×10^{-7}
Toluene	(39)	^oF	0.85713×10^{-1}	-0.87821×10^{-4}	-0.11451×10^{-7}
Toluene	(42)	^oF	0.8595×10^{-1}	-0.92179×10^{-4}	0
Toluene	(41)	^oF	0.84037×10^{-1}	-0.94270×10^{-4}	0.66220×10^{-7}
Toluene	(35)	^oF	0.82272×10^{-1}	-0.9836×10^{-4}	0.55926×10^{-7}
Toluene	(34)	^oF	0.94474×10^{-1}	-0.74691×10^{-4}	0
85 wt % Ethylene Glycol	(43)	^oF	0.16017	0.11198×10^{-3}	-0.12417×10^{-6}
85 wt % Ethylene Glycol	(39)	^oR	0.31854	-0.27845×10^{-2}	0.5417×10^{-7}
50 wt % Ethylene Glycol	(43)	^oR	0.16046	0.30752×10^{-3}	-0.29347×10^{-6}
Heavy Premium Coker	(35)	^oF	0.83998×10^{-1}	-0.46714×10^{-4}	-

TABLE XXVIII (Continued)

$$k_{(Btu/hr\text{-}ft\text{-}^oF)} = a_0 + a_1T + a_2T^2 + a_3T^3$$

	Reference	T (Units)	a_0	a_1	a_2
Heavy Premium Coker	(19)	^oF	0.78087×10^{-1}	-0.51101×10^{-4}	0.10444×10^{-7}
30 wt % Diethanolamine	(43)	^oF	0.23818	0.32519×10^{-3}	-0.37813×10^{-6}
30 wt % Diethanolamine	(51)	^oF	0.23625	0.28898×10^{-3}	-0.29990×10^{-6}
n-Octane	(39)	^oF	0.8243×10^{-1}	-0.98774×10^{-4}	-
n-Octane	(42)	^oF	0.81111×10^{-1}	-0.96006×10^{-4}	-
Water	(22)	^oF	0.30289	0.7029×10^{-3}	-0.1178×10^{-5}
Ethylene Glycol	(44)	^oF	0.1457×10^{-1}	0.42476×10^{-4}	0.40493×10^{-8}

TABLE XXIX

SPECIFIC HEAT EQUATION CONSTANTS FOR TEST FLUIDS

$$Cp_{(Btu/lb-^oF)} = b_0 + b_1T(^oF) + b_2T^2(^oF) + b_3T^3(^oF)$$

	Reference	b_0	b_1	b_2	b_3
Methanol	(41)	0.56115	0.38367×10^{-3}	0.77161×10^{-7}	0
Methanol	(42)	0.55125	0.6801×10^{-3}	-0.4001×10^{-6}	0
Methanol	(39)	0.55156	0.33853×10^{-4}	0.9708×10^{-5}	-0.16226×10^{-7}
Methanol	(38)	0.94107	0.47679×10^{-3}	-0.89024×10^{-6}	0.66483×10^{-8}
Toluene	(39)	0.39604	0.29440×10^{-3}	-0.36689×10^{-6}	0.17319×10^{-8}
Toluene	(42)	0.35999	0.6002×10^{-3}	-0.71232×10^{-14}	0
Toluene	(41)	0.3528	0.73588×10^{-3}	-0.85159×10^{-6}	-
85 wt % Ethylene Glycol	(43)	0.61618	0.25025×10^{-3}	0.25568×10^{-5}	0.53662×10^{-8}
85 wt % Ethylene Glycol	(39)	0.57627	0.81925×10^{-3}	0.88426×10^{-6}	0.11789×15^{-8}
50 wt % Ethylene Glycol	(43)	0.78316	0.31905×10^{-3}	0.12947×10^{-5}	-0.29451×10^{-8}
50 wt % Ethylene Glycol	(39)	0.69192	0.22539×10^{-2}	$-0.1188n \times 10^{-4}$	0.23442×10^{-7}
Heavy Oil Coker*	(35)	0.241	0.3357×10^{-3}	0.47151×10^{-6}	0
Heavy Oil Coker**	(19)	-0.25028×10^{-1}	0.7943×10^{-3}	-0.20603×10^{-6}	0

TABLE XXIX (Continued)

$$Cp_{(Btu/lb-^oF)} = b_0 + b_1T(^oF) + b_2T^2(^oF) + b_3T^3(^oF)$$

	Reference	b_0	b_1	b_2	b_3
30 wt % Diethanolamine	(51)	0.85167	0.25373×10^{-4}	0.10378×10^{-5}	-0.27174×10^{-8}
n-Octane	(39)	0.49579	0.38534×10^{-3}	0.32518×10^{-6}	0
n-Octane	(42)	0.51070	0.20382×10^{-3}	0.51457×10^{-6}	0
Water	(22)	1.01881	-0.4802×10^{-3}	0.3274×10^{-4}	-0.6040×10^{-8}

* Cp in cal/gm-K and T in ^oK
**T in ^oR

TABLE XXX

VISCOSITY EQUATION CONSTANTS FOR TEST FLUIDS

$$\mu_{(centipoise)} = a + bT + cT^2 + dT^3$$

	Reference	T (Units)	a	b	c	d
Methanol	(41)	^oF	0.93871	-0.65583×10^{-2}	0.20264×10^{-4}	-0.2588×10^{-7}
Methanol	(42)	^oF	1.05382	-0.71364×10^{-2}	0.15455×10^{-4}	0
Methanol	(39)	^oF	1.20521	-0.13143×10^{-1}	0.69284×10^{-4}	-0.13531×10^{-6}
Methanol	(35)	^oR	-6.7490*	5256.7*	-319.89*	0
Toluene	(39)	^oF	0.96190	-0.74914×10^{-3}	0.31759×10^{-4}	-0.56290×10^{-7}
Toluene	(42)	^oF	0.873636	-0.44394×10^{-2}	0.75758×10^{-5}	0
Toluene	(41)	^oF	0.94066	-0.67028×10^{-2}	0.24358×10^{-4}	-0.36033×10^{-7}
Toluene	(35)	^oF	-5.8735*	5786.2*	550.0*	0
85 wt % Ethylene Glycol	(35)	^oR	-3.549*	1576.6*	-262.65*	0
85 wt % Ethylene Glycol	(43)	^oF	5.2580	-0.3554×10^{-1}	0.11489×10^{-3}	-0.1668×10^{-6}
85 wt % Ethylene Glycol	(39)	^oR	-2.6719*	1065.9*	-318.99*	-
50 wt % Ethylene Glycol	(35)	^oR	-3.2322*	1012.6*	-305.0*	-
50 wt % Ethylene Glycol	(43)	^oR	-5.25*	2767.7*	-105.6*	-

TABLE XXX (Continued)

$$\mu_{(centipoise)} = a + bT + cT^2 + dT^3$$

	Reference	T (Units)	a	b	c	d
50 wt % Ethylene Glycol	(39)	^oR	-3.6417*	1674.6*	-204.14*	-
Heavy Premium Coker	(35)	^oF	-2.6651*	1223.4*	78.39*	-
Heavy Premium Coker	(19)	^oR	-2.6399*	1241.3*	-398.06*	-
30 wt % Diethanolamine	(35)	^oR	-3.4373*	1290.2*	-250.0*	-
30 wt % Diethanolamine	(51)	^oF	3.5543	-0.2446×15^{-1}	0.50637×10^{-4}	-0.38056×10^{-7}
30 wt % Diethanolamine	(43)	^oF	3.61487	-0.26553×10^{-1}	0.83164×10^{-4}	-0.1602×10^{-6}
n-Octane	(39)	^oF	0.90501	-0.69716×10^{-2}	0.27117×10^{-4}	-0.41279×10^{-7}
n-Octane	(42)	^oF	0.82018	-0.46321×10^{-2}	0.91468×10^{-5}	0
Water	(22)	^oC	1.3272***	0.1053×10^{-2}***	105***	-

*
** Constants for $\ln(\mu) = a + (b/T+c)$
*** μ in lbm/hr-ft
Constants for $\log_{10}(\mu/10^{-3}) = \frac{a(20-T)-b(20-T)^2}{T+c}$ where μ is in NS/s^2

APPENDIX D

NUMERICAL SOLUTION OF WALL TEMPERATURE GRADIENT WITH INTERNAL HEAT GENERATION

A numerical solution of the conduction equation with internal heat generation and variable thermal conductivity and electrical resistivity is presented. The solution was originally developed by Farukhi (21).

Heat Balance on an Incremental Element

Assumptions and Conditions

The following assumptions and conditions are used in deriving the numerical solution (21).

"1. Electrical resistivity of tube wall is a function of temperature.
2. Thermal conductivity of tube wall is a function of temperature.
3. Peripheral and radial wall conduction exist.
4. Axial conduction is negligible.
5. Steady state conditions exist.
6. Heat losses to the atmosphere are present."

The tube wall thickness was divided into ten equal slices (see Figure 21) and the inside surface temperature was obtained directly (since the outside wall temperature was known) by performing heat balances on each node in the radial direction. The tube cross section was divided into quadrant above the axis.

Interior Nodes

Consider the cross-section of a typical interior element as shown in Figure 22.

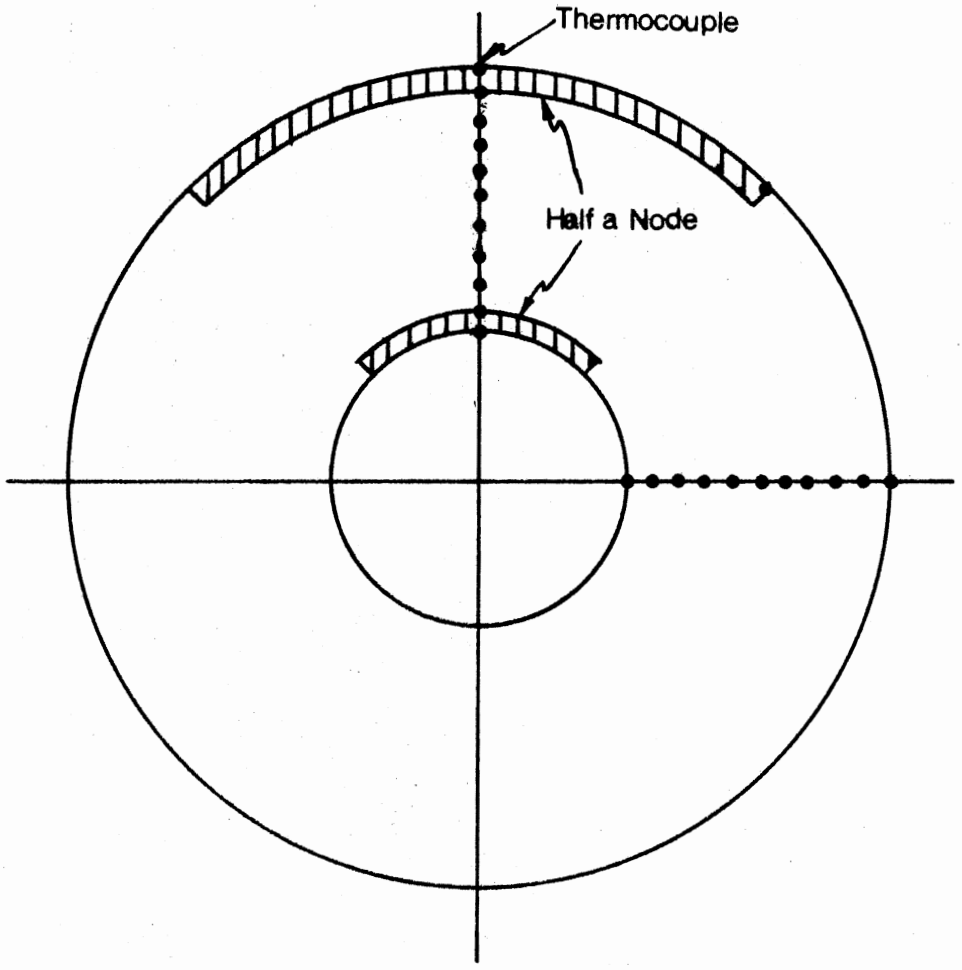

Figure 21. Division of Tube Wall Thickness

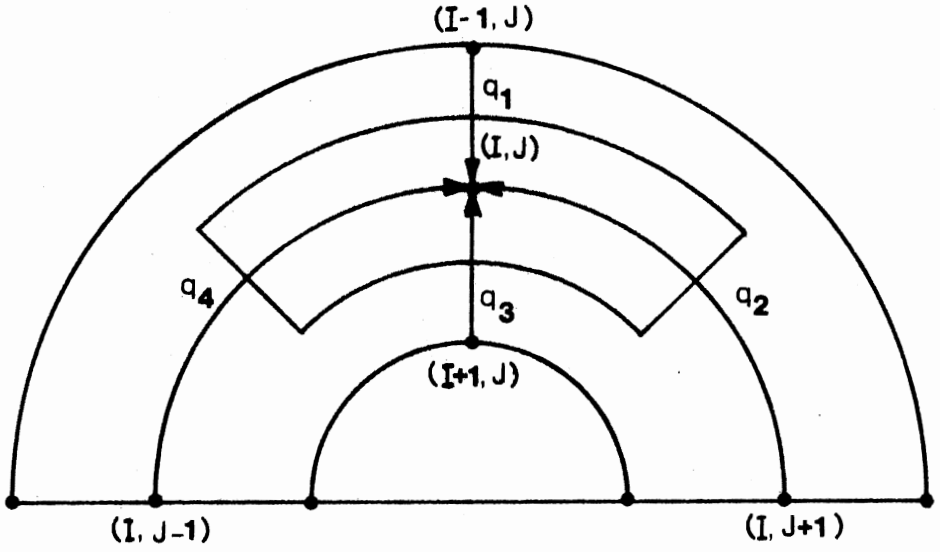

Figure 22. Interior Element

An energy balance on the element gives,

$$\dot{q}_1 + \dot{q}_2 + \dot{q}_3 + \dot{q}_4 + \dot{q}_g = 0 \qquad (D.1)$$

from Fourier's Law we know that

$$\dot{q} = - k A \frac{dT}{dx} \qquad (D.2)$$

Now using subscripts I and J for the radial and peripheral direction respectively (as shown in Figure 22), and writing Fourier's equation for side 1, we obtain

$$\dot{q}_1 = - k_{avg} (r\, d\theta)_{I-\frac{1}{2}} (dz) [T_{I-1,J}] / (r_{I-1} - r_I) \qquad (D.3)$$

where

$$d\theta = \frac{\pi}{2} \quad \text{(four thermocouple locations)}$$

$$r_{I-1} - r_I = \Delta r \quad \text{(taking equal thickness)}$$

$$k_{avg} = (k_{I-1} + k_I) / 2.0$$

$$r_{I-\frac{1}{2}} = \left(r_{I-1} - \frac{\Delta r}{2} \right) \text{ and } r_{I+\frac{1}{2}} = \left(r_{I+1} + \frac{\Delta r}{2} \right).$$

Assuming that heat transfer into the element is positive since Δr is a negative term, the minus sign can be deleted from Equation (D-3).

Substituting the definitions into Equation (D.3) gives

$$\dot{q}_{I-1,J} = (\tfrac{1}{2})(k_{I-1,J} + k_{I,J})(\pi/2)\left(r_{I-1} - \frac{\Delta r}{2}\right) \frac{(T_{I-1,J} - T_{I,J})}{\Delta r} (dz). \qquad (D.4)$$

Similarly for side 3,

$$\dot{q}_{I+1,J} = (\tfrac{1}{2})(k_{I+1,J} + k_{I,J})(\frac{\Pi}{2})(r_{I+1} - \frac{\Delta r}{2})$$

$$(\frac{T_{I+1,J} - T_{I,J}}{\Delta r})\,(dz). \qquad (D.5)$$

Writing Fourier's equation for side 2 gives

$$\dot{q}_2 = \dot{q}_{I,J+1} = k_{avg}(dr)(dz)(T_{I,J+1} - T_{I,J}) / (r_I\, d\theta). \qquad (D.6)$$

Substituting the definitions for some of the variables gives

$$\dot{q}_{I,J+1} = (\tfrac{1}{2})(k_{I,J+1} + k_{I,J})(\Delta r)(\frac{2}{\pi r_I})$$

$$(T_{I,J+1} - T_{I,J})\; dz\,. \qquad (D.7)$$

Similarly for side 4,

$$\dot{q}_{I,J-1} = (\tfrac{1}{2})(k_{I,J-1} + k_{I,J})(\Delta r)(dz)$$

$$(\frac{2}{\pi r_I})(T_{I,J-1} - T_{I,J}). \qquad (D.8)$$

The heat generation term is calculated using Joule's Law as follows:

$$\dot{q}_g = I^2 R \qquad (D.9)$$

where

$$R = \frac{\rho dz}{A_{cs}} \quad (3.41213)$$

ρ = electrical resistivity and a function of temperature at node (I,J)

and

$$A_{cs} = (\tfrac{1}{2})\,\pi r_I\,\Delta r\,. \quad (D\cdot 10)$$

Substituting the above definitions into Equation (D.9) gives

$$\dot{q}_g = (3.412)\left(\frac{2}{\pi r\,\Delta\,r}\right)(\beta)(I^2)\,dz\,. \quad (D.11)$$

Combining Equations (D.4), (D.5), (D.7), (D.8), and (D.11) and rearranging the terms gives:

$$T_{I+1,J} = T_{I,J} - \Big[\frac{3.141213}{(XAREA)}(\rho I^2) + \left(\frac{DPHI}{2\ DELR}\right)(k_{I-1,J} + k_{I,J})$$

$$(r_{I-1} - \frac{DELR}{2})(T_{I-1,J} - T_{I,J}) + \left(\frac{DELR}{2\ DPHI}\right)(k_{I,J-1} + k_{I,J})$$

$$(T_{I,J-1} - T_{I,J})\left(\frac{1}{r_I}\right) + \left(\frac{DELR}{2\ DPHI}\right)(k_{I,J+1} + k_{I,J})$$

$$(T_{I,J+1} - T_{I,J})\left(\frac{1}{r_I}\right)\Big] \Big/ \Big[\left(\frac{DPHI}{2\ DELR}\right)(k_{I+1,J} + k_{I,J})$$

$$(r_{I+1} + \frac{DELR}{2})\Big] \quad (D.12)$$

where

$$DPHI = \pi / 2$$

$$XAREA = r_I \left(\frac{\pi}{2}\right)(\Delta r)$$

$$DELR = \Delta r.$$

Equation (D·12) is used for all the interior elements. For the outside wall element, which is a "half-size" element, Equations (D·5), (D.7), (D.8), and (D.9) are solved simultaneously in conjunction with the following equation, which accounts for the heat loss.

$$\dot{q}_L = \frac{(1/4)\ 2\ \pi\ L\ k_{ins}\ (T_{I,J} - T_{room})}{\ln \frac{d_{ins}}{d_o}} \left(\frac{dz}{L}\right) \qquad (D\cdot13)$$

where

$\dot{q}_L$ = heat loss from the element, Joules/sec

L = Total heated length

k_{ins} = thermal conductivity of insulation, Joules/sec-cm-^{o}C.

For the outside wall node the temperature for nodes (I- 1, J), (I, J +1), and (I,J-1), are known since the first node conditions is given by Equation (D·13) and the other three nodal temperatures are theromocouple readings. Consequently, the temperature at node (I + 1, J) can be calculated. After all the (I + 1, J) temperature values are calculated, successive use of Equation (D.12) gives the temperature at the inside surface.

The above procedure for calculating the inside wall temperature from the measured outer wall temperature was checked and found to agree within 0.2^{o}F with the results of the following Equation (51)

$$T_{w_o} - T_{w_i} = \frac{\dot{q}_{input}}{2 \pi k_{ss} L} \left(\frac{r_o^2 \ln \frac{r_o}{r_i}}{r_o^2 - r_i^2} - \tfrac{1}{2} \right) \qquad (D.14)$$

where

T_{w_o} = outside wall temperature

T_{w_i} = inside wall temperature

k_{ss} = thermal conductivity of stainless steel

r_o = outside tube radius

r_i = inside tube radius

Heat Flux at Inside Wall

The procedure for performing heat balances outlined above gives the radial heat flux at the inside wall when the heat balance is made on the inside surface ("half-size") node. This heat flux value was used in calculating the heat transfer coefficients.

APPENDIX E

HEAT LOSSES

High quality insulation around test section was used to reduce heat losses. The entrance length, test section and exit length were on the axis of a (3½ in.) diameter bed of rigid white hydrous calcium silicate insulation. The thermal conductivity of the insulation is

$$k_{ins} = 3.0812 \times 10^{-5} T_{ins} + 3.86995 \times 10^{-2} \text{ Btu/ft-hr-}^{o}\text{F} \quad (E.1)$$

where

the temperature is in ^{o}F.

Heat loss by way of copper bars was calculated from their dimensions and the assumption that natural convection from the surface to air is controlling.

An attempt to indicate the occurrence of heat losses will be made with reference to Figure 1 as follows:

1. Radial heat flow from entrance length tube through the calcium silicate insulation.

2. Same as No. 1, but for test section.

3. Same as No. 1, but for exit tube.

4. Heat conduction away by the thermocouple leads (negligible)

5. Heat conduction away from entrance of test section through the copper bar.

6. Same as No. 5, but for exit copper bar.

7. Heat conduction away by pressure gauge tubings (neglected).

Using the regular conduction equation and the insulation thermal conductivity Equation (E-1) heat loss for item 1 becomes

$$\dot{q}_{ent} = \frac{2 \pi L_{ent} k_{ins} (T_{w_{in}} - T_I)}{\ln (\frac{d_{ins}}{d_o})} \qquad (E.2)$$

where

$\dot{q}_{ent}$ = heat loss from entrance section

L_{ent} = entrance length of test section

k_{ins} = thermal conductivity of insulation

$T_{w_{in}}$ = outside wall temperature for inlet test section

T_I = temperature at outside surface of insulation.

T_I was eliminated by making use of the natural convection heat transfer coefficient

$$\dot{q}_{ent} = h_c (\pi d_{ins} L_{ent})(T_I - T_{room}) \qquad (E.3)$$

where

h_c = convective heat transfer coefficient.

McAdams (52) gives a free convection correlation from the outside surface of horizontal tubes to air.

$$h_c = 0.5 (\frac{T_I - T_{room}}{d_{ins}})^{0.25} \qquad (E.4)$$

where

$(T_I - T_{room})$ is in ^oF and d_{ins} is in inches.

Heat loss item 2

$$\dot{q}_{test} = \frac{2 \pi L k_{ins} (\bar{T}_{w_o} - T_I)}{\ln (\frac{d_{ins}}{d_o})} \qquad (E.5)$$

where

$\dot{q}_{test}$ = heat loss from test tube section

L = total heated length

$\bar{T}_{w_o}$ = average outside wall temperature for the heated length.

Equation (E.5) is solved for the heat loss in conjunction with Equation (E.4) and replacing the total heated length for the entrance length in Equation (E.3).

Heat loss item 3

$$\dot{q}_{exit} = \frac{2 \pi L_{exit} k_{ins} (T_{w_{out}} - T_I)}{\ln (\frac{d_{ins}}{d_o})} \qquad (E.6)$$

where

$\dot{q}_{exit}$ = heat loss from exit test section

$T_{w_{out}}$ = outside wall temperature for outlet test section.

Equation (E.6) is solved in conjunction with Equation (E.4) and replacing the exit length for the entrance length in Equation (E.3).

Heat loss for items 5 and 6

$$\dot{q}_{cb} = h_{nc} A_{cb} (\bar{T}_{w_{in}} - T_{room}) \qquad (E.7)$$

where

$\dot{q}_{cb}$ = heat loss from copper bar

h_{nc} = convective heat transfer coefficient from plane surfaces

$\bar{T}_{w_{in}}$ = average inside wall temperature

A_{cb} = surface area of copper bar.

The free convection coefficients from the outside vertical surfaces, horizontal upward faces, and horizontal downward faces, are respectively given by McAdams (52) as

$$h_{nc} = 0.28 \left(\frac{\Delta T}{z}\right)^{0.25} \qquad (E.8)$$

$$h_{nc} = 0.38 (\Delta T)^{0.25} \qquad (E.9)$$

$$h_{nc} = 0.2 (\Delta T)^{0.25} \qquad (E\ 10)$$

on an average, the heat loss was found to be of the order of 1.1 percent of heat input.

APPENDIX F

SAMPLE CALCULATIONS

Calculations for experimental data run 541 are presented as a sample calculation. Appendix A gives a listing of the experimental data values for this run. The sample calculations given here are based on the following assumptions and conditions:

1. Electrical resistivity and thermal conductivity of tube walls are functions of temperature.
2. Peripheral and radial wall conduction exist.
3. Axial conduction is negligible.
4. Steady state conditions exist.

Computer programs used by Moshfeghian (22) were modified to perform the calculations on an IBM 370 computer.

Heat Balance Calculations

Heat input rate, Joules/sec = $\dot{q}_{input}$

$$\dot{q}_{input} = (I) \cdot (V)$$

$$= (313.5)(16.81)$$

$$= 5{,}270 \text{ Joules/sec}$$

Heat losses in Joules/sec calculated according to Appendix H are 86.4 Joules/sec.

Heat output rate, Joules/sec = $\dot{q}_{output}$

$$\dot{q}_{output} = \dot{m} \, (Cp) \, [T_{b_{out}} - T_{b_{in}}]$$

The inlet and outlet bulk fluid temperatures measured by the thermocouples were based on their calibration equations. Calibration data for these thermocouples are given in Table XXV in Appendix B.

$$\left\{\begin{matrix}\text{inlet fluid}\\ \text{temperature}\end{matrix}\right\} = 0.99746T_{in} - 0.35678$$

$$= (0.99746)(271.5) - 0.35678$$

$$= 270.5^{o}F = 405.6\ K$$

$$\left\{\begin{matrix}\text{outlet fluid}\\ \text{temperature}\end{matrix}\right\} = 0.99881T_{out} - 0.051831$$

$$= (0.99881)(295.2) + 0.051831$$

$$= 294.9^{o}F = 419.2\ K$$

From Appendix C, for heavy premium coker (gas-oil) and using FPRI data (35)

$$Cp = 0.241 + (0.3357)(10^{-3})\ (T) + (0.47151)(10^{-6})(T^{2})$$

where

$$T = \frac{1}{2}\ (T_{b_{in}} + T_{b_{out}})$$

$$= \frac{1}{2}\ (405.6 + 419.2)$$

$$= 412.4\ K$$

$$Cp = 0.241 + (0.3357)(10^{-3})(412.4) + (0.47151)(10^{-6})(412.4^{2})$$

$$= 0.45963 cal/\ g\text{-}K$$

$$\dot{q}_{output} = (1616.9)(0.4596)(294.9\text{-}270.5)$$

$$= 0.181x10^{5}\ Btu/hr$$

$$= 5{,}305\ Joules/sec$$

$$\text{Percent error in heat balance} = \frac{\dot{q}_{input} - \dot{q}_{output} - \dot{q}_{loss}}{\dot{q}_{input}} \times 100.0$$

$$= \frac{5{,}270 - 5{,}305 - 86.4}{5{,}270} \times 100$$

$$= -2.3\%$$

Similar heat balance calculations were carried out using different sets of heat capacity data for each run.

Calculation of the Local Inside Wall Temperature and the Inside Wall Radial Heat Flux

As indicated in Chapter V, a numerical solution developed by Owhadi (27), and Crain (28) was used to compute the inside wall temperatures and the inside wall radial heat flux at each thermocouple location. The calculations were checked and found to agree with the results of an equation used by Mclaughlin (99) and presented in Appendix D of this thesis. The trial-and-error solution is complex and hence a sample calculation is not presented; however, the derivation of equations which were given by Farukhi (20) are presented in Appendix D.

Tables XXXI to XXXIII give the outside surface temperatures, the computed inside wall temperatures and the inside wall radial heat fluxes for every thermocouple located on the test section.

Local Heat Transfer Coefficient Calculations

The local heat transfer coefficient, h_i, is calculated for thermocouple 4-1 (thermocouple station 4, peripheral position 1):

$$h_4 = \frac{(\dot{q}/A)}{(T_{w_4} - T_{b_4})}$$

$$T_{b_4} = T_{b_{in}} + \left(\frac{L_4}{L_{total}}\right)\left(T_{b_{out}} - T_{b_{in}}\right)$$

$$= 270.5 + \left(\frac{67.65}{84.0}\right)(294.9 - 270.5)$$

$$= 290.1^{\circ}F = 416.5\ K$$

TABLE XXXI

OUTSIDE SURFACE TEMPERATURES FOR RUN 541

Thermocouple* Station Number	Outside Surface Temperature, °F Peripheral Location			
	1	2	3	4
1	357.6	357.5	357.2	358.8
2	358.6	359.2	357.3	359.3
3	364.0	362.7	362.1	364.2
4	364.2	366.0	366.4	336.7

*See the position of each thermocouple on Figure 2.

TABLE XXXII

COMPUTED INSIDE SURFACE TEMPERATURES FOR RUN 541

Thermocouple Station Number	Inside Wall Temperature, °F Peripheral Location			
	1	2	3	4
1	354.2	354.1	353.7	355.4
2	355.2	355.8	353.8	355.9
3	360.6	359.2	358.6	360.8
4	360.7	362.6	362.9	363.3

TABLE XXXIII

RADIAL HEAT FLUX FOR INSIDE SURFACE FOR RUN 541

Thermocouple Station Number	Radial Heat Flux for Inside Surface, Btu/hr-ft^2 Peripheral Location			
	1	2	3	4
1	22,815.9	22,796.6	22,869.6	22,668.0
2	22,834.9	22,713.6	22,938.9	22,705.8
3	22,808.8	22,879.8	22,966.1	22,784.4
4	23,063.7	22,854.2	22,893.3	22,810.1

$$h_i = \frac{23{,}063.7}{(360.7-290.1)}$$

$$= 326.8 \text{ Btu/hr-ft}^2\text{-}^\circ\text{F}$$

$$= 1{,}855.7 \text{ Joule/sec-m}^2\text{-K}$$

Results of the calculations for the local heat transfer coefficient at the other thermocouple locations at station 4 are presented in Table XXIV.

The peripheral average heat transfer coefficient at station 4 is calculated as follows:

$$\bar{h} = (\tfrac{1}{4}) \sum_{i=1}^{4} h_i$$

$$= (\tfrac{1}{4})(326.8 + 315.6 + 314.4 + 311.9)$$

$$= 317.2 \text{ Btu/hr-ft}^2\text{-}^\circ\text{F}$$

$$= 1801.1 \text{ Joules/sec-m}^2\text{-K}$$

Calculation of Relevant Dimensionless Numbers at Station 4

Physical Properties:

Using the two sets of physical property data given in Appendix C, viscosity, specific heat, density, thermal conductivity, and thermal expansion coefficient of heavy oil were calculated. Sample calculations are presented for FPRI (35) physical property data, and results are tabulated and compared with API (19) physical property data.

1. Viscosity

$$\mu_{(T)} = \exp(-2.6651 + (1223.4/(T+78.39)))$$

TABLE XXXIV

PERIPHERAL HEAT TRANSFER COEFFICIENT
AT STATION 4 FOR RUN 541

	Peripheral Location			
	1	2	3	4
h, Btu/(hr-ft^2-^{o}F)	326.8 (Top)	315.6	314.4 (Bottom)	311.9

where T is ^{o}F and μ in centipoise

at $T_{b_4} = 290.1^{o}F$

$$\mu_b = \exp\ (-2.6651 + (1223.4/(290.1 + 78.39)))$$

$$\mu_b = 1.9243 \text{ centipoise} = 1.9243 \times 10^{-3} \text{ gr/(cm-sec)}.$$

Similarly, for average inside surface temperature, $\overline{T}_{w_i}$:

$$\overline{T}_{w_i} = (\tfrac{1}{4}) \sum_{i=1}^{4} (T_{w_i})$$

$$= (\tfrac{1}{4})(360.7 + 362.6 + 362.9 + 363.3)$$

$$= 362.4^{o}F$$

$$\mu_w = 1.1169 \text{ centiposie} = 1.1169 \times 10^{-3} \text{ gr/(cm-sec)}.$$

Also, for average film temperature, $\overline{T}_F$

$$\overline{T}_F = (\overline{T}_{w_i} + T_{b_4})/2$$

$$= 326.3^{o}F$$

$$\mu_F = 1.4309 \text{ centipoise} = 1.4309 \times 10^{-3} \text{ gr/(cm-sec)}.$$

2. Specific Heat:

$$Cp = 0.241 + (0.3357)(10^{-3})(T) + (0.47151)(10^{-6})(T^2)$$

where T is K and Cp is in cal/(gr-K)

at $T_{b_4} = 416.5$ K

$$Cp_b = 0.241 + (0.3357)(10^{-3})(416.5) + (0.47151)(10^{-6})(416.5)^2$$

$$= 0.4627 \text{ cal/(gr-K)}$$

$$= 1.8772 \text{ Joules/(gr-K)}$$

Similarly at $\overline{T}_F = 436.7$K

$$Cp_F = 0.4\text{-}75 \text{ cal/(gr-K)}$$

$$= 1.9372 \text{ Joules/(gr-K)}.$$

3. Density

$$\rho = (A)(B)^{-(1-T/C)^{(2/7)}}$$

$A = 0.35325$, $B = 0.29051$, $C = 1620.3$

where T is ^{o}R and ρ is in gm/cm^3

at $T_{b_4} = 749.8^{o}R$

$$\rho_b = (0.35325)(0.29051)^{-\left(1-\frac{749.8}{1620.3}\right)^{(2/7)}}$$

$$= 0.9945 - gm/cm^3$$

Similarly at $T_F = 786.0^{o}R$

$$\rho_F = 0.9821\ gms/cm^3$$

4. Thermal Conductivity

$$k = 0.083998 - (4.6714)(10^{-5})(T)$$

where T is ^{o}F and k is in $Btu/(hr\text{-}ft\text{-}^{o}F)$

at $T_{b_4} = 290.1^{o}F$

$$k = 0.083998 - (4.6714)(10^{-5})(290.1)$$

$$k = 0.07045\ Btu/(hr\text{-}ft\text{-}^{o}F)$$

$$= 0.12193\ Joules/(sec\text{-}cm\text{-}^{o}C)$$

Similarly at $T_F = 326.3^{o}F$

$$k_F = 0.06876\ Btu/(hr\text{-}ft\text{-}^{o}F)$$

$$= 0.11901\ Joules/(sec\text{-}cm\text{-}^{o}C)$$

5. Thermal Expansion Coefficient

$$\beta = -\frac{1}{\rho}\frac{d\rho}{dT}$$

$$\frac{d\rho}{dT} = (\rho)(2)\left(1 - \frac{T}{C}\right)^{\left(-\frac{5}{7}\right)} \ln\beta/(7C)$$

at $T_{b_4} = 749.8^{\circ}R$

$$\beta = -(2)\left(1 - \frac{749.8}{1620.3}\right)^{-(\frac{5}{7})} \ln(0.29051)/(7)(1620.3)$$

$$\beta = 3.3973\text{x}10^{-4}(1/^{\circ}R)$$

Dimensionless Numbers:

1. Reynolds Number: Re

$$Re_b = (d_i)(G)/\mu_b$$

where $G = \dot{m}/(\pi d_i^2/4)$

$$= 1616.9/(\pi(.43/12)^2/4)$$

$$= 1.603\text{x}10^6 \text{ lbm/(hr-ft}^2)$$

$$Re_b = (.43/12)(1.603\text{x}10^6)/(1.9243)(2.42)$$

$$= 1.23\text{x}10^4$$

Similarly $Re_F = 1.66\text{x}10^4$

2. Prandtl Number: Pr

$$Pr_b = (Cp)(\mu)/k$$

$$= (0.4627)(1.9243)(2.42)/(0.07045)$$

$$= 30.6$$

Similarly $Pr_w = 19.8$

3. Peripheral Average Nusselt Number

$$Nu = (\bar{h})(d_i)/k$$

$$= (317.2)(.43/12)/(0.7045)$$

$$= 161.3$$

4. Grashof Number: Gr

$$Gr = (d_i^3)(\rho^2)(g)(\beta)(\bar{T}_w - T_b)/(\mu^2)$$

where $G = 4.17\text{x}10^8 \text{ ft/hr}^2$

$$Gr = (.43/12)^3(62.08)^2(4.17\text{x}10^8)(3.3973\text{x}10^4)(822.1-749.8)/$$
$$(1.9243)^2(2.42)^2$$

$$= 0.84\text{x}10^5.$$

5. Gr/Re^2

$$Gr/Re^2 = (0.84x10^5)/(1.23x10^4)^2$$

$$= 5.60x10^{-4}$$

6. Graetz Number: Gz

$$Gz = (\dot{m})(Cp)/(K)(L)$$

$$= (1616.9)(0.4627)/(0.07045)(67.51/12)$$

$$= .189x10^4$$

7. Dimensionless Axial Distance: X^*

$$X^* = \pi/(4(Gz)$$

$$X^* = 4.16x10^{-4}$$

Table XXXV gives a comparison of the dimensionless numbers computed using FPRI and API physical property data.

TABLE XXXV

COMPARISON OF DIMENSIONLESS NUMBERS COMPUTED USING FPRI AND API PHYSICAL PROPERTY DATA FOR RUN 541

Dimensionless Number	Computed Using FPRI Data	Computed Using API Data
Re	$1.23x10^4$	$2.36x10^4$
Pr	30.6	17.2
Nu	161.3	177.0
Gr	$0.84x10^5$	$0.38x10^6$
Gr/Re^2	$5.6x10^{-4}$	$6.78x10^{-4}$
Gz	$0.189x10^4$	$0.204x10^4$
X^*	$4.16x10^{-4}$	$3.85x10^{-4}$

Comparison of Experimental Data with Literature

Heat transfer coefficients are calculated using available literature equations, FPRI physical property data, and API physical property data. Results of the calculations are compared with experimental data.

1. Sieder-Tate equation

   a. Using FPRI physical property data

$$\bar{h}_{ST} = 0.023(k/d_i)(Re^{0.8})(Pr^{0.333})(\mu_b/\mu_w)^{0.14}$$

$$= (0.023)(0.0705/(0.43/12))(1.23\times10^4)^{0.8}(30.6)^{0.333}$$

$$(1.924/1.117)^{0.14}$$

$$= 285.1 \text{ Btu/(hr-ft}^2\text{-}^\circ\text{F)}$$

$$= 1618.9 \text{ J/m}^2\text{.S.K}$$

At Station 4 the peripheral average heat transfer coefficient was calculated to be 317.2 Btu/hr-ft^2-$^\circ$F.

$$\text{ratio of heat transfer coefficients (experimental to Sieder-Tate)} = \frac{317.2}{285.1} = 1.11$$

   b. Similarly using API physical property data

$$\bar{h}_{ST} = 368.6 \text{ Btu/(hr-ft}^2\text{-}^\circ\text{F)}$$

$$\text{ratio of heat transfer coefficients (experimental to Sieder-Tate)} = \frac{317.2}{368.6} = 0.86$$

2. Dittus-Boelter equation

   a. Using FPRI physical property data

$$\bar{h}_{DB} = 0.023(k/d_i)(Re^{0.8})(Pr^{0.4})$$

$$= (0.023)(0.0705/(0.43/12))(1.23\times10^4)^{0.8}(30.6)^{0.4}$$

$$\bar{h}_{DB} = 332.3 \text{ (Btu/hr-ft}^2\text{-}^\circ\text{F)}$$

$$= 1886.9 \text{ J/m}^2\text{.S.K}$$

ratio of heat transfer coefficient (experimental to Dittus-Boelter) $= \frac{317.2}{332.3} = 0.95$

b. Using API data

$\bar{h}_{DB} = 406.7$ (Btu/hr-ft^2-^{o}F)

$= 2309.3$ J/m^2.S.K

ratio of heat transfer coefficient (experimental to Dittus-Boelter) $= 0.78$

3. Petukhov correlation

a. Using FPRI physical property data

$f = (1.82 \log Re - 1.64)^{-2}$

$$\bar{h}_{PK} = \left[(k/d_i)(Re)(Pr)(f/8) \Big/ (1.07+12.7(Pr^{2/3}-1)(\sqrt{f/8}))\right] \left(\frac{\mu_b}{\mu_w}\right)^{0.11}$$

$f = (1.82 \log 1.23 \times 10^4 - 1.64)^{-2}$

$f = 0.0297$

$$\bar{h}_{PK} = \left[(0.0705/(0.43/12))(1.23\times10^4)(30.6)(0.0297/8) \Big/ (1.07+12.7((30.6)^{2/3}-1)(0.0297/8))\right] (1.924/1.117)^{0.11}$$

$\bar{h}_{PK} = 373.2$ Btu/(hr-ft^2-^{o}F)

$= 2119.1$ J/m^2.S.K

ratio of heat transfer coefficient (experimental to Petukhov) $= \frac{317.2}{373.2} = 0.85$

b. Using API data

$\bar{h}_{PK} = 480.6$ Btu/(hr-ft^2-^{o}F)

$= 2729.0$ J/m^2.S.K

ratio of heat transfer coefficient (experimental to Petukhov) $= \frac{317.2}{480.6} = 0.66$

APPENDIX G

CALCULATED RESULTS

LIT(1) = Ratio of the experimental heat transfer coefficient (H_1) to that predicted by Sieder-Tate correlation (for Re > 2100).

LIT(1) = Ratio of the experimental heat transfer coefficient (H_1) to that predicted by Morcos-Bergles correlation (for Re < 2100)

LIT(2) = Ratio of the experimental heat transfer coefficient (H_1) to that predicted by Dittus-Boelter (for Re > 2100).

LIT(2) = Ratio of the experimental heat transfer coefficient (H_2) to that predicted by Morcos-Bergles correlation (for Re < 2100).

LIT(3) = Ratio of the experimental heat transfer coefficient (H_1) to that predicted by Petukhov correlation (for Re > 2100).

The calculated results for those experimental runs which were presented in Appendix A are presented here. The rest of the calculated results are available at:

School of Chemical Engineering
Oklahoma State University
Stillwater, Oklahoma 74074 USA

RUN NUMBER 702

AVERAGE REYNOLDS NUMBER	= 0.216E 05	
AVERAGE PRANDTL NUMBER	= 0.884E 01	
MASS FLUX	= 0.710E 06	LBM/(SQ.FT-HR)
AVERAGE HEAT FLUX	= 0.356E 04	BTU/(SQ.FT-HR)
Q=AMP*VOLT	= 0.312E 04	BTU/HR
Q=MW*CP*(TOUT-TIN)	= 0.327E 04	BTU/HR
HEAT LOST	= 0.379E 00	BTU/HR
HEAT BALANCE ERROR %	=-0.486E 01	

PERIPHERAL HEAT TRANSFER COEFFICIENT BTU/(SQ.FT-HR-DEG.F)

	1	2	3	4
1	321.8	328.1	330.5	339.5
2	321.4	331.5	333.7	335.4
3	321.8	331.5	333.9	336.0
4	318.3	328.1	326.9	332.0

AVERAGE HEAT TRANSFER COEFFICIENT-BTU/(SQ.FT.HR-DEG.F)

	1	2	3	4
(H1)	320.8	329.8	331.2	335.7
(H2)	320.8	329.8	331.2	335.7
LIT(1)	1.17	1.20	1.20	1.21
LIT(2)	1.02	1.05	1.05	1.06
LIT(3)	0.92	0.94	0.94	0.95

RUN NUMBER 705

AVERAGE REYNOLDS NUMBER	= 0.329E 05	
AVERAGE PRANDTL NUMBER	= 0.819E 01	
MASS FLUX	= 0.972E 06	LBM/(SQ.FT-HR)
AVERAGE HEAT FLUX	= 0.996E 04	BTU/(SQ.FT-HR)
Q=AMP*VOLT	= 0.787E 04	BTU/HR
Q=MW*CP*(TOUT-TIN)	= 0.807E 04	BTU/HR
HEAT LOST	= 0.257E 02	BTU/HR
HEAT BALANCE ERROR %	=-0.284E 01	

PERIPHERAL HEAT TRANSFER COEFFICIENT BTU/(SQ.FT-HR-DEG.F)

	1	2	3	4
1	444.9	456.9	455.4	469.3
2	442.0	450.9	465.1	466.3
3	444.9	464.4	470.6	461.7
4	437.4	448.4	455.1	456.2

AVERAGE HEAT TRANSFER COEFFICIENT-BTU/(SQ.FT.HR-DEG.F)

	1	2	3	4
(H1)	442.3	455.2	461.5	463.4
(H2)	442.3	455.1	461.5	463.3
LIT(1)	1.20	1.22	1.23	1.23
LIT(2)	1.06	1.08	1.09	1.09
LIT(3)	0.93	0.95	0.96	0.95

RUN NUMBER 710

AVERAGE REYNOLDS NUMBER	= 0.577E 05	
AVERAGE PRANDTL NUMBER	= 0.618E 01	
MASS FLUX	= 0.111E 07	LBM/(SQ.FT-HR)
AVERAGE HEAT FLUX	= 0.412E 05	BTU/(SQ.FT-HR)
Q=AMP*VOLT	= 0.327E 05	BTU/HR
Q=MW*CP*(TOUT-TIN)	= 0.322E 05	BTU/HR
HEAT LOST	= 0.155E 03	BTU/HR
HEAT BALANCE ERROR %	= 0.823E 00	

PERIPHERAL HEAT TRANSFER COEFFICIENT BTU/(SQ.FT-HR-DEG.F)

	1	2	3	4
1	581.6	606.2	605.0	629.2
2	585.9	602.3	620.4	621.5
3	594.5	609.4	631.0	627.9
4	578.1	595.1	603.5	614.8

AVERAGE HEAT TRANSFER COEFFICIENT-BTU/(SQ.FT.HR-DEG.F)

	1	2	3	4
(H1)	585.0	603.2	615.0	623.3
(H2)	585.0	603.2	614.8	623.3
LIT(1)	1.18	1.20	1.20	1.20
LIT(2)	1.09	1.11	1.11	1.11
LIT(3)	0.93	0.94	0.94	0.94

RUN NUMBER 708

AVERAGE REYNOLDS NUMBER	= 0.451E 05	
AVERAGE PRANDTL NUMBER	= 0.729E 01	
MASS FLUX	= 0.112E 07	LBM/(SQ.FT-HR)
AVERAGE HEAT FLUX	= 0.215E 05	BTU/(SQ.FT-HR)
Q=AMP*VOLT	= 0.170E 05	BTU/HR
Q=MW*CP*(TOUT-TIN)	= 0.170E 05	BTU/HR
HEAT LOST	= 0.697E 02	BTU/HR
HEAT BALANCE ERROR %	=-0.572E 00	

PERIPHERAL HEAT TRANSFER COEFFICIENT BTU/(SQ.FT-HR-DEG.F)

	1	2	3	4
1	541.0	561.9	559.8	577.1
2	545.6	555.9	569.6	567.4
3	549.1	563.6	575.4	570.0
4	539.2	550.9	554.2	560.5

AVERAGE HEAT TRANSFER COEFFICIENT-BTU/(SQ.FT.HR-DEG.F)

	1	2	3	4
(H1)	543.7	558.1	564.7	568.8
(H2)	543.7	558.1	564.6	568.7
LIT(1)	1.22	1.24	1.24	1.23
LIT(2)	1.09	1.11	1.11	1.11
LIT(3)	0.94	0.96	0.96	0.96

RUN NUMBER 606

AVERAGE REYNOLDS NUMBER	= 0.153E 05	
AVERAGE PRANDTL NUMBER	= 0.107E 02	
MASS FLUX	= 0.140E 07	LBM/(SQ.FT-HR)
AVERAGE HEAT FLUX	= 0.780E 04	BTU/(SQ.FT-HR)
Q=AMP*VOLT	= 0.621E 04	BTU/HR
Q=MW*CP*(TOUT-TIN)	= 0.643E 04	BTU/HR
HEAT LOST	= 0.581E 02	BTU/HR
HEAT BALANCE ERROR %	=-0.462E 01	

PERIPHERAL HEAT TRANSFER COEFFICIENT BTU/(SQ.FT-HR-DEG.F)

	1	2	3	4
1	1182.0	1261.1	1181.2	1332.3
2	1159.9	1196.5	1239.7	1237.5
3	1201.7	1218.8	1285.9	1241.5
4	1106.2	1196.5	1141.6	1177.0

AVERAGE HEAT TRANSFER COEFFICIENT-BTU/(SQ.FT.HR-DEG.F)

	1	2	3	4
(H1)	1162.4	1218.2	1212.1	1247.1
(H2)	1161.4	1217.7	1209.8	1244.8
LIT(1)	1.34	1.39	1.38	1.41
LIT(2)	1.15	1.20	1.19	1.22
LIT(3)	1.05	1.09	1.08	1.10

RUN NUMBER 607

AVERAGE REYNOLDS NUMBER	= 0.162E 05	
AVERAGE PRANDTL NUMBER	= 0.101E 02	
MASS FLUX	= 0.140E 07	LBM/(SQ.FT-HR)
AVERAGE HEAT FLUX	= 0.111E 05	BTU/(SQ.FT-HR)
Q=AMP*VOLT	= 0.884E 04	BTU/HR
Q=MW*CP*(TOUT-TIN)	= 0.900E 04	BTU/HR
HEAT LOST	= 0.635E 02	BTU/HR
HEAT BALANCE ERROR %	=-0.255E 01	

PERIPHERAL HEAT TRANSFER COEFFICIENT BTU/(SQ.FT-HR-DEG.F)

	1	2	3	4
1	1188.2	1266.9	1204.1	1332.1
2	1185.9	1219.6	1278.1	1263.6
3	1216.3	1251.5	1311.3	1266.9
4	1133.3	1205.1	1203.4	1204.3

AVERAGE HEAT TRANSFER COEFFICIENT-BTU/(SQ.FT.HR-DEG.F)

	1	2	3	4
(H1)	1180.9	1235.8	1249.2	1266.7
(H2)	1180.2	1235.3	1247.6	1265.3
LIT(1)	1.32	1.37	1.37	1.38
LIT(2)	1.15	1.19	1.19	1.20
LIT(3)	1.03	1.07	1.07	1.08

RUN NUMBER 613

AVERAGE REYNOLDS NUMBER	= 0.255E 05	
AVERAGE PRANDTL NUMBER	= 0.601E 01	
MASS FLUX	= 0.132E 07	LBM/(SQ.FT-HR)
AVERAGE HEAT FLUX	= 0.280E 05	BTU/(SQ.FT-HR)
Q=AMP*VOLT	= 0.222E 05	BTU/HR
Q=MW*CP*(TOUT-TIN)	= 0.220E 05	BTU/HR
HEAT LOST	= 0.117E 03	BTU/HR
HEAT BALANCE ERROR %	= 0.102E 00	

PERIPHERAL HEAT TRANSFER COEFFICIENT BTU/(SQ.FT-HR-DEG.F)

	1	2	3	4
1	1357.7	1440.4	1416.3	1511.3
2	1356.0	1383.8	1446.3	1449.8
3	1372.3	1408.8	1464.5	1443.9
4	1300.7	1369.0	1362.0	1410.0

AVERAGE HEAT TRANSFER COEFFICIENT-BTU/(SQ.FT.HR-DEG.F)

	1	2	3	4
(H1)	1346.7	1400.5	1422.3	1453.8
(H2)	1346.2	1400.0	1421.3	1452.9
LIT(1)	1.21	1.23	1.22	1.23
LIT(2)	1.11	1.13	1.12	1.13
LIT(3)	0.97	0.99	0.99	0.99

RUN NUMBER 616

AVERAGE REYNOLDS NUMBER	= 0.230E 05	
AVERAGE PRANDTL NUMBER	= 0.618E 01	
MASS FLUX	= 0.123E 07	LBM/(SQ.FT-HR)
AVERAGE HEAT FLUX	= 0.431E 05	BTU/(SQ.FT-HR)
Q=AMP*VOLT	= 0.341E 05	BTU/HR
Q=MW*CP*(TOUT-TIN)	= 0.355E 05	BTU/HR
HEAT LOST	= 0.125E 03	BTU/HR
HEAT BALANCE ERROR %	=-0.452E 01	

PERIPHERAL HEAT TRANSFER COEFFICIENT BTU/(SQ.FT-HR-DEG.F)

	1	2	3	4
1	1146.0	1217.8	1226.8	1307.0
2	1141.5	1192.7	1229.1	1263.2
3	1149.4	1253.2	1262.5	1256.8
4	1111.8	1178.2	1198.7	1235.2

AVERAGE HEAT TRANSFER COEFFICIENT-BTU/(SQ.FT.HR-DEG.F)

	1	2	3	4
(H1)	1137.2	1210.5	1229.3	1265.6
(H2)	1137.0	1209.9	1228.9	1265.1
LIT(1)	1.09	1.13	1.09	1.09
LIT(2)	1.02	1.06	1.03	1.03
LIT(3)	0.88	0.91	0.89	0.89

RUN NUMBER 619

AVERAGE REYNOLDS NUMBER	= 0.101E 05	
AVERAGE PRANDTL NUMBER	= 0.142E 02	
MASS FLUX	= 0.121E 07	LBM/(SQ.FT-HR)
AVERAGE HEAT FLUX	= 0.707E 04	BTU/(SQ.FT-HR)
Q=AMP*VOLT	= 0.560E 04	BTU/HR
Q=MW*CP*(TOUT-TIN)	= 0.602E 04	BTU/HR
HEAT LOST	= 0.361E 02	BTU/HR
HEAT BALANCE ERROR %	=-0.803E 01	

PERIPHERAL HEAT TRANSFER COEFFICIENT BTU/(SQ.FT-HR-DEG.F)

	1	2	3	4
1	768.5	793.5	785.7	843.8
2	748.7	781.9	794.4	810.0
3	768.6	813.9	805.6	811.5
4	739.9	772.2	765.5	799.7

AVERAGE HEAT TRANSFER COEFFICIENT-BTU/(SQ.FT.HR-DEG.F)

	1	2	3	4
(H1)	756.4	790.4	787.8	816.2
(H2)	756.3	790.1	787.6	815.9
LIT(1)	1.13	1.17	1.15	1.19
LIT(2)	0.96	1.00	0.98	1.01
LIT(3)	0.88	0.92	0.90	0.93

RUN NUMBER 623

AVERAGE REYNOLDS NUMBER	= 0.226E 05	
AVERAGE PRANDTL NUMBER	= 0.561E 01	
MASS FLUX	= 0.110E 07	LBM/(SQ.FT-HR)
AVERAGE HEAT FLUX	= 0.316E 05	BTU/(SQ.FT-HR)
Q=AMP*VOLT	= 0.250E 05	BTU/HR
Q=MW*CP*(TOUT-TIN)	= 0.247E 05	BTU/HR
HEAT LOST	= 0.126E 03	BTU/HR
HEAT BALANCE ERROR %	= 0.660E 00	

PERIPHERAL HEAT TRANSFER COEFFICIENT BTU/(SQ.FT-HR-DEG.F)

	1	2	3	4
1	1097.7	1163.5	1146.3	1227.2
2	1100.8	1142.4	1183.0	1185.1
3	1123.7	1207.6	1214.3	1191.7
4	1079.8	1137.8	1131.5	1170.5

AVERAGE HEAT TRANSFER COEFFICIENT-BTU/(SQ.FT.HR-DEG.F)

	1	2	3	4
(H1)	1100.5	1162.8	1168.8	1193.6
(H2)	1100.3	1162.2	1168.0	1193.3
LIT(1)	1.11	1.15	1.12	1.13
LIT(2)	1.02	1.06	1.04	1.04
LIT(3)	0.90	0.93	0.92	0.92

RUN NUMBER 509

AVERAGE REYNOLDS NUMBER	= 0.716E 03	
AVERAGE PRANDTL NUMBER	= 0.364E 03	
MASS FLUX	= 0.143E 07	LBM/(SQ.FT-HR)
AVERAGE HEAT FLUX	= 0.361E 04	BTU/(SQ.FT-HR)
Q=AMP*VOLT	= 0.293E 04	BTU/HR
Q=MW*CP*(TOUT-TIN)	= 0.303E 04	BTU/HR
HEAT LOST	= 0.872E 02	BTU/HR
HEAT BALANCE ERROR %	=-0.638E 01	

PERIPHERAL HEAT TRANSFER COEFFICIENT BTU/(SQ.FT-HR-DEG.F)

	1	2	3	4
1	60.0	51.8	46.6	45.5
2	62.9	54.6	50.5	48.9
3	67.1	56.1	49.5	46.4
4	62.7	52.9	43.2	39.3

AVERAGE HEAT TRANSFER COEFFICIENT-BTU/(SQ.FT.HR-DEG.F)

	1	2	3	4
(H1)	63.2	53.9	47.4	45.0
(H2)	63.1	53.8	47.4	44.9
LIT(1)	2.28	1.83	1.53	1.41
LIT(2)	2.28	1.83	1.52	1.41

RUN NUMBER 510

AVERAGE REYNOLDS NUMBER	= 0.906E 03	
AVERAGE PRANDTL NUMBER	= 0.294E 03	
MASS FLUX	= 0.144E 07	LBM/(SQ.FT-HR)
AVERAGE HEAT FLUX	= 0.479E 04	BTU/(SQ.FT-HR)
Q=AMP*VOLT	= 0.388E 04	BTU/HR
Q=MW*CP*(TOUT-TIN)	= 0.389E 04	BTU/HR
HEAT LOST	= 0.107E 03	BTU/HR
HEAT BALANCE ERROR %	=-0.316E 01	

PERIPHERAL HEAT TRANSFER COEFFICIENT BTU/(SQ.FT-HR-DEG.F)

	1	2	3	4
1	60.1	51.8	46.6	44.0
2	65.0	56.5	52.9	51.5
3	70.5	59.1	52.4	49.5
4	64.6	54.8	44.1	40.6

AVERAGE HEAT TRANSFER COEFFICIENT-BTU/(SQ.FT.HR-DEG.F)

	1	2	3	4
(H1)	65.0	55.5	49.0	46.4
(H2)	64.9	55.5	48.9	46.2
LIT(1)	2.05	1.65	1.37	1.26
LIT(2)	2.05	1.64	1.37	1.26

RUN NUMBER 516

AVERAGE REYNOLDS NUMBER	= 0.610E 03	
AVERAGE PRANDTL NUMBER	= 0.307E 03	
MASS FLUX	= 0.101E 07	LBM/(SQ.FT-HR)
AVERAGE HEAT FLUX	= 0.739E 04	BTU/(SQ.FT-HR)
Q=AMP*VOLT	= 0.596E 04	BTU/HR
Q=MW*CP*(TOUT-TIN)	= 0.557E 04	BTU/HR
HEAT LOST	= 0.141E 03	BTU/HR
HEAT BALANCE ERROR %	= 0.437E 01	

PERIPHERAL HEAT TRANSFER COEFFICIENT BTU/(SQ.FT-HR-DEG.F)

	1	2	3	4
1	60.3	50.9	42.2	40.3
2	63.6	54.6	51.2	49.0
3	67.5	58.8	55.0	53.8
4	63.8	55.4	48.1	46.0

AVERAGE HEAT TRANSFER COEFFICIENT-BTU/(SQ.FT.HR-DEG.F)

	1	2	3	4
(H1)	63.8	54.9	49.1	47.3
(H2)	63.7	54.8	48.9	47.1
LIT(1)	1.77	1.42	1.19	1.11
LIT(2)	1.77	1.41	1.18	1.10

RUN NUMBER 513

AVERAGE REYNOLDS NUMBER	= 0.132E 04	
AVERAGE PRANDTL NUMBER	= 0.155E 03	
MASS FLUX	= 0.106E 07	LBM/(SQ.FT-HR)
AVERAGE HEAT FLUX	= 0.377E 04	BTU/(SQ.FT-HR)
Q=AMP*VOLT	= 0.311E 04	BTU/HR
Q=MW*CP*(TOUT-TIN)	= 0.301E 04	BTU/HR
HEAT LOST	= 0.135E 03	BTU/HR
HEAT BALANCE ERROR %	=-0.125E 01	

PERIPHERAL HEAT TRANSFER COEFFICIENT BTU/(SQ.FT-HR-DEG.F)

	1	2	3	4
1	49.7	42.6	38.4	36.0
2	57.0	49.7	48.2	48.0
3	64.2	54.3	49.1	47.3
4	56.6	48.5	39.5	37.6

AVERAGE HEAT TRANSFER COEFFICIENT-BTU/(SQ.FT.HR-DEG.F)

	1	2	3	4
(H1)	56.9	48.8	43.8	42.2
(H2)	56.6	48.6	43.6	42.0
LIT(1)	1.56	1.26	1.07	1.01
LIT(2)	1.55	1.25	1.07	1.01

RUN NUMBER 518

AVERAGE REYNOLDS NUMBER	= 0.165E 03	
AVERAGE PRANDTL NUMBER	= 0.920E 03	
MASS FLUX	= 0.866E 05	LBM/(SQ.FT-HR)
AVERAGE HEAT FLUX	= 0.368E 04	BTU/(SQ.FT-HR)
Q=AMP*VOLT	= 0.296E 04	BTU/HR
Q=MW*CP*(TOUT-TIN)	= 0.283E 04	BTU/HR
HEAT LOST	= 0.587E 02	BTU/HR
HEAT BALANCE ERROR %	= 0.244E 01	

PERIPHERAL HEAT TRANSFER COEFFICIENT BTU/(SQ.FT-HR-DEG.F)

	1	2	3	4
1	57.8	51.0	48.4	46.9
2	56.7	49.3	43.7	41.6
3	56.9	47.9	42.6	39.8
4	55.8	47.5	40.8	38.4

AVERAGE HEAT TRANSFER COEFFICIENT-BTU/(SQ.FT.HR-DEG.F)

	1	2	3	4
(H1)	56.8	48.9	43.9	41.7
(H2)	56.8	48.9	43.8	41.6
LIT(1)	2.48	2.00	1.70	1.57
LIT(2)	2.48	2.00	1.70	1.57

RUN NUMBER 519

AVERAGE REYNOLDS NUMBER	= 0.974E 02	
AVERAGE PRANDTL NUMBER	= 0.146E 04	
MASS FLUX	= 0.822E 06	LBM/(SQ.FT-HR)
AVERAGE HEAT FLUX	= 0.230E 04	BTU/(SQ.FT-HR)
Q=AMP*VOLT	= 0.185E 04	BTU/HR
Q=MW*CP*(TOUT-TIN)	= 0.189E 04	BTU/HR
HEAT LOST	= 0.403E 02	BTU/HR
HEAT BALANCE ERROR %	=-0.431E 01	

PERIPHERAL HEAT TRANSFER COEFFICIENT BTU/(SQ.FT-HR-DEG.F)

	1	2	3	4
1	50.5	44.1	40.1	38.9
2	50.0	42.6	37.8	35.4
3	50.8	42.6	38.2	35.5
4	49.5	42.2	36.1	33.8

AVERAGE HEAT TRANSFER COEFFICIENT-BTU/(SQ.FT.HR-DEG.F)

	1	2	3	4
(H1)	50.2	42.9	38.1	35.9
(H2)	50.2	42.9	38.0	35.8
LIT(1)	2.65	2.14	1.81	1.66
LIT(2)	2.65	2.14	1.81	1.66

RUN NUMBER 540

AVERAGE REYNOLDS NUMBER	= 0.108E 05	
AVERAGE PRANDTL NUMBER	= 0.328E 02	
MASS FLUX	= 0.153E 07	LBM/(SQ.FT-HR)
AVERAGE HEAT FLUX	= 0.227E 05	BTU/(SQ.FT-HR)
Q=AMP*VOLT	= 0.182E 05	BTU/HR
Q=MW*CP*(TOUT-TIN)	= 0.181E 05	BTU/HR
HEAT LOST	= 0.296E 03	BTU/HR
HEAT BALANCE ERROR %	=-0.892E 00	

PERIPHERAL HEAT TRANSFER COEFFICIENT BTU/(SQ.FT-HR-DEG.F)

	1	2	3	4
1	282.4	295.6	297.4	316.2
2	282.6	290.4	304.1	305.5
3	284.0	300.6	307.1	306.8
4	276.8	289.6	295.4	302.4

AVERAGE HEAT TRANSFER COEFFICIENT-BTU/(SQ.FT.HR-DEG.F)

	1	2	3	4
(H1)	281.5	294.0	301.0	307.8
(H2)	281.4	294.0	300.9	307.7
LIT(1)	1.08	1.11	1.11	1.12
LIT(2)	0.93	0.96	0.96	0.96
LIT(3)	0.84	0.86	0.86	0.86

RUN NUMBER 541

AVERAGE REYNOLDS NUMBER	= 0.115E 05	
AVERAGE PRANDTL NUMBER	= 0.324E 02	
MASS FLUX	= 0.160E 07	LBM/(SQ.FT-HR)
AVERAGE HEAT FLUX	= 0.224E 05	BTU/(SQ.FT-HR)
Q=AMP*VOLT	= 0.180E 05	BTU/HR
Q=MW*CP*(TOUT-TIN)	= 0.182E 05	BTU/HR
HEAT LOST	= 0.295E 03	BTU/HR
HEAT BALANCE ERROR %	=-0.272E 01	

PERIPHERAL HEAT TRANSFER COEFFICIENT BTU/(SQ.FT-HR-DEG.F)

	1	2	3	4
1	292.5	305.8	307.1	326.8
2	292.6	301.7	313.6	315.6
3	294.7	312.8	317.4	314.4
4	286.1	301.2	305.9	311.9

AVERAGE HEAT TRANSFER COEFFICIENT-BTU/(SQ.FT.HR-DEG.F)

	1	2	3	4
(H1)	291.5	305.4	311.0	317.2
(H2)	291.5	305.3	310.9	317.1
LIT(1)	1.07	1.11	1.10	1.11
LIT(2)	0.92	0.95	0.95	0.95
LIT(3)	0.83	0.85	0.85	0.85

RUN NUMBER 415

AVERAGE REYNOLDS NUMBER	= 0.188E 05	
AVERAGE PRANDTL NUMBER	= 0.104E 02	
MASS FLUX	= 0.153E 07	LBM/(SQ.FT-HR)
AVERAGE HEAT FLUX	= 0.125E 05	BTU/(SQ.FT-HR)
Q=AMP*VOLT	= 0.996E 04	BTU/HR
Q=MW*CP*(TOUT-TIN)	= 0.100E 05	BTU/HR
HEAT LOST	= 0.766E 02	BTU/HR
HEAT BALANCE ERROR %	=-0.159E 01	

PERIPHERAL HEAT TRANSFER COEFFICIENT BTU/(SQ.FT-HR-DEG.F)

	1	2	3	4
1	1144.2	1222.8	1185.6	1307.8
2	1130.2	1159.7	1236.6	1249.3
3	1179.2	1149.8	1223.2	1212.2
4	1097.7	1148.2	1185.9	1185.2

AVERAGE HEAT TRANSFER COEFFICIENT-BTU/(SQ.FT.HR-DEG.F)

	1	2	3	4
(H1)	1137.8	1170.1	1207.8	1238.6
(H2)	1137.1	1169.4	1207.4	1237.1
LIT(1)	1.29	1.32	1.35	1.37
LIT(2)	1.12	1.15	1.17	1.20
LIT(3)	1.01	1.03	1.05	1.07

RUN NUMBER 416

AVERAGE REYNOLDS NUMBER	= 0.182E 05	
AVERAGE PRANDTL NUMBER	= 0.101E 02	
MASS FLUX	= 0.145E 07	LBM/(SQ.FT-HR)
AVERAGE HEAT FLUX	= 0.128E 05	BTU/(SQ.FT-HR)
Q=AMP*VOLT	= 0.102E 05	BTU/HR
Q=MW*CP*(TOUT-TIN)	= 0.952E 04	BTU/HR
HEAT LOST	= 0.739E 02	BTU/HR
HEAT BALANCE ERROR %	= 0.596E 01	

PERIPHERAL HEAT TRANSFER COEFFICIENT BTU/(SQ.FT-HR-DEG.F)

	1	2	3	4
1	1166.7	1259.8	1199.5	1279.7
2	1153.3	1195.0	1236.3	1224.5
3	1190.1	1161.1	1224.2	1202.0
4	1131.2	1171.2	1163.4	1164.2

AVERAGE HEAT TRANSFER COEFFICIENT-BTU/(SQ.FT.HR-DEG.F)

	1	2	3	4
(H1)	1160.3	1196.8	1205.9	1217.6
(H2)	1160.0	1195.7	1205.3	1216.3
LIT(1)	1.36	1.40	1.39	1.40
LIT(2)	1.19	1.21	1.21	1.22
LIT(3)	1.06	1.09	1.09	1.09

RUN NUMBER 417

AVERAGE REYNOLDS NUMBER	= 0.267E 05	
AVERAGE PRANDTL NUMBER	= 0.694E 01	
MASS FLUX	= 0.145E 07	LBM/(SQ.FT-HR)
AVERAGE HEAT FLUX	= 0.205E 05	BTU/(SQ.FT-HR)
Q=AMP*VOLT	= 0.163E 05	BTU/HR
Q=MW*CP*(TOUT-TIN)	= 0.171E 05	BTU/HR
HEAT LOST	= 0.122E 03	BTU/HR
HEAT BALANCE ERROR %	=-0.604E 01	

PERIPHERAL HEAT TRANSFER COEFFICIENT BTU/(SQ.FT-HR-DEG.F)

	1	2	3	4
1	1253.7	1379.7	1305.3	1417.7
2	1243.2	1301.9	1361.3	1344.9
3	1288.1	1268.5	1342.4	1309.9
4	1211.1	1275.5	1269.7	1280.8

AVERAGE HEAT TRANSFER COEFFICIENT-BTU/(SQ.FT.HR-DEG.F)

	1	2	3	4
(H1)	1249.0	1306.4	1319.7	1338.3
(H2)	1248.5	1305.0	1318.8	1336.5
LIT(1)	1.21	1.25	1.24	1.25
LIT(2)	1.08	1.12	1.11	1.12
LIT(3)	0.95	0.99	0.99	0.99

RUN NUMBER 418

AVERAGE REYNOLDS NUMBER	= 0.250E 05	
AVERAGE PRANDTL NUMBER	= 0.559E 01	
MASS FLUX	= 0.109E 07	LBM/(SQ.FT-HR)
AVERAGE HEAT FLUX	= 0.262E 05	BTU/(SQ.FT-HR)
Q=AMP*VOLT	= 0.208E 05	BTU/HR
Q=MW*CP*(TOUT-TIN)	= 0.194E 05	BTU/HR
HEAT LOST	= 0.158E 03	BTU/HR
HEAT BALANCE ERROR %	= 0.615E 01	

PERIPHERAL HEAT TRANSFER COEFFICIENT BTU/(SQ.FT-HR-DEG.F)

	1	2	3	4
1	1185.4	1297.6	1241.5	1343.7
2	1177.7	1216.9	1280.8	1291.6
3	1203.3	1176.6	1261.0	1246.6
4	1143.7	1186.6	1209.8	1225.7

AVERAGE HEAT TRANSFER COEFFICIENT-BTU/(SQ.FT.HR-DEG.F)

	1	2	3	4
(H1)	1177.5	1219.4	1248.3	1276.9
(H2)	1177.1	1217.7	1247.7	1275.4
LIT(1)	1.27	1.30	1.31	1.32
LIT(2)	1.16	1.18	1.19	1.21
LIT(3)	1.03	1.05	1.06	1.08

APPENDIX H

ERROR ANALYSIS

A general analysis of the probable error in local heat transfer coefficient determinations can be made on the basis of Eq.(5.4) as suggested by Singh (21).

$$h = \frac{\dot{q}/A}{[T_w - T_b]} = F\,(\dot{q}/A,\ T_w,\ T_b) \qquad (H.1)$$

or

$$dh = \frac{\partial f}{\partial(\dot{q}/A)} \cdot d\,(\dot{q}/A) + \frac{\partial f}{\partial T_w} \cdot dT_w + \frac{\partial f}{\partial T_b} \cdot dT_b \qquad (H.2)$$

from (H-1)

$$\frac{\partial f}{\partial(\dot{q}/A)} = \frac{1}{(T_w - T_b)}\ ;\ \frac{\partial f}{\partial T_w} = -\frac{\dot{q}/A}{(T_w - T_b)^2}\ ;\ \frac{\partial f}{\partial T_b} = \frac{\dot{q}/A}{(T_w - T_b)^2}$$

substituting in Equation (H-2)

$$dh = \frac{1}{(T_w - T_b)} \cdot d\,(\dot{q}/A) - \frac{\dot{q}/A}{(T_w - T_b)^2} \cdot dT_b + \frac{\dot{q}/A}{(T_w - T_b)^2} \cdot dT_b$$

or

$$\frac{dh}{h} = \frac{d\,(\dot{q}/A)}{(\dot{q}/A)} - \frac{dT_w}{(T_w - T_b)} + \frac{dT_b}{(T_w - T_b)} \qquad (H.3)$$

To estimate the error in h, the error in the measurement of $(\dot{q}/A)$, T_w and T_b will be estimated.

The error in the heat flux, $\dot{q}/A$, depends upon the error associated with the primary measurements used to determine the heat flux. These measurements together with an estimate of their error are:

1.	Test section current	$\pm$ 0.15
2.	Test section voltage	$\pm$ 0.25%
3.	Test section dimensions	$\pm$ 0.1%
4.	Inside wall temperature	$\pm$ 1.0%
5.	Room temperature	$\pm$ 0.5%

If all of the above mentioned measurements were in error to the extent indicated and in the same direction, the maximum error in the heat flux is 5.1%.

The calibrations were performed using the Doric Digital Thermocouple Indicator to measure the thermocouple outputs. The Digital Thermocouple Indicator had a stated accuracy of $\pm$ 0.27°F for the -320.0°F to 800.0°F range. Since the calibrations were made in-situ, the corrections reflect the inaccuracies of the Digital Thermocouple Indicator and the associated thermocouple wires.

Based on the above data, the average error in the bulk fluid temperature and the surface of the test section was estimated to be 0.27°F and 0.5°F, respectively.

The inside wall temperature was determined by a numerical solution. The average error in the wall temperature would be affected by the errors in the test section dimensions, the room temperature, the flow rate, and any computational errors. Considering all the errors, Singh (21) reported the combined total error in the inside wall temperature to be 1%.

Rewriting Equation (H-3):

$$\frac{dh}{h} = \frac{d(\dot{q}/A)}{\dot{q}/A} - \frac{(dT_w)/T_w}{[1-(T_b/T_w)]} + \frac{(dT_b)/T_b}{[(T_w/T_b)-1]} \qquad (H.4)$$

The average bulk fluid and inside wall temperature were estimated to be 195°F and 260°F, respectively.

The maximum error in the heat transfer coefficient would occur when the errors in the independent variables are all additive. Therefore,

$$\frac{dh}{h} = 0.051 + \frac{\frac{0.5}{720}}{[1-\frac{655}{720}]} + \frac{\frac{0.27}{655}}{[\frac{720}{655}-1]}$$

$$= 0.063$$

$$= 6.3\%$$

However, the most likely error in heat transfer coefficient is estimated to be about 3%.

VITA

Mitri S. Najjar

Candidate for the Degree of

Doctor of Philosophy

Thesis: AN INVESTIGATION OF THE EFFECT OF IMPROVED PHYSICAL PROPERTY DATA ON HEAT TRANSFER COEFFICIENT PREDICTION

Major Field: Chemical Engineering Minor Field: Civil Engineering

Biographical:

Personal Data: Born in El-Koura, North Lebanon, May 21, 1952, the son of Salim Najjar and Wahibi Shaheen.

Education: Attended elementary and high school in Bishmizzen, El-Koura, North Lebanon; graduated from Bishmizzen High School in 1968; attended American University at Beirut and received the Bachelor of Science degree in 1973 with a major in Chemistry + teaching diploma; received the Master of Science degree in Chemical Engineering from Oklahoma State University in May, 1977; completed the requirements for Doctor of Philosophy degree at Oklahoma State University in May, 1980.

Professional Experience: Instructor, Greenfield College, St. Mary Orthodox College and the Ministry of Education, Beirut, Lebanon, 1973-1975; Research Associate, Institute of Gas Technology, Chicago, summer, 1976; Graduate Teaching, Research Assistant, School of Chemical Engineering and Chemistry Department, Oklahoma State University, 1975-1980; Member of Omega Chi Epsilon.